TECHNISCHE UNIVERSITÄT WIEN

Diplomarbeit

Investigation of the reactivity of PCP pincer ligands with $Co_2(CO)_8$ under solvothermal conditions

ausgeführt zum Zwecke der Erlangung des akademischen Grades eines Diplom-Ingenieurs

unter der Leitung von

Univ.Prof. Dr. Karl Kirchner

Dr. Daniel Himmelbauer

Institut für Angewandte Synthesechemie E163

Getreidemarkt 9/163, A-1060 Wien

eingereicht an der Technischen Universität Wien

Fakultät für Technische Chemie

von

Heiko Schratzberger

Matr. Nr. 01525179

Altendorf 41, A-4793 Sankt Roman

Wien, August 2020

_____

Heiko Schratzberger

Ich habe zur Kenntnis genommen, dass ich zur Drucklegung meiner Arbeit unter der Bezeichnung

Diplomarbeit

nur mit Bewilligung der Prüfungskommission berechtigt bin.

Ich erkläre weiters Eides statt, dass ich meine Diplomarbeit nach den anerkannten Grundsätzen für wissenschaftliche Abhandlungen selbstständig ausgeführt habe und alle verwendeten Hilfsmittel, insbesondere die zugrunde gelegte Literatur, genannt habe.

Weiters erkläre ich, dass ich dieses Diplomarbeitsthema bisher weder im In- noch Ausland (einer Beurteilerin/einem Beurteiler zur Begutachtung) in irgendeiner Form als Prüfungsarbeit vorgelegt habe und dass diese Arbeit mit der vom Begutachter beurteilten Arbeit übereinstimmt.

Wien, August 2020

_____

Heiko Schratzberger

Acknowledgements

First of all, I want to thank Prof. Karl Kirchner for providing me the opportunity to perform my master thesis in his research group. I am grateful for the interesting research topic and the introduction to the concepts of organometallic chemistry.

I would also like to thank my supervisor Daniel Himmelbauer for giving me guidance and support during my work on my thesis as well as the entertaining karaoke evenings and nice moments in one of Vienna's high quality bars.

Furthermore, I like to express special thanks to the research group, the pincer boys. Julian Brünig and Stefan Weber for introducing me to the diversity of beer. Wolfgang Eder for guidance during my work as well as extensive talks about a plethora of topics. Gerald Tomsu for entertaining remarks and having a good time. Jan Pecak and Sarah Fleissner for some nice chats. Ines Blaha, Claudia Rabijasz and Dina Iebed for the fun moments during student labs. And last but not least my diploma colleague Daniel Zobernig for the mutual support during our master thesis and plenty nice memories while drinking coffee.

I would also like to mention my friends who started studying with me in 2015. Anna, Carola, Fabio, Flo, Hansi, Irina, Klausi and Meli for giving me motivation and support during the time at university. Special thanks to my friend Benedikt for proofreading my master thesis.

Finally, I want to express my gratitude to my parents and family for providing me never-ending support during my life. Without them, it would have been impossible to achieve this milestone in my life.

Abstract

In recent years, the field of organometallic chemistry has shifted the focus of interest towards earth abundant transition metal complexes, thus investigating how sustainable catalysts can be developed. One way of enhancing the catalytic properties of base metal complexes is to introduce spectator ligands like the so-called pincer ligands. This tridentate ligand system can be modified in a controlled manner to change the stereoelectronic properties of the metal center. Therefore, in this work the synthesis of cobalt PCP pincer complexes was investigated with special focus on the oxidative addition of the PCP ligands bearing NH and CH_2 spacer groups. To enhance the complex formation, halogens (X = Br, Cl) are introduced to the *ipso*-carbon of the PCP pincer ligand in order to weaken the C–X bond and facilitate the oxidative addition. It could be demonstrated that this approach enables the oxidative addition of PCP-X ligands with cobalt(0)octacarbonyl ($Co_2(CO)_8$) under solvothermal conditions. Several cobalt PCP^{NH} complexes that were otherwise not accessible could be synthesized via this approach. Depending on the temperature of the solvothermal reaction, disproportionation of the cobalt precursor $Co_2(CO)_8$ was observed, affording a dicarbonyl Co^{I} species and a dihalide Co^{III} species. Under elevated temperatures, only the square planar complexes [$Co^{II}(PCP^{NH}$-*t*Bu)X] (X = Br, Cl) were isolated when using PCP^{NH}-*t*Bu. All compounds were characterized by means of NMR, HR-MS and ATR-IR spectroscopy as well as single crystal XRD methods.

Kurzfassung

In den letzten Jahren verlagerte sich der Schwerpunkt der metallorganischen Chemie zu Komplexen mit Metallen, die in der Erdkruste vermehrt vorkommen, um nachhaltige Katalysatoren zu entwickeln. Eine Möglichkeit, die katalytischen Eigenschaften von Metallkomplexen der ersten Übergangsmetallreihe zu erhöhen, ist die Einführung von Liganden wie zum Beispiel die sogenannten Pincer Liganden. Dieses tridentate Ligandensystem kann gezielt modifiziert werden, um die stereoelektronischen Eigenschaften des Zentralatoms anzupassen. Daher wird in dieser Arbeit die Synthese von Cobalt PCP Pincer Komplexen mit besonderem Augenmerk auf die oxidative Addition der PCP Liganden mit NH und CH_2 Spacergruppen untersucht. Zur Erleichterung der Komplexbildung wurden Halogene (X = Br, Cl) an den *ipso*-Kohlenstoff der PCP Pincer Liganden eingeführt und dadurch die C–X Bindung geschwächt, um die oxidative Addition zu begünstigen. Es konnte gezeigt werden, dass durch diesen Ansatz die oxidative Addition der PCP-X Liganden mit Cobalt(0)octacarbonyl ($Co_2(CO)_8$) unter Solvothermalbedingungen ermöglicht wird. Einige Cobalt PCP^{NH} Komplexe konnten so hergestellt werden, die über andere Methoden nicht zugänglich waren. Abhängig von der Temperatur der Solvothermalreaktion wurde eine Disproportionierung der Cobalt Vorstufe $Co_2(CO)_8$ zu einer Co^{I} Dicarbonylspezies und einer Co^{III} Dihalogenidspezies beobachtet. Bei erhöhter Temperatur wurden bei Verwendung von PCP^{NH}-*t*Bu nur die quadratisch planaren Komplexe [$Co^{II}(PCP^{NH}$-*t*Bu)X] (X = Br, Cl) isoliert. Alle Verbindungen wurden mittels NMR, HR-MS und ATR-IR Spektroskopie sowie Einkristallröntgendiffraktion (XRD) charakterisiert.

TABLE OF CONTENTS

1. Introduction

Well defined catalysts are used to minimize the generation of waste and/or by-products for the production of bulk, fine and pharmaceutical chemicals.[1] The design of benign chemicals as well as catalytic reactions, in contrast to using stoichiometric reagents, are key aspects of the 12 principles of green chemistry (Figure 1) in order to accomplish the ultimate goal of sustainable chemical syntheses.[2,3]

1	WASTE PREVENTION	5	BENIGN SOLVENTS & AUXILIARIES	9	CATALYSIS
2	ATOM ECONOMY	6	ENERGY EFFICIENCY	10	DEGRADATION
3	SAFER SYNTHESIS	7	RENEWABLE FEEDSTOCK	11	POLLUTION PREVENTION
4	SAFER CHEMICALS	8	REDUCE DERIVATIVES	12	ACCIDENT PREVENTION

Figure 1: The 12 Principles of Green Chemistry[2,3]

However, in common industrial-scale processes, the utilized catalysts comprise noble metals like Pd, Pt, Rh. Even though these catalysts show a high efficiency and selectivity, they contain low abundant elements and some of them feature a high inherent toxicity. On the contrary, base metal catalyst usually exhibit a lower efficiency and selectivity as well as a reduced stability under reaction conditions suitable for noble metals.[4] To achieve the transition from precious to more abundant metals while addressing the problem of selectivity and efficiency, the development and synthesis of complexes containing so-called pincer ligands is a possible approach. This ligand system allows, due to its modular scaffold, the tuning of the stereoelectronic properties of the metal center and thus renders the utilization of base metals in homogenous catalysis possible.[5]

A pincer ligand is a tridentate chelating ligand system that coordinates to the metal center due to its rigid structure in a meridional fashion. Figure 2 depicts the basic scaffold of pincer ligands: they consist of an aliphatic or aromatic backbone tethered to two donor moieties via spacer groups. The nomenclature of pincer ligands is derived from the order of the coordinating atoms according to the scheme DED‘.

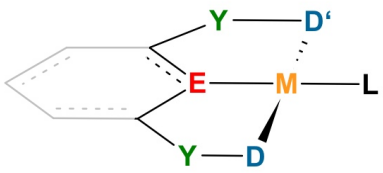

metal center: M = transiton metal
co-ligand: L = CO, Hal, H, NHC, etc.
backbone: E = C_{sp2}, C_{sp3}, N, P, etc.
spacer Y = C, N, O, S, etc.
neutral 2e⊖ donor: D/D‘ = P, N, S, etc.

Figure 2: Scaffold of a pincer ligand

Shaw *et. al.* reported the first pincer complexes (PCP) in the mid 1970s[6], although the name „pincer“ was introduced by van Koten in the 1980s.[7]

The approach of pincer containing base metal complexes was successful, which is indicated by many publications regarding PNP bearing base metal catalysts.[8-10] Unlike PNP systems, the number of published catalysts with the older PCP system is scarce, which makes them a popular topic in current research in the field of organometallic chemistry. The reason for the lack of PCP complexes are the limited supply for suitable metal precursor as well as aromatic and aliphatic precursors, which require multi-step syntheses, and the high stability of the *ipso* C–H bond.[11] There are several approaches to circumvent these limitations:

a) Transmetalation, for example, with *n*-BuLi in the absence of acidic groups in the pincer scaffold
b) Increasing of the C–H acidity by variation of the spacer groups. Kirchner and coworkers introduced a NMe containing PCP pincer that was able to form Ni and Co pincer complexes[12]
c) Substitution of the *ipso*-H with halides or other leaving groups which facilitates the oxidative addition due to the lower bond-enthalpy of C–X (X = Cl, Br, I, OTf) in comparison to C–H[11]

1.1. Aim of this thesis

This work focused on the synthesis of PCP complexes that contain Co as central atom. The respective complexes were synthesized via the approach of solvothermal synthesis, which means that the reactions are performed in sealed pressure vials in order to exceed the solvent's atmospheric boiling point. $Co_2(CO)_8$ was used as metal precursor and the process of oxidative addition of the different PCP ligands was investigated with respect to the formed species. The obtained complexes were characterized by means of ATR-IR, NMR, HR-MS and XRD measurements.
This thesis continues the work of Kirchner *et. al.* regarding the solvothermalreactions of $Cr(CO)_6$, $Fe(CO)_5$ and $Co_2(CO)_8$ with POCOP and PCP^{NMe} systems which reacted differently depending on the substituents of the phosphines with respect to disproportionation (Scheme 1).[13] Disproportionation, in this context, describes the conversion of a compound with an intermediate oxidation state into one compound with a higher and another with a lower oxidation number.

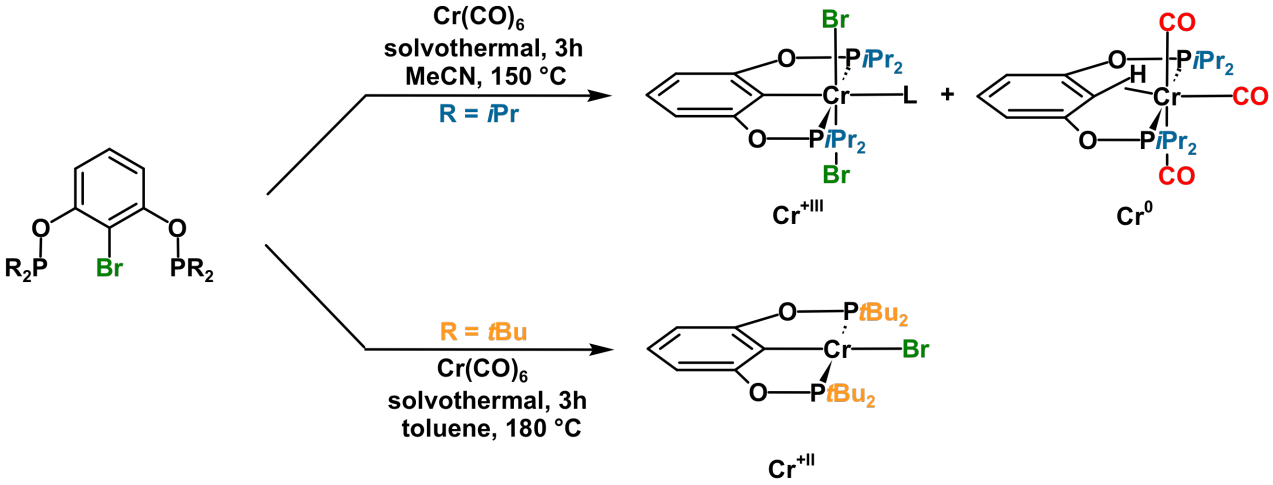

Scheme 1: Findings with POCOP ligands and $Cr(CO)_6$

The process of oxidative addition of the *ipso*-halogenated PCP pincers with $Co_2(CO)_8$ resulted in different formed complexes, depending on spacer and phosphine donor groups from the ligand. In addition, ATR-IR measurements allowed a fast interpretation of the formed species via the CO stretching frequencies. Hence, cobalt was chosen for the investigation of the process of oxidative addition with the systems PCP^{NH} and PCP^{CH_2} (Figure 3).

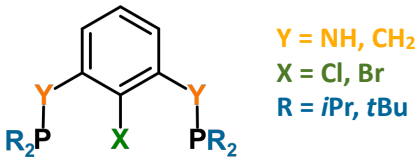

Figure 3: Structure of the used pincer ligands

The solvothermalreactions were performed under different reaction conditions with variation of reaction time (4 h and 20 h) and reaction temperature (110°C and 130 °C).

1.2. PCP pincer ligands

PCP pincers constitute one of the oldest classes of pincer ligands and were first published in the 1970s by Shaw and coworkers who reported the synthesis of PCP^{CH_2} complexes with group 10 transition metals (Figure 4).[6]

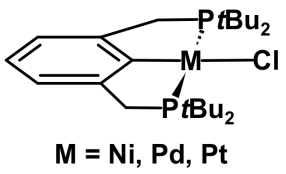

Figure 4: PCP^{CH_2} complexes established by Shaw and coworkers[6]

Since then, a plethora of PCP ligands have been published, some common PCP scaffolds are represented in Figure 5.[5]

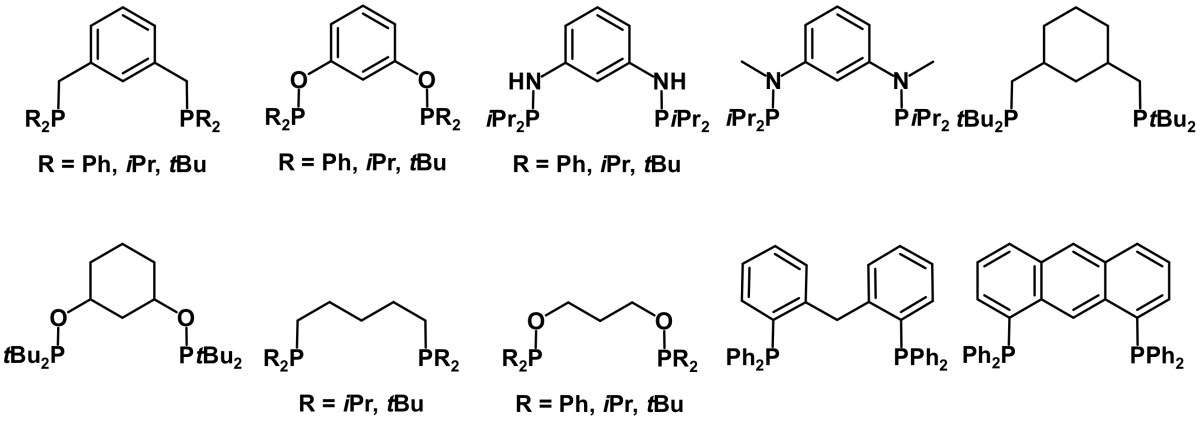

Figure 5: Overview of common PCP motifs[5]

The main difference between anionic PCP ligands and PNP ligands, for example, is the direct M–C bond, which is the origin of their slightly enhanced stability in comparison to PNP ligands.[14] Though the M–C bond is usually very strong, many first row metals fail to activate the C–H bond or the corresponding hydride complex turns out to be unstable. In some cases, an agostic species has been isolated, which feature a σ-complex motif, i. e. the C–H bond coordinates to the metal center.[15]

In recent years, a great variety of spacer groups have been established as common motifs in PCP ligands, which allow the modulation of stereoelectronic properties, introduce chirality or give control over the ligand's bite angle.[5] The spacers have strong influence on the ligand's stability as well. There are several publications that deal with the stability of P–N bond of aminophosphines under acidic conditions. Due to the higher electronegativity, the P–N bond is polarized and the phosphorus is more sensitive to oxidation and displacement by another nucleophile than P–C containing phosphines.[16]
Depending on the spacer groups, the pincer ligand can take part in the chemical transformation via metal ligand cooperation (MLC) as well, which is an essential prerequisite for certain reaction pathways to take place.[17]

1.3. Cobalt PCP pincer complexes in literature

Until 2015, there were no applications for Co-PCP pincer complexes for any catalytic reaction.[5] Since then, only few publications were submitted regarding catalysis with PCP complexes (see below). Contrary is the situation with other Co pincer complexes, for example with PNP, NNN or CCC pincer ligands. With these Co pincers, catalytic (de)hydrogenations, transfer hydrogenations, hydroborations, hydrosilylations and dehydrogenative couplings have been reported.[17]

The first Co containing PCP complex was synthesized by Li and coworkers in 2009. Via oxidative addition of the C–H bond of $(Ph_2POCH_2)_2CH_2$ with $[Co(Me)(PMe_3)_4]$, followed by the release of methane, the complex $[Co(POC(sp^3)OP)(PMe_3)_2]$ (**Co1**) could be obtained (Scheme 2).[18]

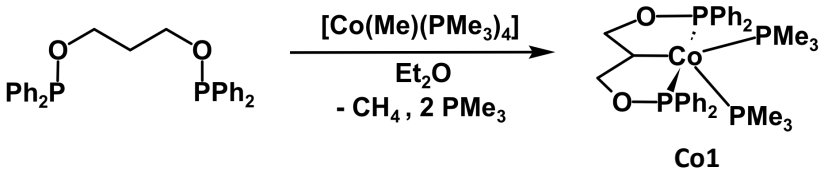

Scheme 2: Synthesis of the first Co PCP complex[18]

One year later, Li *et. al.* published the synthesis of the first Co POC(sp^2)OP complex (**Co2**) as well. The POCOP ligand was stirred with [Co(PMe$_3$)$_4$] in Et$_2$O for 48 h and after workup, the complex could be obtained as red crystals (Scheme 3). Interestingly, only the complex without a Co–H bond was detected, which would be expected after oxidative addition of the POCOP ligand.[19]

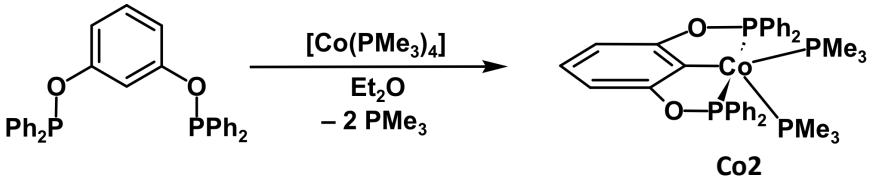

Scheme 3: Synthesis of the first aromatic Co POCOP complex[19]

Heinekey and coworkers described the synthesis of the cobalt POCOP complex [Co(POCOP-*t*Bu)I] (**Co3**) via transmetalation with *n*-BuLi and CoI$_2$•THF in 2011 (Scheme 4). The structure was determined via XRD measurements and magnetic susceptibility measurements are in agreement with a d^7 low spin configuration.[20]

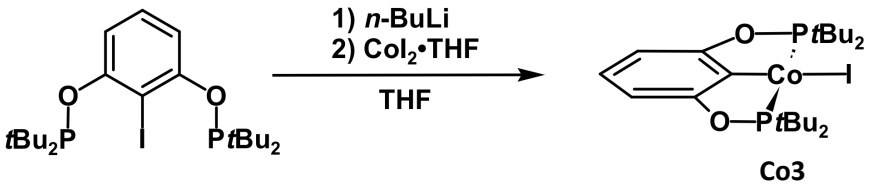

Scheme 4: Co POCOP complex via transmetalation[20]

The square planar iodide POCOP (**Co3**) was further reduced by sodium amalgam to yield a mercury bridged dimer [{(POCOP)Co}$_2$Hg]. Exposure of the bridged complex to H$_2$ resulted in the formation of the corresponding dihydrogen complex [Co(POCOP)(H$_2$)] (**Co4**), and under increased hydrogen pressure the dihydride complex [Co(POCOP)H$_2$(H$_2$)] (**Co5**) was obtained, which was not stable above 220 K (Figure 6).[20]

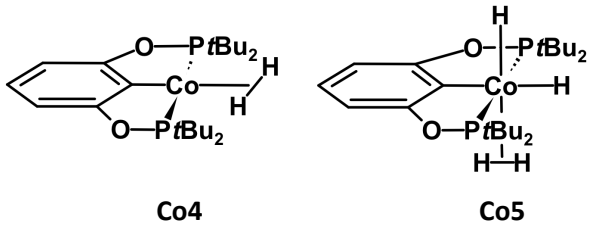

Figure 6: Hydrogen and hydride complexes obtained from **Co3**[20]

In 2016, Kirchner *et. al.* published the catalytic dehydrogenative coupling of primary alcohols and primary amines with a Co^{II} PCP complex comprising a N-alkylated 1,3-benzendiamine scaffold (Scheme 5).[21]

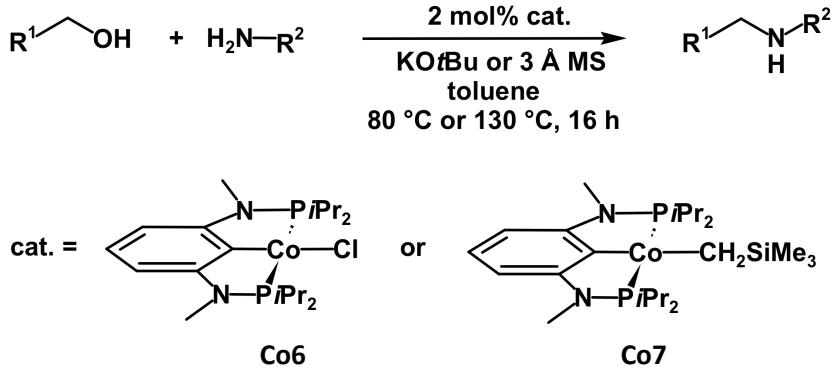

Scheme 5: Dehydrogenative coupling of primary alcohols and primary amines[21]

While both complexes alkylate aromatic amines with primary alcohols, the cobalt halide complex (**Co6**) required the addition of a base. In contrast, the complex bearing the basic TMS group (**Co7**) worked under base-free conditions at the cost of elevated reaction temperatures.

Inspired by the results of Li regarding the synthesis of cobalt PCP complexes via the route of C–H activation, Guan and coworkers adapted Li's approach and used $Co_2(CO)_8$ as precursor material (Scheme 6), since $Co(PMe_3)_4$ distorts the usual planar conformation of bulkier PCP ligands, thus making the C-H activation thermodynamically less favorable.[22]

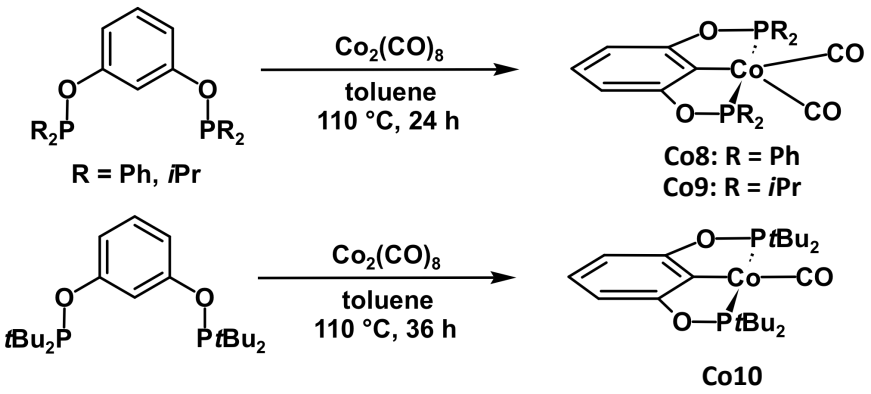

Scheme 6: C–H activation of POCOP ligands by $Co_2(CO)_8$[22]

They successfully applied complexes **Co8-10** for catalytic hydrosilylation of carbonyl functionalities (Scheme 7).[22]

The initial entries 1-2, which were performed in sealed J. Young NMR tubes, showed zero to low conversion of the starting material. In entry 3, a mixture of several silylated products was obtained, most likely due to alkoxide exchange reactions.

CO abstraction from **Co9** via addition of Me_3NO, an approach which was previously successfully applied by Guan *et*. al. before to generate vacant sites at the metal center, did not improve the catalytic activity at all.[23]

Entry 9 was performed under irradiation of UV light resulting in the increase of the overall conversion, although it failed to form the hydrosilylated product instead of photoproducts.

Guan and coworkers concluded from the findings of entries 1-5 that loss of CO was essential for the formation of the active species, a monocarbonyl complex, and that an open system is required in order to form this species in higher amounts.

This consideration was in agreement with entries 6-7, in which quantitative conversion and yields were detected with the model reaction when the CO could escape via the open Schlenk line. Contrary results were obtained when the Schlenk line was filled with CO, thus inhibiting the formation of the active species. Despite **Co10** already being a coordinatively unsaturated 16-electron complex, the reaction still required an open system to be catalytically active. Guan reasoned that in order to generate the active species, **Co10** had to lose another CO, which seemed to be a necessity only for the sterically hindered *t*Bu-phosphine complex.[22]

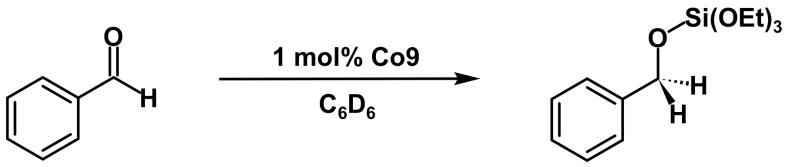

entry	conditions	conversion (%)	yield (%)
1	50 °C, 24 h, closed	0	0
2	80 °C, 24 h, closed	10	7
3	80 °C, 24 h followed by 100 °C for 24 h	78	78
4	50 °C, 1 mol% Me_3NO, 24 h, closed	0	0
5	23 °C, hv (365 nm), 24 h, closed	87	15
6	50 °C, 24 h, open to argon	> 99	> 99
7	50 °C, 24 h, open to CO	0	0
8	23 °C, 24 h, open to argon	12	10
9	23 °C, hv (365 nm), 24 h, open to argon	94	42

Scheme 7: Hydrosilylation of PhCHO with $(EtO)_3SiH$[22]

Similar cobalt carbonyl complexes bearing a PCP^{NMe} pincer ligand were reported by Kirchner and coworkers in 2014. These Co^{I} and Co^{II} carbonyls were prepared from the square planar [Co(PCP^{NMe})Cl] (**Co6**) which was treated with CO and KC_8 or $AgSbF_6$ (Scheme 8).[24]

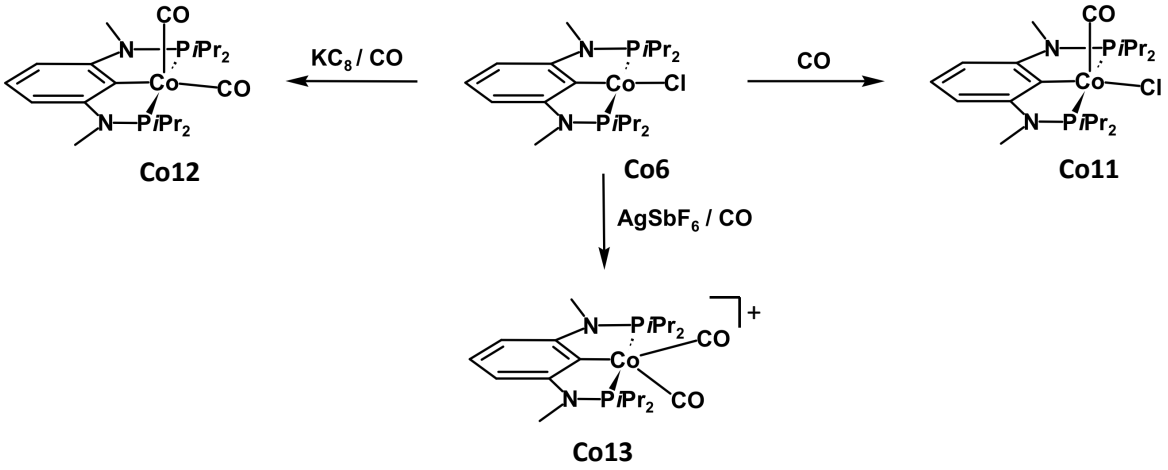

Scheme 8: Reaction of [Co(PCP^{NMe})Cl] (**Co6**) with CO[24]

DFT calculations suggested that the loss of CO from **Co12** is an endergonic process by 9.3 kcal mol^{-1}. Thus, the formation of the monocarbonyl complex like **Co10** is unfavorable for iPr_2P-donors with the PCP^{NMe} system at the applied reaction conditions.

Heinekey *et. al.* investigated the behavior of **Co10** under exposure to CO (Scheme 9). They proved that the dicarbonyl complex [Co(POCOP)$(CO)_2$] (**Co14**) can be obtained from **Co10** by exposure to CO gas (1 atm), unlike the higher homologs Rh and Ir, or by treating [Co(POCOP)I] (**Co3**) with Na/Hg and > 2 equiv. of CO. However, when treating [Co(POCOP)I] (**Co3**) directly with CO gas and without adding a reducing agent, [Co(POCOP)I(CO)] (**Co15**) was obtained.[25]
Both **Co14** and **Co15** transform to the respective starting material upon heating or longer periods of vacuum.

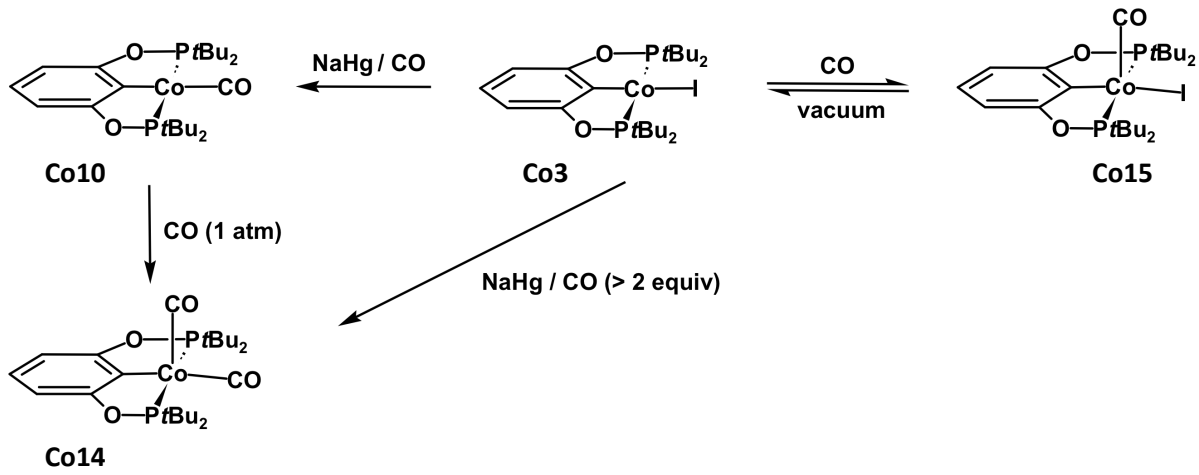

Scheme 9: Cobalt carbonyl-complexes with POCOP-*t*Bu[25]

The first agostic cobalt PCP complex was reported by Kirchner *et. al.* in 2016. Via protonation of **Co12** with $HBF_4 \bullet Et_2O$, complex **Co17** was afforded, which features a η^2-C_{aryl}–H agostic bond in addition to two CO ligands. The formation of the agostic species was reversible due to the high acidity of the agostic proton. Hence, the addition of a weak base, such as pyridine, led to the re-formation of the starting material **Co12** (Scheme 10).[26]

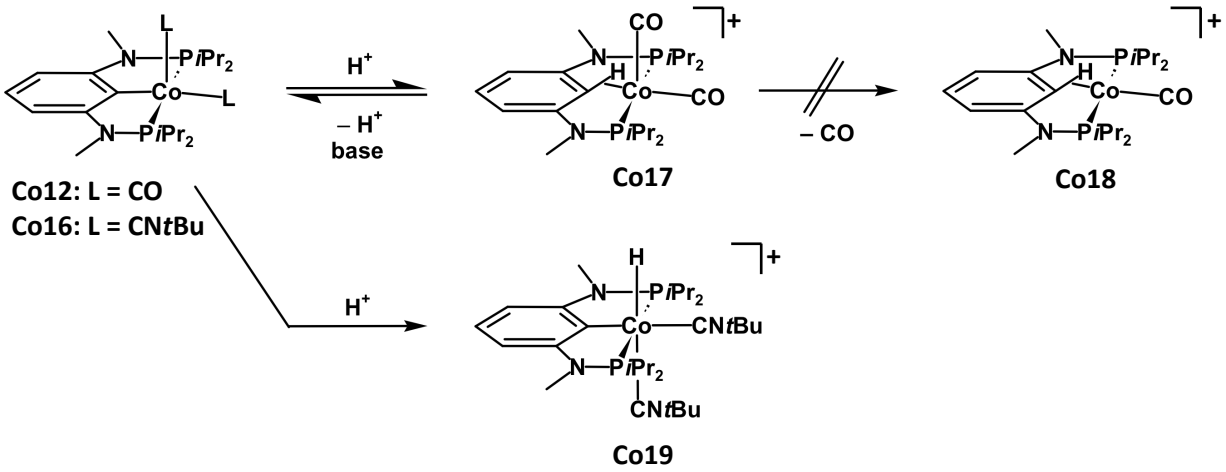

Scheme 10: Agostic cobalt PCP pincers upon protonation[26]

Unlike **Co12**, the analogous di-isonitrile complex **Co16** did not form an agostic complex but resulted in the corresponding hydride **Co20**. Much like **Co12**, the loss of one of the CO of the cationic complex **Co17** to obtain the monocarbonyl complex **Co18** was not observed. The dicarbonyl species **Co17** is more stable than the monocarbonyl species **Co18** which is supported by the means of DFT calculations.

The first nitrosyl containing cobalt PCP complexes were reported by Kirchner and coworkers in 2020. A series of [Co(PCP-*i*Pr)X] (X = Br, Cl) complexes with different spacer groups were exposed to nitric oxide (NO) and the resulting nitrosyl complexes were characterized via XRD, solution magnetic susceptibility measurements, ATR-IR and CV (Scheme 11).[27]

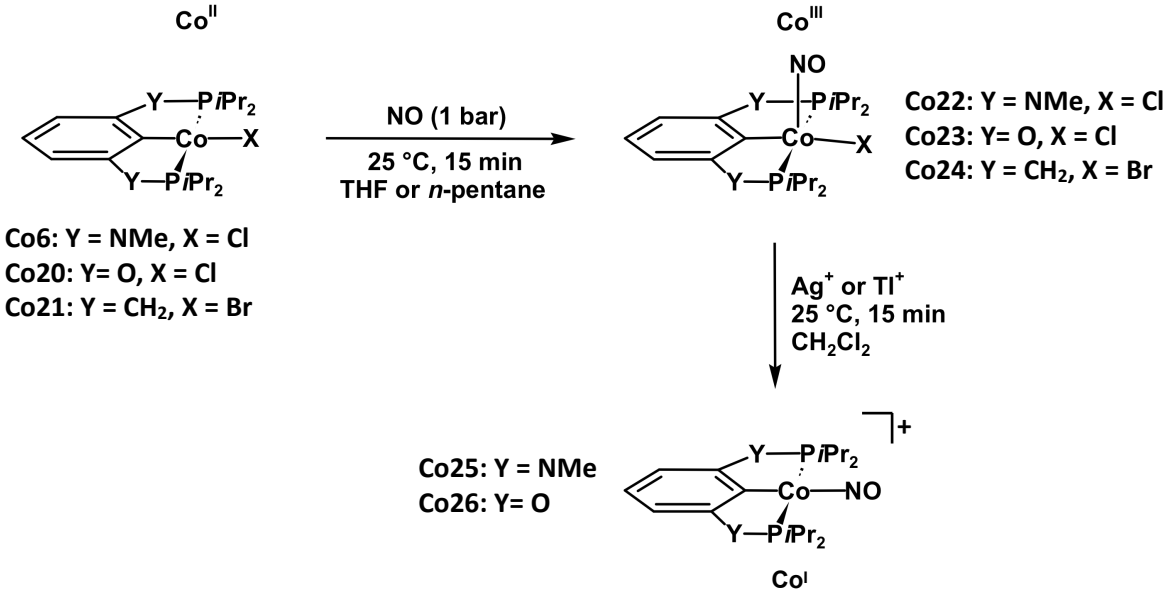

Scheme 11: Synthesis of nitrosyl cobalt PCP complexes and halide abstraction by Ag^+ or Tl^+ [27]

Direct nitrosylation of **Co6**, **Co20** and **Co21** with nitric oxide afforded the five-coordinated Co^{III} nitrosyl complexes **Co22-24**. Via single crystal XRD measurements, the structures of the complexes **Co22-23** were determined and they showed a slightly distorted square pyramidal geometry, in which the nitrosyl ligand occupied the apical position.
ATR-IR measurements displayed characteristic N–O stretching modes at 1643 (**Co22**), 1650 (**Co23**) and 1639 (**Co24**) cm^{-1}, which is indicative for NO being in a bent coordination mode and the nitrosyl ligand is therefore formally considered to be a NO^- anion. These N–O vibrations, which are shifted due to different π-backbonding from the metal center, are in accordance with Tolman's series of electronic parameters, which sort the phosphine donors according to their donor strengths ($CH_2 \approx NR > O$).[27]
Treating the complexes **Co22-23** with halogen scavengers like $AgBF_4$, $TlPF_6$ afforded the square planar diamagnetic cationic nitrosyl complexes **Co25-26**. Unlike the five-coordinated nitrosyl complexes **Co22-23**, the NO exhibited a linear coordination mode, which is underlined by the ATR-IR spectra displaying NO vibrations at 1806 (**Co25**) and 1861 (**Co26**) cm^{-1}.[27]

1.4. Carbonyl ligands

Carbon monoxide (CO) is one of the best studied ligands in coordination and organometallic chemistry. It forms a strong σ-bond to the metal center via its highest occupied molecular orbital (HOMO) and is able to accept π-backdonation from the metal center in its lowest unoccupied molecular orbital (LUMO) (Figure 7). Due to the appropriate energy levels, the LUMO is accessible for efficient backdonation, which results in a high ligand field splitting. Thus, homoleptic first row transition metal carbonyl complexes usually follow the 18-electron rule of coordination chemistry.[28]

A big advantage of CO ligands is the relatively easy detection by various methods including IR spectroscopy, ^{13}C-NMR spectroscopy and XRD measurements.[28] IR-based detection methods are most common, since the number and intensity of carbonyl bands give additional information about the number of CO ligands attached to the metal center, the local symmetry of the metal center as well as its electronic properties.[29]
Depending on the degree of backdonation from the metal's d_π orbitals into the LUMO of carbon monoxide, the bond strength is weakened and the bond length increases. Consequently, the signal of the C–O stretching mode in the IR spectra is shifted to lower wave numbers ν_{CO}.

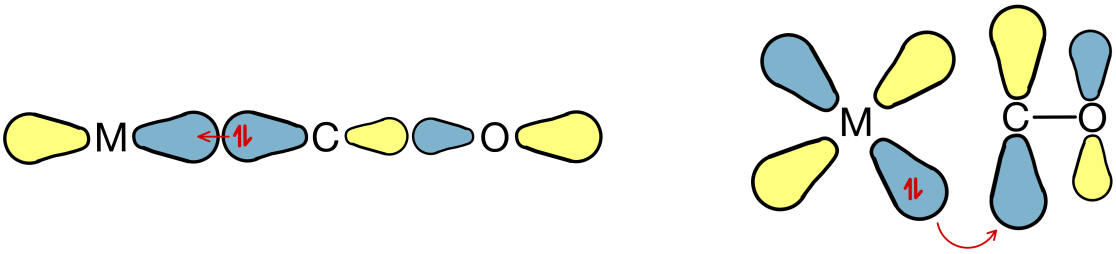

σ-bonding: HOMO → metal s, p or d	**π-backbonding: metal d_π → LUMO**
bond order M–C increases	bond order M–C increases
bond order C–O increases slightly	bond order C–O decreases
ν_{CO} increases	ν_{CO} decreases

Figure 7: σ- and π-bonding of CO with the metal center[28]

Metal carbonyls are widely used in organometallic chemistry as precursor substances, since CO can be substituted by many other ligands, such as Lewis bases, olefins and arenes (Scheme 12). Additionally, after the substitution of one carbonyl ligand, the remaining CO ligands stabilize the resulting complex in regard to thermal decomposition and oxidation.[28]

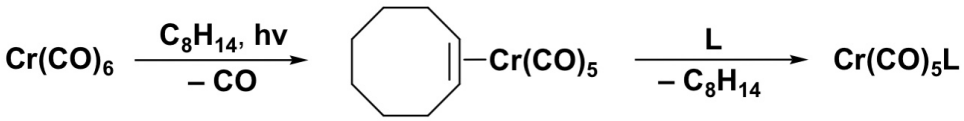

Scheme 12: Photochemical supported ligand exchange of homoleptic metal carbonyls[28]

Ligand exchange can be supported by means of photochemistry. Via selective absorption of UV light, CO dissociation is facilitated. Further irradiation of light can either result in the loss of another carbonyl ligand and the substitution by another ligand L or the dissociation of the previously introduced ligand L (Scheme 13).[30]

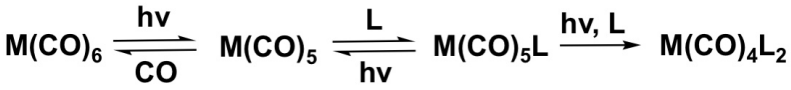

Scheme 13: Photochemically supported ligand exchange of homoleptic metal carbonyls[30]

1.5. Phosphines

In homogenous catalysis, phosphine ligands have been applied for a long time, since they allow control over electronic and steric properties that can be tuned independently from each other. Tolman and coworkers investigated the properties of several phosphine ligands and established a plot, which sorts the phosphines according to their electronic properties and their steric demand (Figure 8).[31,32]

Similarly to carbon monoxide, phosphines can accept backdonation from the metal center in the antibonding $\sigma^*_{P\text{-}C}$ orbital. In accordance with Tolman‘s plot, the π-acidity of phosphines increases

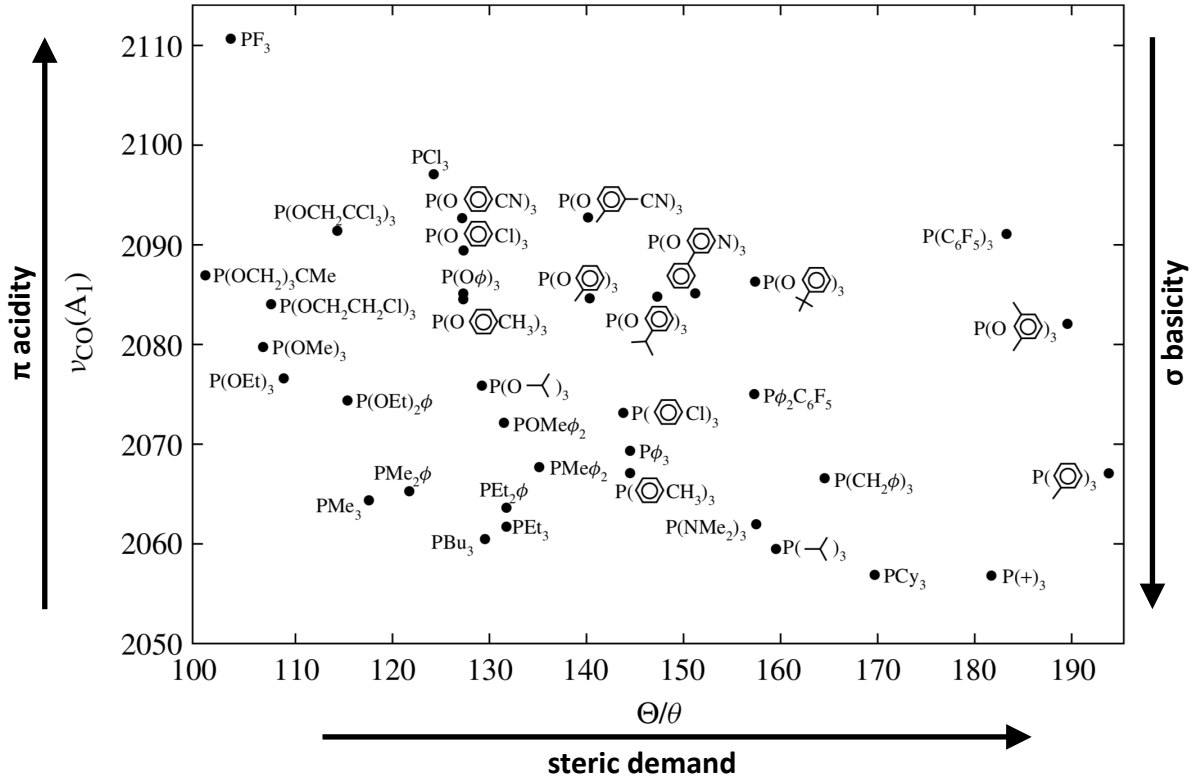

Figure 8: Electronic and steric correlation plot of various phosphines according to Tolman[32]

with the electronegativity of the substituents, since the energy levels of the $\sigma^*_{P\text{-}C}$ orbital are lowered and are therefore more accessible for π-backdonation (Figure 9).[32]

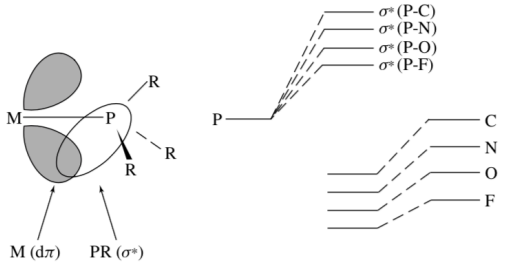

Figure 9: π backdonation in phosphine ligands[32]

Since ^{31}P has a natural abundance of 100 % and a nuclear spin of ½, it is an excellent nucleus for routine NMR experiments such as monitoring the reaction progress. Furthermore, the shift of ^{31}P of phosphines is altered significantly upon complexation, which gives information whether the phosphine donors are attached to a metal center or not.

1.6. Oxidative addition

A major goal in organometallic chemistry is to achieve selective and efficient C–H and C–C bond activation via transition metal catalysts, hence eliminating the necessity to functionalize reagents in order to perform a chemical transformation.[33]
One main step in the process of C–H and C–C activation is the oxidative addition of the respective bond. Apart from chemical transformations, the process of oxidative addition is a possible route for the cyclometalation of pincer ligands.[15,22]

There are three main mechanism regarding oxidative addition: the concerted addition, the S_N2 pathway and the radical mechanism. For non-polar bonds like C–H and arylhalides (Ar–X), the concerted pathway is usually the predominant one.[32]
In the concerted oxidative addition, the precoordination of the C–Y bond (Y = H, Cl, Br, I,…) is a necessity for a successful cleavage. As a consequence, a vacant site for the formation of the intermediately forming σ-complex is necessary. Via backdonation of electron density from occupied d-orbitals into the $\sigma^*_{R\text{-}Y}$ orbital, cleavage of the C–Y bond is achieved. Since the net transfer of electron density is a key element for a successful oxidative addition, the cleavage is accomplished easier by low valent late transition metals.[31] When comparing the first row transition metals regarding their ability to achieve the oxidative addition of the *ipso*-C–H bond of PCP ligands, there is a general trend from left to right in the periodic table of the elements (Figure 10).[15,22,34]

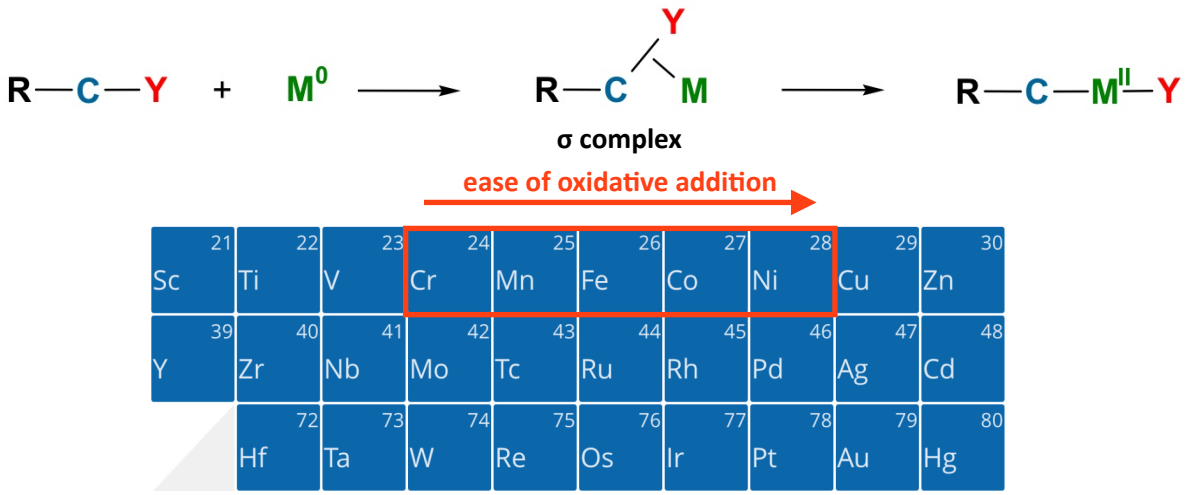

Figure 10: Schematic mechanism of the oxidative addition and general trend for first row transition metals

Early transition metals like chromium have a lack of the electron density to achieve the cleavage of the C–H bond of PCP ligands, hence the σ-complex can be afforded as main product if the agostic complex is stable enough (Figure 11).[15]

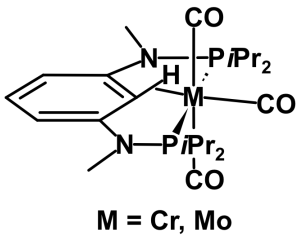

Figure 11: Agostic chromium and molybdenum PCP complexes obtained from $M(CO)_6$ [15]

An approach to circumvent the insufficient oxidative addition by first row transition metals is to employ *ipso*-halogenated P(C-X)P ligands as starting material (Figure 2). Due to the lower bond enthalpy of C–X bonds in comparison to C–H bonds, the oxidative addition is facilitated.[11] Applying this approach made several new PCP pincer complexes available with the group 6 elements, chromium, molybdenum and tungsten as well as manganese and iron (Figure 12).[13,35-37]

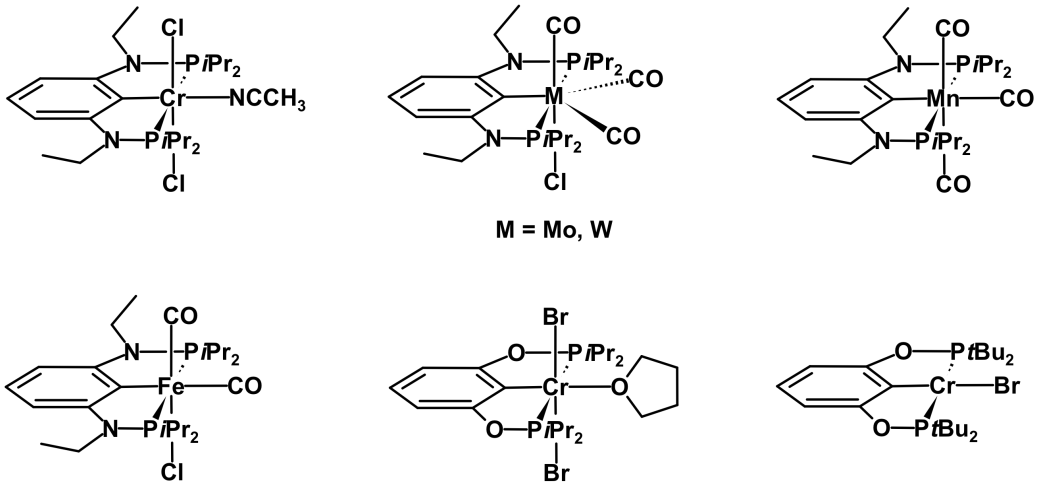

Figure 12: PCP complexes accessible via oxidative addition of P(C-X)P ligands[13,35-37]

2. Results and Discussion

As outlined in section 1.6., the oxidative addition of unfunctionalized compounds is not readily achieved by first row transition metals. In order to enhance the cleavage of the bond at the *ipso*-position, a common approach is the polarization, i. e. weakening, of the covalent bond by substituting the C–H bond with C–X (X = Cl, Br).[11,35-37]
During this thesis, the oxidative addition of several PCP^{NH} and PCP^{CH_2} pincer ligands (Figure 13) was investigated with $Co_2(CO)_8$ as metal precursor under solvothermal conditions. The reaction were carried out in sealed microwave vessels in order to withstand the built-up pressure of the solvent and the determination of the formed species was carried out via ATR-IR and NMR methods as well as HR-MS and XRD measurements (see following sections).

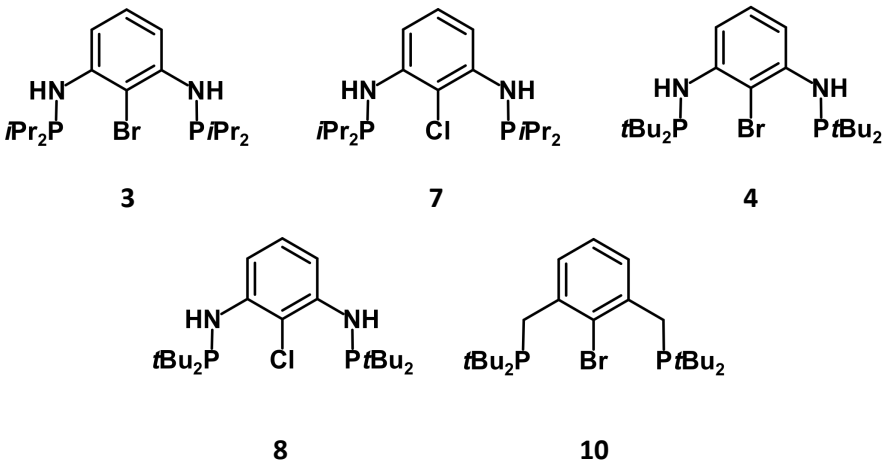

Figure 13: Overview of the synthesized pincer ligands of this thesis

The synthesis of the ligands and their reactivity in regard to the oxidative addition with $Co_2(CO)_8$ is described in the following section. It has to be noted that similar ligand systems have been previously applied by Kirchner *et. al.* for several first row metals including cobalt. Solvothermalreactions with $Co_2(CO)_8$ as metal precursor for the oxidative additions of P(C-X)P ligands displayed a stronger dependency on the spacer groups and the phosphine donors than other transition metals like iron or chromium with the similar POCOP and PCP^{NMe} systems.[13,35-37]

2.1. Synthesis of PCP^{NH} ligands

Starting from 1,3-dinitroaniline, the respective halide (X = Cl, Br) was introduced to the *ipso*-carbon (**1,5**) via a Sandmeyer reaction. The reduction of the two nitro groups to primary amines (**2,6**) was carried out by the addition of iron powder in the acidic solvent mixture EtOH/AcOH/H_2O under exposure to ultrasound irradiation. The ultrasound-supported reaction with iron powder has the advantage of utilizing rather inexpensive and benign reagents in comparison to other reducing agents, such as $SnCl_2$ or heterogenous reduction on Pd/C, at the cost of the overall yield of the reaction. With R_2P-Cl (R = *i*Pr, *t*Bu) and the addition of a base, the phosphine donors were introduced and the final PCP^{NH} ligands were obtained as a colorless oil (R = *i*Pr: **3**, X = Br, **7**, X = Cl) or a colorless solid (R = *t*Bu: **4**, X = Br, **8**, X = Cl) after the filtration through a pad of silica and the removal of all volatiles under reduced pressure (Scheme 14).

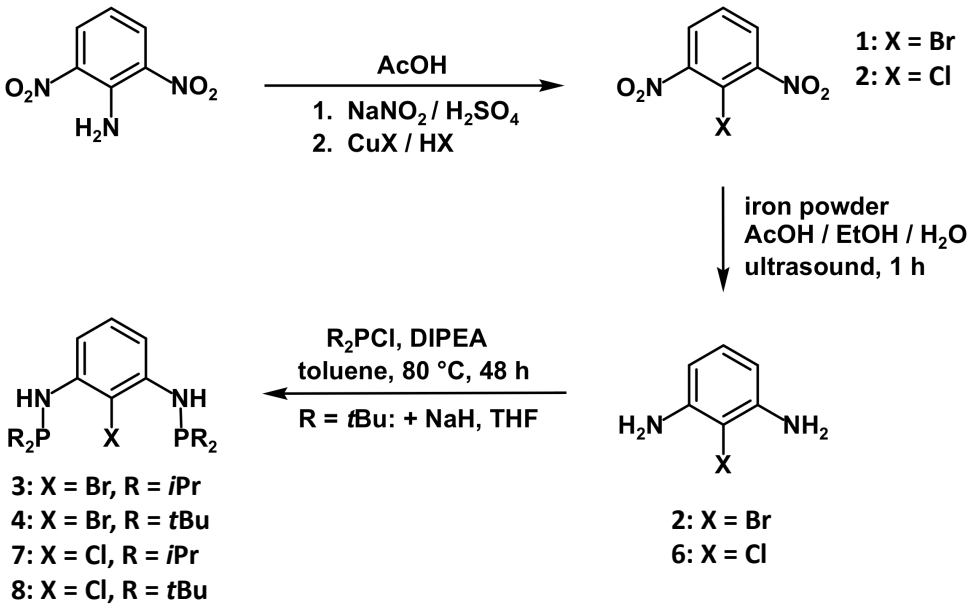

Scheme 14: Synthesis of PCP^{NH} ligands

The phosphorylation was performed according to the procedure for the analogous *ipso*-H PCP^{NH} ligand, although the exchange of NEt_3 with di(isopropyl)ethylamine (DIPEA) was necessary as full conversion of the added chlorophosphine did not occur with NEt_3.[38] Intriguingly, DIPEA as sole base was not able to selectively transform **2** or **6** to the respective PCP ligands. Besides DIPEA, it was necessary to add NaH or *n*-BuLi so as to obtain the desired product. Even though *n*-BuLi can potentially perform metal-halide exchange, no dehalogenated product was detected after purification. However, traces of the respective PCP^{NH}-*t*Bu-Cl ligand were detected when synthesizing **4** due to halogen scrambling.

In comparison to *n*-BuLi/DIPEA, the reaction with NaH/DIPEA increased the yield of **4** with less side products, which was in accordance to the colorless appearance. Hence, the phosphorylation of **2** with *t*Bu_2P-Cl was preferentially carried out with NaH as the tedious cooling steps when handling *n*-BuLi were not required. When performing the reaction only with NaH as base, full conversion of **2** to one species was confirmed via $^{31}P\{^1H\}$-NMR. Nevertheless, the isolated product had lost the *ipso*-halide. Hence, for the PCP ligands bearing *t*Bu_2P-donors, it seemed to be essential to add a stronger secondary base besides a non-nucleophilic amine base, while *i*Pr_2P-donors can be introduced only by adding a bulky amine such as DIPEA as hydrochloric acid scavenger.

2.2. Synthesis of PCP^{CH_2} ligands

As starting material for the *ipso*-bromide bearing PCP^{CH_2} ligands, the commercially available 2-bromoxlyene was utilized. After dibromination via N-bromosucccinimide (NBS) and dibenzoyl peroxide (DBPO) as radical starter in CCl_4, the benzylic tribromide **9** was obtained as colorless solid. The advantage of using CCl_4, despite its environmental issues, was that the resulting succinimide was insoluble in CCl_4 and could be readily separated via filtration through a pad of celite allowing to continue with the crude product. Nucleophilic substitution of the benzylic bromides with *t*Bu_2PH afforded the corresponding phosphonium salt, which was deprotonated, after solvent exchange from MeOH to toluene, with DIPEA resulting in the formation of **10** as a colorless solid (Scheme 15).

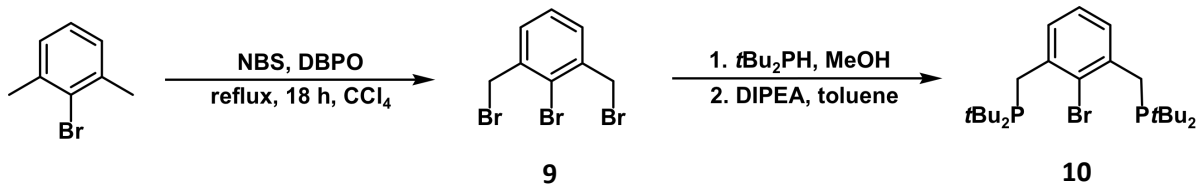

Scheme 15: Synthesis of PCP^{CH_2}-*t*Bu-Br (**10**)

2.3. Solvothermalsynthesis of cobalt complexes with PCP ligands

The complexation with the above described PCP ligands was realized via oxidative addition under solvothermal conditions. For the reactions, acetonitrile (MeCN) was chosen as solvent and the reaction was investigated at 110 °C and 130 °C. To gain further insight in the process of oxidative addition, the reaction time was varied as well. Consequently, the reactions were stopped after 4 h or 20 h. The workflow for the solvothermal reactions is depicted in Scheme 16.

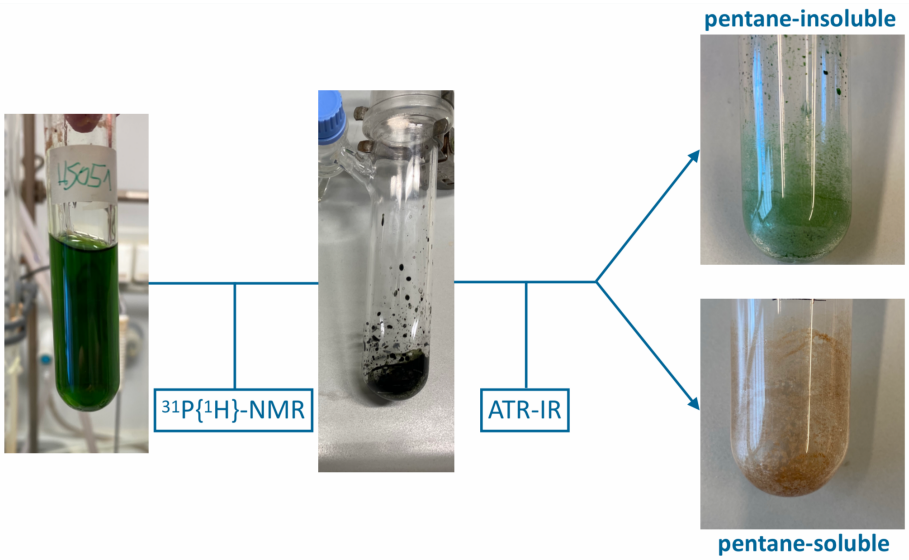

Scheme 16: General solvothermal reaction workflow

After putting the starting materials in a sealed microwave vial, the reaction mixture was heated to 110 °C or 130 °C respectively and after 4 h or 20 h, the heating was stopped. The progress of the reaction was determined via measurement of $^{31}P\{^{1}H\}$-NMR spectra, although the signal of the free ligand had often been suppressed by the presence of paramagnetic Co^{II} or Co^{III} complexes. The reaction mixture was transferred into a Schlenk flask and all volatiles were removed under reduced pressure. ATR-IR measurements of the obtained solid gave first information about the formed species. Dicarbonyl complexes could usually be separated from the other species via extraction with *n*-pentane. Further characterization was realized by means of NMR, ATR-IR, HR-MS and single crystal XRD measurements. Single crystals were obtained by slow evaporation of the solvent from a solution of the respective complex or by slow gas diffusion of a non-solvent (*n*-pentane) into a solution of the complex in THF.

2.4. Solvothermalreactions with PCP^{NH} ligands

All PCP^{NH} ligands showed moderate to no solubility in MeCN at ambient conditions. This was more prominent with the PCP^{NH}-*t*Bu ligands, since the colorless solid dissolved only in the course of the reaction. With increasing conversion, the color of the mixture changed from the yellow-red to brown or green.

PCP^{NH}-*i*Pr-X (X = Br, Cl) ligands:

When heating up a mixture of PCP^{NH}-*i*Pr-X (**3:** X = Br, **7:** X = Cl) and $Co_2(CO)_8$ in MeCN in a sealed microwave vial to 110 °C for 20 h, a mixture of two species was obtained, [Co^{I}(PCP^{NH}-*i*Pr)(CO)$_2$] (**11**) and [Co^{III}(PCP^{NH}-*i*Pr)X$_2$] (**12:** X = Br, **13:** X = Cl) (Scheme 17).

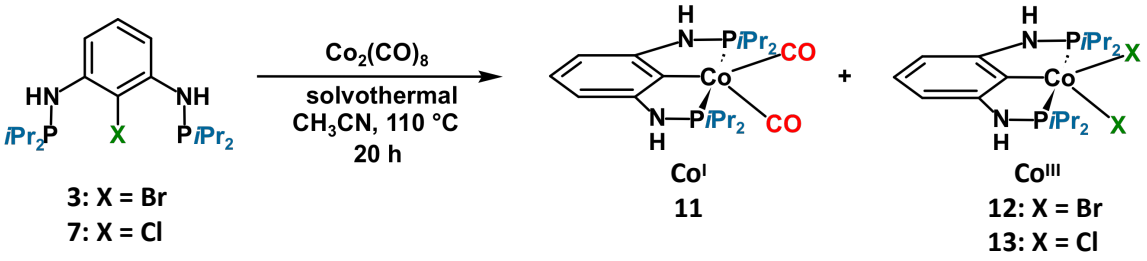

Scheme 17: Solvothermalreactions of PCP^{NH}-*i*Pr-X (X = Cl, Br) with $Co_2(CO)_8$ at 110 °C

The outcome of the reaction did not change upon decreasing the reaction time to 4 h and there was no difference detected between the PCP^{NH}-*i*Pr bearing an *ipso*-bromide (**3**) and an *ipso*-chloride (**4**) in terms of reactivity.

The dicarbonyl complex was separated via extraction with *n*-pentane. ATR-IR measurements of the dicarbonyl species (**11**) displayed two C–O vibrations at 1896 and 1956 cm^{-1} and the structure of the complex could be determined via single crystal XRD measurements. Single crystals were obtained from the slow solvent evaporation of a solution of **11** in *n*-pentane at -20 °C (Figure 14).

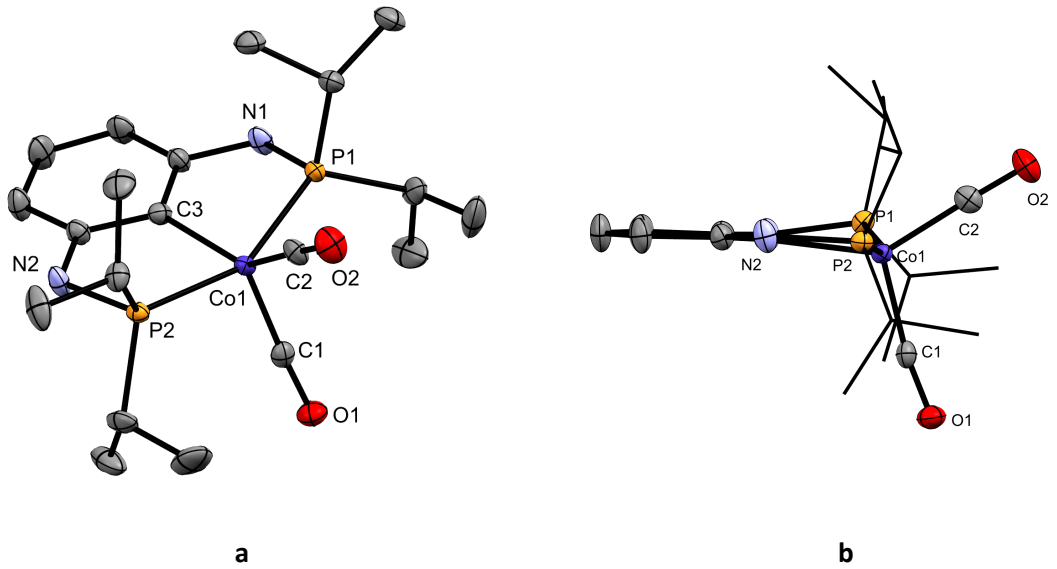

a **b**

Figure 14: ORTEP view of [Co(PCP^{NH}-*i*Pr)(CO)$_2$] (**11**) showing 50 % thermal ellipsoids (H atoms omitted for clarity). Selected bond lengths (Å) and bond angles (deg): Co1-C1 1.783(3), Co1-C2 1.753(3), Co1-P1 2.1803(9), Co1-P2 2.1830(9), Co1-C3 2.022(3), C1-O1 1.158(4), C2-O2 1.150(4), P1-Co1-P2 153.46, C1-Co1-C2 108.32(15), C2-Co1-C3 141.09(14), C1-Co-1-C3 110.59(14)

The solid state structure of **11** reveals the PCP ligand to coordinate in the usual meridional fashion, although there is a slight distortion in the plane formed by the PCP ligand and the metal center due to the steric strain of the bulky *i*Pr-chains of the phosphine donors (Figure 13b). Overall, the complex shows a distorted square pyramidal coordination geometry of the ligands around the cobalt center (τ = 0.21). The C–O distance (in average 1.152 Å) gives information about the degree of backbonding from the Co^{I} center. The NH spacers appear to have little influence on the electronic properties of the cobalt center in comparison to NMe spacer groups, since the similar [Co^{I}(PCP^{NMe}-*i*Pr)(CO)$_2$] exhibits C–O distances of 1.150 Å.[24] The analogous POCOP complex [Co^{I}(POCOP-*i*Pr)(CO)$_2$] **Co9** has average

C–O distances of 1.147 Å , which emphasizes the stronger donor abilities of NR spacers in comparison to O spacers.[22] One broad carbonyl signal at 207.4 ppm was present in the $^{13}C\{^1H\}$ NMR spectrum of **11**. Due to the broad signal, a J_{CP} coupling constant could not be stated. HR-MS measurements (positive ion ESI) resulted in the detection of the fragment $[Co(PCP^{NH}\text{-}iPr)(CO)]^+$ (m/z = 426.1401 u) which corresponds to $[M\text{-}CO]^+$.

Characterization of the second species was quite unsuccessful, since it seemed to be a paramagnetic species. It has not yet been possible to obtain single crystals for XRD measurements to determine the structure. HR-MS (positive ion ESI) measurements showed the fragment $[Co(PCP^{NH}\text{-}iPr)]^+$ (m/z = 399.1528 u) which corresponds to $[M\text{-}2Br]^+$ and results from the loss of two bromide ligands. To verify the existence of the dihalide species, the residue from the *n*-pentane extraction was dissolved in MeCN-d_3 and excess $AgBF_4$ was added, whereupon an instantaneous color change was observed from a greenish blue to an intensive pink-purple. The separation of the solution from the AgX (X = Br, Cl) was accomplished via filtration through a syringe filter. NMR measurements displayed a singlet at 106.5 ppm in the $^{31}P\{^1H\}$-spectra. Since a octahedral diamagnetic cobalt species $[Co^{III}(PCP^{NH}\text{-}iPr)(CH_3CN)_3](BF_4)_2$ (**14**) could only result from a Co^{III} halide, the existence of $[Co^{III}(PCP^{NH}\text{-}iPr)X_2]$ was therefore demonstrated (Scheme 18). **14** was characterized by its resonances in ^1H- and $^{31}P\{^1H\}$-NMR spectra, which are in agreement with the similar $[Co^{III}(PCP^{NH}iPr)(CH_3CN)_3](BF_4)_2$.[24]

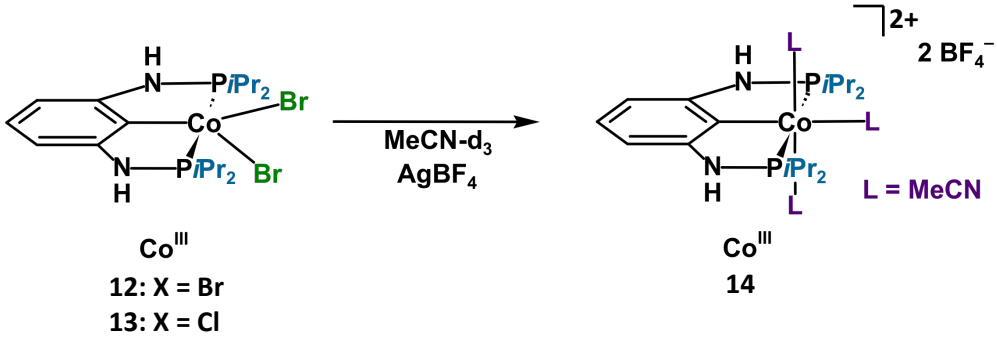

Scheme 18: Halide abstraction from Co^{III} dihalides with $AgBF_4$ in MeCN-d_3

When heating a mixture of PCP^{NH}-*i*Pr-Br (**3**) and $Co_2(CO)_8$ in MeCN in a sealed microwave vial to 130 °C for 20 h, no dicarbonyl species was afforded. ATR-IR measurements of the crude reaction mixture displayed one major C–O vibration and one minor one. Unlike the reaction at 110 °C, it seemed that only one species had formed. In both the extracted layer as well as the residue, the same monocarbonyl species was detected, which featured a C–O vibration at 1963.0 cm^{-1} and a weak band at 1903.6 cm^{-1}. This weaker vibration could result from traces of a side product (Figure 15).

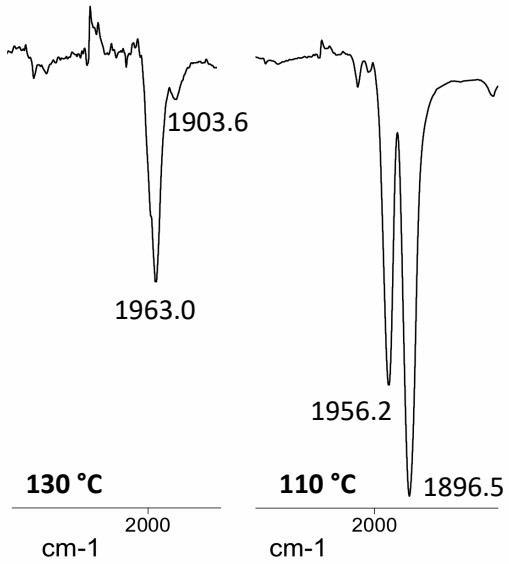

Figure 15: Selected part of the ATR-IR spectra (C–O region) from the solvothermalreaction of PCP^{NH}-*i*Pr-Br with $Co_2(CO)_8$ at 130 and 110 °C

The monocarbonyl species had a similar C–O vibration like other reported Co^{II} PCP complexes featuring one carbonyl ligand as well as one halide ligand (Scheme 19).[24,25] Hence, it appears that at higher temperatures, [Co^{II}(PCP^{NH}-*i*Pr)X(CO)] (**15:** X = Br, **16:** X = Cl) is the main species formed in the reaction. It was not possible to obtain single crystals for structure determination via XRD.

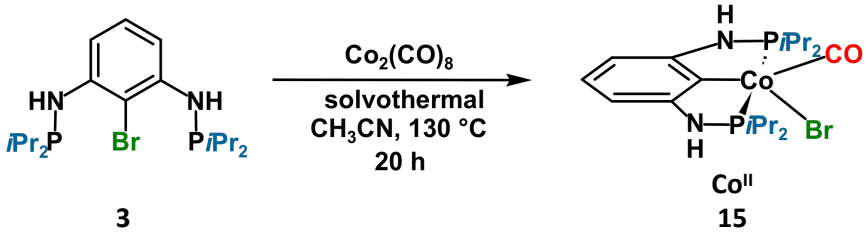

Scheme 19: Solvothermalreactions of PCP^{NH}-*i*Pr-Br (**3**) with $Co_2(CO)_8$ at 130 °C

When performing the reaction with PCP^{NH}-*i*Pr-Cl (**7**) at 130 °C for 20 h, the dicarbonyl species (**11**) was still detected like when stirring at 110 °C for 20 h. The reason for the different behavior of PCP^{NH}-*i*Pr-Br (**3**) at 130 °C to **7** is unclear. The main difference of **3** is the lower bond enthalpy of the *ipso* C–Br bond. Thus oxidative addition is facilitated over cleavage of C–Cl and the monocarbonyl species (**15**) is kinetically favored over the dicarbonyl species.

PCP^{NH}-*t*Bu-X (X = Br, Cl) ligands:

When heating up a mixture of PCP^{NH}-*t*Bu-X (**4:** X = Br, **8:** X = Cl) and $Co_2(CO)_8$ in MeCN in a sealed microwave vial to 110 °C for 20 h, a mixture of three species, [Co^{I}(PCP^{NH}-*t*Bu)$(CO)_2$] (**16**), [Co^{I}PCP^{NH}-*t*Bu)(CO)] (**17**) and [Co^{III}(PCP^{NH}-*t*Bu)X_2] (**18:** X = Br, **19:** X = Cl), was afforded (Scheme 20).

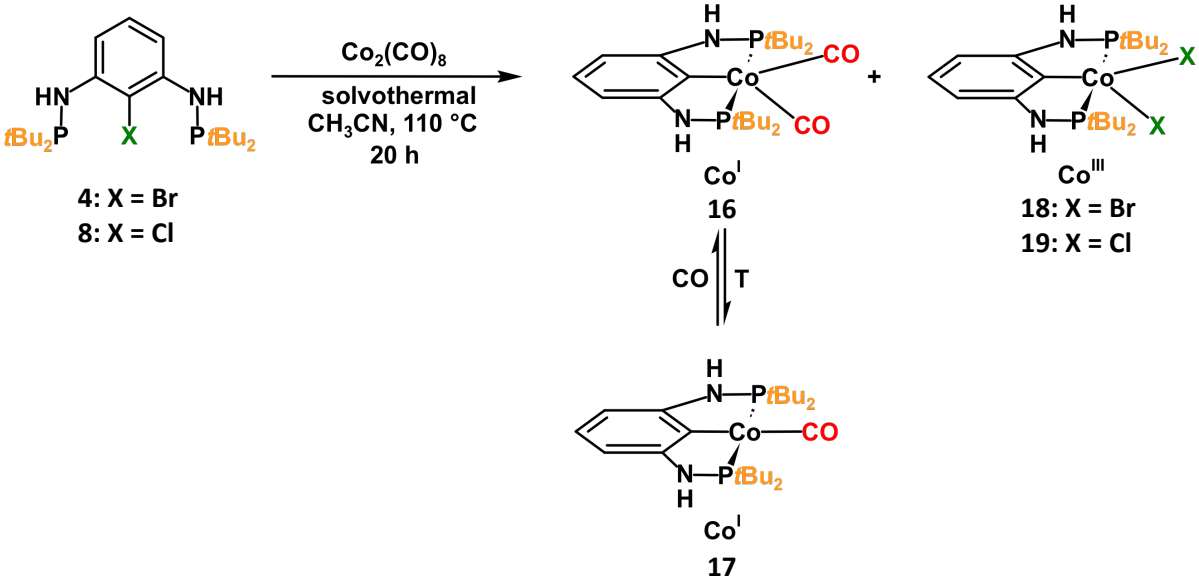

Scheme 20: Solvothermalreaction with PCP^{NH}-*t*Bu-X (X = Br, Cl) with $Co_2(CO)_8$ at 110 °C

Much like with the PCP^{NH}-*i*Pr-X system, a disproportionation to two cobalt species was observed. Additionally, the dicarbonyl species (**16**) appeared to be unstable at higher temperatures. Hence, under solvothermal conditions an equilibrium between the dicarbonyl species (**16**) and the monocarbonyl species (**17**) was perceived. The situation seemed to be similar to the cobalt POCOP system, which was reported by Heinekey *et. al*.[25]

Whereas the dicarbonyl species (**16**) displayed a singlet in the $^{31}P\{^{1}H\}$-NMR spectra at 170.0 ppm, it was rather unstable, even after isolation. Hence, no pure ^{1}H and $^{13}C\{^{1}H\}$ NMR spectra of substance **16** could be obtained. After ATR-IR measurements showed C–O vibrations at 1957.8 and 1902.8 cm^{-1}, the color of the orange-red solid changed to brown, whereupon another ATR-IR no longer displayed any carbonyl vibrations. The monocarbonyl species (**17**) could be detected from the crude reaction mixture along the dicarbonyl species and in the *n*-pentane extracted residue with a C–O vibration at 1853.2 cm^{-1} (Figure 16). **17**, unlike **16**, was rather insoluble in *n*-pentane, which is why it was not possible to separate it from the dihalide species and neither yields nor spectra could be obtained.

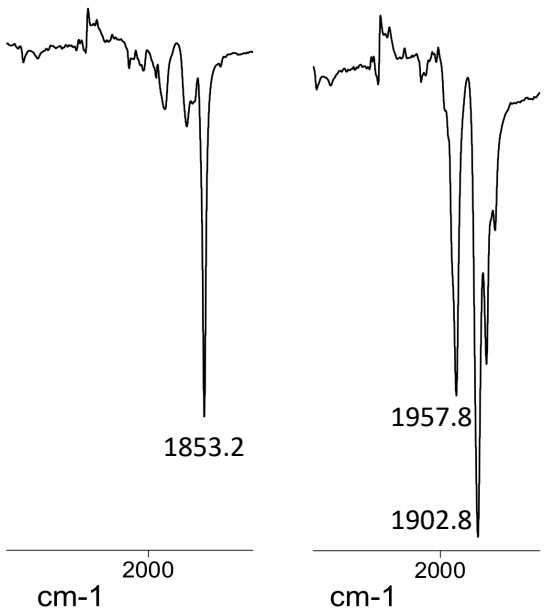

Figure 16: Selected part of the ATR-IR spectra (C–O region) of the residue (left) and *n*-pentane soluble layer (right) of the reaction of PCP^{NH}-*t*Bu-X (X = Br, Cl) with $Co_2(CO)_8$ at 110 °C

However, the C–O vibration of the monocarbonyl species was not consistent with reported $[Co^{II}(PCP)X(CO)]$ complexes, since these show the vibration at a range between 1940-1990 cm^{-1} (Figure 16).[24,25] Although the C–O vibration was not in agreement with the $[Co^{II}(PCP)Cl(CO)]$, it was in the range of the $[Co^{I}(PCP)(CO)]$, as Heinekey and coworkers reported the similar Co^{I} POCOP complex with a C–O stretching mode at 1899 cm^{-1}.[24] Since PCP complexes with N–R spacers are better donor ligands than ones containing O, the C–O vibration is expected at a lower wavenumber.[27]

The dihalide species (**18**, **19**) were detected in a similar manner like the PCP^{NH}-*i*Pr-X system. After adding $AgBF_4$ in MeCN-d_3, a diamagnetic dicationic complex $[Co^{III}(PCP^{NH}\text{-}Bu)(CH_3CN)_3](BF_4)_2$ (**20**) was obtained. Unlike the analogous *i*Pr-containing complex, the NMR spectra showed three resonances, which most likely resulted from side reactions of the dicarbonyl species (**17**) with the halogen scavenger. As a result, no pure ^{1}H-NMR spectra could be given (Scheme 21).

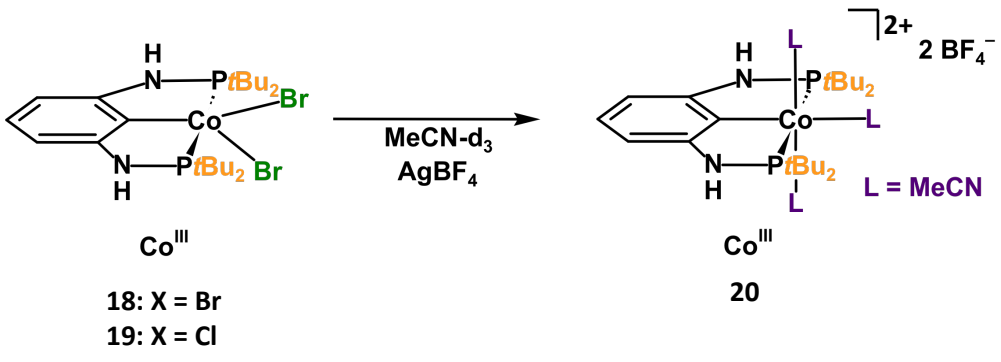

Scheme 21: Halide abstraction from a Co^{III} dihalide with $AgBF_4$ in MeCN-d_3

Intriguingly, when decreasing the reaction time to 4 h, only the monocarbonyl species was observed for the PCP^{NH}-*t*Bu-Cl ligand (**8**). In the case of the analogous bromide bearing ligand (**4**), both the mono- and dicarbonyl species are detected via ATR-IR measurements. As a result, the weaker C–Br bond in comparison to the C–Cl bond appeared to accelerate the progress of the reaction in regard to oxidative addition. According to Heinekey, the decay of the dicarbonyl species to the monocarbonyl species was observed at temperatures of 70 °C or higher with the analogous Co POCOP system. Under exposure to CO gas (p = 1 atm), the dicarbonyl species can be restored.[25]

Concluding from the findings, it appeared that at higher temperatures, the monocarbonyl species for the PCP-*t*Bu systems were thermodynamically more stable than their dicarbonyl counterparts. When the reaction was performed in a sealed microwave vial, the precursor $Co_2(CO)_8$ gradually lost CO until the active species was able to accomplish the oxidative addition of the PCP ligand. Consequently, the CO partial pressure in the closed system increased. At short reaction times, i. e. lower conversion, the CO partial pressure was too low to stabilize the, at high temperatures, unfavored dicarbonyl species and only the monocarbonyl species was isolated. Since the PCP^{NH}-*t*Bu-Br (**4**) appeared to react faster, a higher CO partial pressure had built up at 4 h reaction time compared to PCP^{NH}-*t*Bu-Cl (**8**). As a result, both carbonyl species were detected when performing the reaction with **4** as the amount of free CO seemed to partially stabilize the presence of the dicarbonyl species (**16**).

When performing the same reaction at 130 °C, no carbonyl species was observed at all. The oxidative addition was achieved forming the square planar cobalt complex [Co^{II}(PCP^{NH}-*t*Bu)X] (**21:** X = Br, **22:** X = Cl) (Scheme 22).

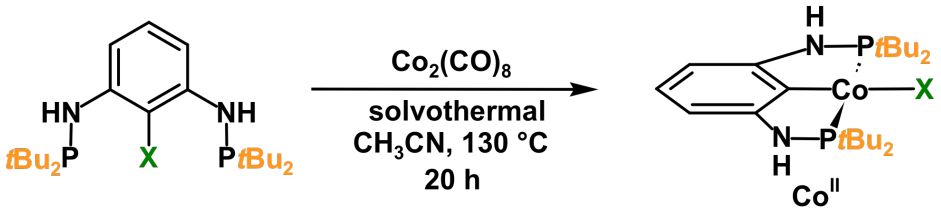

4: X = Br
8: X = Cl

21: X = Br
22: X = Cl

Scheme 22: Solvothermalreaction of PCP^{NH}-*t*Bu-X (X = Br, Cl) with $Co_2(CO)_8$ at 130 °C

In HR-MS measurements (positive ion ESI) of **22**, the fragment [Co(PCP^{NH}-*t*Bu)]$^+$ (m/z = 454.2079 u) which corresponds [M-Cl]$^+$ was detected.

The structure of **21** was confirmed via single crystal XRD measurements. Single crystals were obtained from the slow evaporation of the solvent from a solution of the complex in *n*-pentane (Figure 17).
The solid state structure of **21** displays the PCP pincer ligand coordinating in a meridional coordination mode and constitutes a plane with Co1 and Br1. The complex features a square planar geometry around the metal center and slight distortions at the phosphine donors occur due to the steric strain of the *t*-butyl groups. The plane formed by the benzene ring and the NH spacers indicates strong π-interaction between the lone pair of the nitrogen atom and the electron density of the aromatic system. The bond lengths and angles are in agreement with the similar square planar [Co(POCOP-*t*Bu)I] **Co3**, which was reported by Heinekey and coworkers.[20]

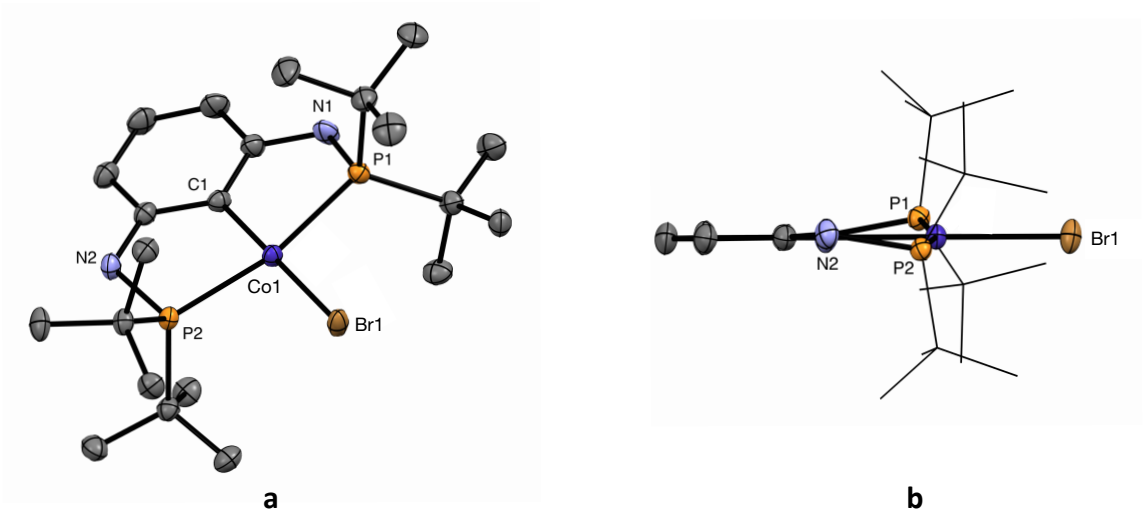

Figure 17: ORTEP view of [Co(PCP^{NH}-*t*Bu)Br] (**21**) showing 50 % thermal ellipsoids (H atoms and solvent omitted for clarity). Selected bond lengths (Å) and bond angles (deg): Co1-Br1 2.3686(3), Co1-P1 2.2395(4), Co1-P2 2.2332(4), Co1-C1 1.9301(15), C1-Co1-Br1 179.87(5), P1-Co1-P2 165.219(17)

When exposing the 15-electron complex **21** to nitric oxide (NO) in CH_2Cl_2, a mixture of two nitrosyl complexes was obtained, [Co^{I}(PCP^{NH}-*t*Bu)(NO)]Br (**23**) and [Co^{III}(PCP^{NH}-*t*Bu)Br(NO)] (**24**) (Scheme 23).

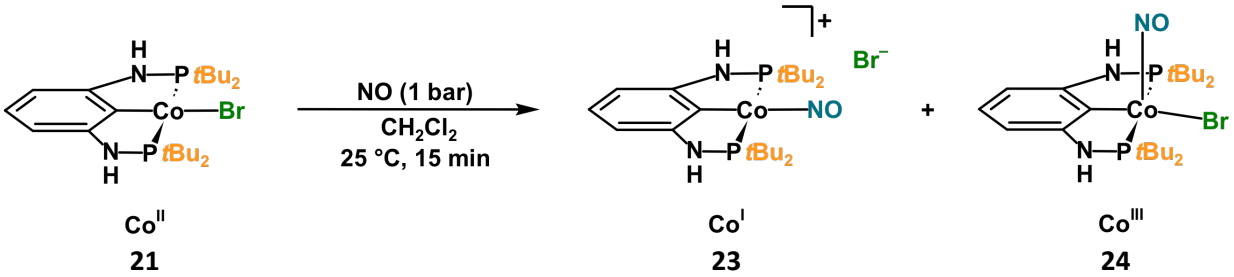

Scheme 23: Exposing [Co(PCP^{NH}-*t*Bu)Br] (**21**) to nitric oxide (NO) at 25 °C

After the exposure of the orange-red complex [Co(PCP^{NH}-*t*Bu)Br] (**21**) to NO, the solution in CH_2Cl_2 turned deep red. ATR-IR measurements displayed two N–O vibrations indicating a mixture of two nitrosyl complexes. The vibration at 1803.3 cm^{-1} corresponds to a linear coordination, formally NO^{+} (**23**) and the vibration at 1651.1 cm^{-1} correlates with NO^{-} in a bent coordination mode (**24**) (Figure 18).[27]

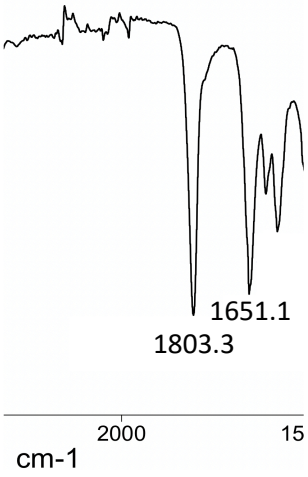

Figure 18: Selected part of the ATR-IR spectra (N–O region) of the deep red solid obtained from the reaction of **21** with nitric oxide (NO)

A $^{31}P\{^{1}H\}$-NMR spectrum displayed two resonances for each nitrosyl complex along resonances of decay products, a singlet at 156.8 ppm (**23**) and one at 131.2 ppm (**24**). Unlike the recently published *i*Pr-systems reported by Kirchner and coworkers, two coordination modes were observed after exposing **21** to NO. Cobalt PCP-*i*Pr systems selectively formed the bent coordination mode, affording Co^{III} complexes. Further halide abstraction by halogen scavengers ($AgBF_4$ or $TlPF_6$) resulted in the formation of the cationic Co^{I} species with NO in a linear binding mode.[27] With the *t*Bu-system, a direct pathway to the cationic Co^{I} nitrosyl complex was possible. The steric demand of the bulky *t*Bu-groups appeared to be the driving force for the direct dissociation of the bromide, whereupon the cationic Co^{I} complex (**23**) was formed in one step. However, the estimation of the ratio between **23**:**24** according to $^{31}P\{^{1}H\}$-NMR suggested a distribution of 1:5. Hence, the five-fold coordinated nitrosyl complex [Co^{III}(PCP^{NH}-*t*Bu)Br(NO)] (**24**) was the main product after exposure to nitric oxide (NO) gas.

2.5. Solvothermalreactions with PCP^{CH_2}-*t*Bu-Br

When heating up a mixture of PCP^{CH_2}-*t*Bu-Br (**10**) and $Co_2(CO)_8$ in MeCN to 110 °C for 20 h in a sealed microwave vial, two species were formed, [Co(PCP^{CH_2}-*t*Bu)$(CO)_2$] (**24**) and [Co(PCP^{CH_2}-*t*Bu)Br_2] (**25**) (Scheme 24).

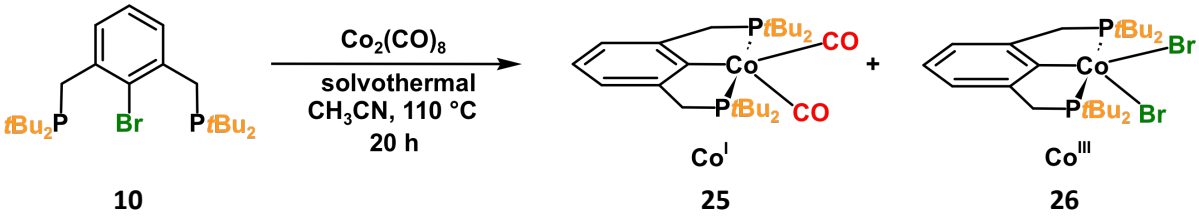

Scheme 24: Solvothermalreaction of PCP^{CH_2}-*t*Bu-Br with $Co_2(CO)_8$ at 110 °C

25 displayed two C–O vibrations in the ATR-IR spectra at 1962.2 and 1904.5 cm^{-1}. The measurement of a $^{13}C\{^{1}H\}$-NMR spectrum was futile, since the dicarbonyl complex appeared to be rather unstable in solution and the decay to free and to decomposed ligand was observed in $^{31}P\{^{1}H\}$ as well as ^{1}H spectra. The fragment Co(PCP^{CH_2}-*t*Bu)$(CO)]^+$ (m/z = 480.2116 u), which corresponds to $[M\text{-}CO]^+$, was detected in HR-MS measurements (positive ion ESI).
Unlike the similar PCP^{NH}-*t*Bu system, the formation of a monocarbonyl species [Co(PCP^{CH_2}-*t*Bu)(CO)] was not observed at all with the CH_2-spacer groups. Perhaps due to the higher degree of flexibility of the PCP^{CH_2} scaffold, caused by the sp^3 hybridization of the CH_2 carbon and the absence of π-cloud interaction with the aromatic system, the formation of the dicarbonyl species is more favorable than with the PCP^{NH}-*t*Bu scaffold.

In a similar manner to the PCP^{NH} system, the existence of the dihalide species (**26**) was proven via halide abstraction by adding $AgSbF_6$ to a solution of the green compound **26** in MeCN-d_3. Upon adding $AgSbF_6$, the color of the suspension changed from green to beige-brown, affording the complex [Co^{III}(PCP^{CH_2}-*t*Bu)$(CH_3CN)_3$]$(SbF_6)_2$ (**27**). After filtration through a syringe filter, NMR measurements of the solution displayed a single resonance at 68.9 ppm in the $^{31}P\{^{1}H\}$-NMR spectra (Scheme 25).

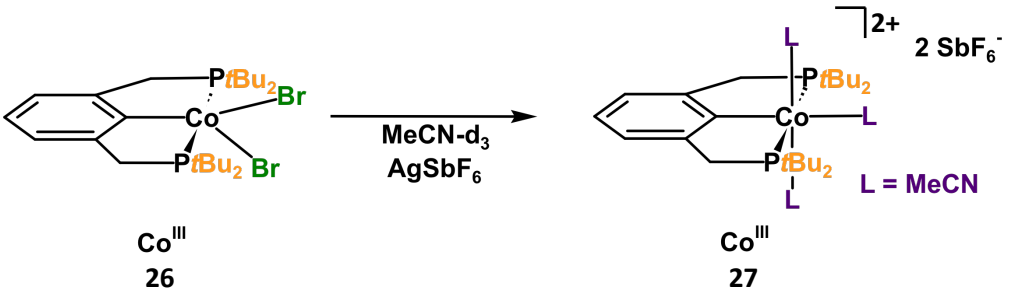

Scheme 25: Bromide abstraction from [Co(PCP^{CH_2}-*t*Bu)Br_2] (**26**) with $AgSbF_6$ in MeCN-d_3

Additionally, HR-MS measurement displayed the fragment $[Co(PCP^{CH_2}\text{-}t\text{Bu})]^+$ (m/z = 452.2157) which corresponds to $[M\text{-}2Br]^+$.

Unlike the similar PCP^{NH}-*t*Bu system, no change in the outcome of the reaction was observed when the reaction temperature was increased to 130 °C instead of 110 °C. Furthermore, there were no differences upon stopping the reaction after 4 h. Hence, it appeared that the solvothermalreaction with PCP^{CH_2} system was overall faster than with the PCP^{NH} systems, since a color change of the reaction mixture was observed before even heating up to the reaction temperature. After less than 15 minutes of heating and stirring, the reaction mixture turned green. No further color change was observed after prolonged heating of the reaction mixture.

3. Experimental part

3.1. General considerations

If not stated otherwise, all manipulations were performed under an inert atmosphere of argon by using Schlenk techniques or an MBraun inert-gas glovebox. The solvents were purified according to standard procedures.[39] The deuterated solvents were purchased by Aldrich and dried over 3 Å molecular sieves. All starting materials are known compounds and were used as obtained from commercial suppliers. The nitric oxide (NO) gas was purchased from Messer (Austria) with a 10 Vol% concentration and the rest being N_2. ^{1}H-, ^{13}C{^{1}H}- and ^{31}P{^{1}H}-NMR spectra were recorded on Bruker AVANCE-250, AVANCE-400 and AVANCE-600 spectrometers. ^{1}H- and ^{13}C{^{1}H}-NMR spectra were referenced internally to residual protio-solvent and solvent resonances, respectively, and are reported relative to tetramethylsilane (δ = 0 ppm). ^{31}P{^{1}H}-NMR spectra were referenced externally to H_3PO_4 (85 %) (δ = 0 ppm). High resolution-accurate mass spectra were recorded on a hybrid Maxis Qq-aoTOF mass spectrometer (Bruker Daltonics, Bremen, Germany) fitted with an ESI-source. Measured accurate mass data of the $[M]^+$ ions for confirming calculated elemental compositions were typically within 5 ppm accuracy. The mass calibration was done with a commercial mixture of perfluorinated trialkyl-triazines (ES Tuning Mix, Agilent Technologies, Santa Clara, CA, USA). All IR measurements were performed on a Bruker Tensor 27 with an ATR unit. Single crystals suitable for the X-ray studies were selected under a polarizing microscope and measured on a Bruker SMART-CCD area diffractometer system with a Mo-K_α-radiation and a graphite monochromator. The data were processed with the SADABS[40] algorithm and the crystal structures were solved and refined with the SHELXTL[41] software suite. Aluminum-capped 10 mL microwave vials from Biotage were used for the solvothermal reactions as reaction vessels.

3.2. Synthesis of PCP^{NH} ligands

Synthesis of 2-bromo-1,3-dinitrobenzene (**1**)

H_2SO_4 (96 %, 30 mL) was placed in a 250 mL three-necked round flask and $NaNO_2$ (2.10 g, 30.0 mmol) was added in portions under cooling with an ice bath. After complete addition, the temperature was raised to 70 °C until all $NaNO_2$ had dissolved.
The mixture was cooled to room temperature and a solution of 2,6-dinitroaniline (98 %, 5.10 g, 27.3 mmol) in hot conc. acetic acid (100 %, 60 mL) was added in portions to avoid the reaction mixture's temperature to exceed 40 °C. To complete the formation of the diazonium salt, the mixture was stirred at 40 °C for 30 min.
Meanwhile, CuBr (8.69 g, 60.2 mmol) was dissolved in hydrobromic acid (48 %, 120 mL) in an Erlenmeyer flask and the resulting solution was cooled with an ice bath.
The diazonium mixture was added to the CuBr-solution in portions. After the bubbling had slackened, the mixture was heated to 80 °C for 20 min. The mixture was poured onto H_2O dest. (250 mL) and was cooled with an ice bath, which resulted in the formation of a yellow-brown precipitate. The solid was filtered off and washed with H_2O dest. After drying of the solid, 5.87 g (87 %) of **1** was obtained as a yellow powder. **1** was used without further purification.
^{1}H-NMR (250 MHz, CD_2Cl_2, 20 °C, ppm): δ = 7.94 (d, J = 9.4 Hz, 2H, CH), 7.67 (t, J = 8.3 Hz, 1H, CH).

Synthesis of 2-bromobenzen-1,3-diamine (**2**)

To a 100 mL one-necked round flask were added **1** (1.50 g, 6.1 mmol), iron powder (3.37 g, 60.3 mmol) and a solvent mixture of ethanol/acetic acid/water (40 mL, 2:2:1).
The flask was exposed to ultrasonic irradiation for 1 h, resulting in a brown suspension. NaOH solution (2 M, 100 mL) was added to the mixture and the formed dark-brown precipitate was filtered through a pad of celite and the residue was washed with ethyl acetate. The filtrate was extracted with ethyl acetate and the combined organic layers were dried over anhydrous Na_2SO_4. All volatiles were removed under reduced pressure, whereupon a yellow solid was formed. The solid was redissolved in

ethyl acetate (20 mL) and after adding 2 spatula of activated carbon, the suspension was stirred for 10 min at room temperature.
After the filtration through a pad of silica, all volatiles were removed under reduced pressure and the yellow solid was recrystallized from a n-heptane/CH_3Cl-mixture resulting in the isolation of 0.45 g (40 %) of **2** as colorless needles.
^{1}H-NMR (400 MHz, CD_2Cl_2, 20 °C, ppm): δ = 6.87 (t, J = 8.0 Hz, 1H, CH), 6.18 (d, J = 7.8 Hz, 2H, CH), 4.07 (s, broad, 4H, NH_2).

Synthesis of 2-bromo-N,N'-bis[di(isopropyl)phosphino]-1,3-benzendiamine (PCP^{NH}-*i*Pr-Br) (**3**)

2 (0.403 g, 2.2 mmol) and DIPEA (1.106 g, 8.6 mmol) were added to a Schlenk flask and dissolved in toluene (10 mL). Chlorodi(isopropyl)phosphine (96 %, 0.697 g, 4.4 mmol) was dissolved in toluene (8 mL) and added dropwise to the reaction mixture while cooling with an ice bath, whereupon the mixture turned opaque. After complete addition, the mixture was stirred at 100 °C for 3 days. The reaction mixture was reduced to 10 mL and was filtered through a pad of celite. All volatiles were removed under reduced pressure resulting in the formation of an off-white viscous liquid. The oil was redissolved in *n*-pentane and filtered through a pad of silica. After removing all volatiles, **3** was obtained as a colorless oil with a yield of 0.703 g (78 %).
^{1}H-NMR (400 MHz, CD_2Cl_2, 20 °C, ppm): δ = 6.97 (d, J = 8.2 Hz, 1H, CH), 6.81 (m, 2H, CH), 4.42 (d, J = 10.2 Hz, 2H, N-H), 1.82 (m, 4H, C*H*$(CH_3)_2$), 1.11 (m, 24H, CH(C*H*$_3)_2$).
^{31}P{^{1}H}-NMR (162 MHz, CD_2Cl_2, 20 °C, ppm): δ = 50.7 (s, P).
^{13}C{^{1}H}-NMR (101 MHz, CD_2Cl_2, 20 °C, ppm): δ = 147.2 (d, J = 17.3 Hz, C-N), 128.2 (s, CH), 106.7 (d, J = 23.3 Hz, CH), 103.0 (s, C-Br), 27.3 (d, J = 12.3 Hz, P-CH), 19.2 (d, J = 20.3 Hz, CH(*C*$H_3)_2$), 17.5 (d, J = 7.7 Hz, CH(*C*$H_3)_2$).
HR-MS (ESI$^+$, CH_3CN/MeOH + 1 % H_2O): m/z calcd for $C_{18}H_{33}BrN_2P_2$ $[M+H]^+$ 419.1375, found 419.1375.

Synthesis of 2-bromo-N,N'-bis[di(tertbutyl)phosphino]-1,3-benzendiamine (PCP^{NH}-*t*Bu-Br) (**4**)

2 (0.42 g, 2.2 mmol) and DIPEA (0.58 g, 4.5 mmol) were added to a Schlenk flask and dissolved in toluene (10 mL). Chlorodi(tertbutyl)phosphine (96 %, 0.866 g, 4.6 mmol) was added dropwise while cooling with an ice bath. Then NaH (116 mg, 4.8 mmol), dissolved in THF (10 mL), was transferred into the Schlenk flask and the mixture was stirred at 80 °C for 24 h.
All volatiles were removed under reduced pressure resulting in the formation of a beige solid which was redissolved in *n*-pentane, filtered through a pad of silica and washed with *n*-pentane. After removing all volatiles under reduced pressure at 80 °C, **4** was afforded as a colorless solid with a yield of 0.586 g (56 %).
^{1}H-NMR (400 MHz, CD_2Cl_2, 20 °C, ppm): δ = 6.94 (t, J = 8.1 Hz, 1H, CH), 6.79 (dd, J = 8.1, 3.5 Hz, 2H, CH), 4.75 (d, J = 10.1 Hz, 2H, N-H), 1.15 (d, J = 11.8 Hz, 36 H, C(C*H*$_3)_3$).
^{31}P{^{1}H}-NMR (162 MHz, CD_2Cl_2, 20 °C, ppm): δ = 60.5 (s, P).
^{13}C{^{1}H}-NMR (101 MHz, CD_2Cl_2, 20 °C, ppm): δ = 147.4 (d, J = 17.8 Hz, C-N), 128.1 (s, CH), 106.7 (d, J = 23.3 Hz, CH), 102.6 (s, C-Br), 34.7 (d, J = 20.2 Hz, *C*$(CH_3)_3$), 28.4 (d, J = 15.2 Hz, C(*C*$H_3)_3$).

Synthesis of 2-chloro-1,3-dinitrobenzene (**5**)

H_2SO_4 (96 %, 30 mL) was placed in a 250 mL three-necked round flask and $NaNO_2$ (2.54 g, 36.8 mmol) was added in portions under cooling with an ice bath. After complete addition, the temperature was raised to 70 °C until all $NaNO_2$ had dissolved.
The mixture was cooled to room temperature and a solution of 2,6-dinitroaniline (98 %, 6.11 g, 32.7 mmol) in hot conc. acetic acid (100 %, 70 mL) was added in portions to avoid the reaction mixture's temperature to exceed 40 °C. To complete the formation of the diazonium salt, the mixture was stirred at 40 °C for 30 min.
Meanwhile, CuCl (7.35 g, 74.2 mmol) was dissolved in hydrochloric acid (37 %, 70 mL) in an Erlenmeyer flask and the resulting solution was cooled with an ice bath.
The diazonium mixture was added to the CuCl-solution in portions. After the bubbling had slackened, the mixture was heated to 80 °C for 20 min. The mixture was poured onto H_2O dest. (160 mL) and was cooled with an ice bath, which resulted in the formation of a yellow precipitate. The solid was

filtered off and washed with H_2O dest. After drying of the solid, 6.25 g (93 %) of **5** was obtained as a yellow powder. **5** was used without further purification.

Synthesis of 2-chlorobenzen-1,3-diamine (**6**)

To a 250 mL one-necked round flask were added **5** (6.25 g, 30.9 mmol), iron powder (17.15 g, 308.6 mmol) and a solvent mixture of ethanol/acetic acid/water (80 mL, 2:2:1).
The flask was exposed to ultrasonic irradiation for 1 h resulting in the formation of a red-brown suspension. NaOH solution (6 M, 80 mL) was added, whereupon a dark brown-black precipitate was formed. The suspension was filtered off through a pad of celite and the residue was washed with ethyl acetate.
The filtrate was extracted with ethyl acetate and the combined organic layers were dried over Na_2SO_4. All volatiles were removed under reduced pressure, whereupon an orange solid was formed. The solid was redissolved in ethyl acetate (20 mL) and after adding 2 spatula of activated carbon, the suspension was stirred for 10 min at room temperature.
After the filtration through a pad of silica, all volatiles were removed under reduced pressure and the orange solid was recrystallized from a *n*-heptane/CH_3Cl resulting in the isolation of 1.84 g (42 %) of **6** as colorless needles.
^{1}H-NMR (250 MHz, DMSO-d_6, 20 °C, ppm): δ = 6.68 (t, J = 7.9 Hz, 1H, CH), 6.02 (d, J = 7.9 Hz, 2H, CH), 5.00 (s, broad, 4H, -NH_2).

Synthesis of 2-chloro-N,N‘-bis[di(isopropyl)phosphino]-1,3-benzendiamine (PCP^{NH}-*i*Pr-Cl) (**7**)

6 (0,50 g, 3.5 mmol) and DIPEA (1,11 g, 8.6 mmol) were added to a Schlenk flask and dissolved in toluene (10 mL). Chlorodi(isopropyl)phosphine (96 %, 1,381 g, 9.0 mmol) was dissolved in toluene (8 mL) and added dropwise to the reaction mixture while cooling with an ice bath, whereupon the mixture turned opaque. After complete addition, the mixture was stirred at 80 °C for 6 days.
The reaction mixture was reduced to 10 mL and filtered through a pad of celite. All volatiles were removed under reduced pressure resulting in the formation of a off-white viscous liquid. The oil was redissolved in *n*-pentane and filtered through a pad of silica. After removing all volatiles, **7** was obtained as a colorless oil with a yield of 1.06 g (80 %).
^{1}H-NMR (600 MHz, CD_2Cl_2, 20 °C, ppm): δ = 6.82 (t, J = 8.2 Hz, 1H, CH), 6.69 (dd, J = 8.1, 3.3 Hz, 2H, CH), 4.25 (d, J = 10.3 Hz, 2H, NH), 1.69 (m, 4H, C*H*(CH_3)$_2$), 0.98 (m, 24H, CH(C*H*$_3$)$_2$).
^{31}P{^{1}H}-NMR (243 MHz, CD_2Cl_2, 20 °C, ppm): δ = 50.0 (s, P).
^{13}C{^{1}H}-NMR (151 MHz, CD_2Cl_2, 20 °C, ppm): δ = 146.1 (d, J = 17.3 Hz, C-N), 127.43 (s, CH), 109.1 (s, C-Cl), 106.4 (d, J = 23.0 Hz, CH), 27.3 (d, J = 12.2 Hz, P-CH), 19.2 (d, J = 20.3 Hz, CH(*C*H_3)$_2$), 17.4 (d, J = 7.6 Hz, CH(*C*H_3)$_2$).
HR-MS (ESI$^+$, CH_3CN/MeOH + 1 % H_2O): m/z calcd for $C_{18}H_{33}ClN_2P_2$ $[M+H]^+$ 375.1880, found 375.1885.

Synthesis of 2-chloro-N,N‘-bis[di(tertbutyl)phosphino]-1,3-benzendiamine (PCP^{NH}-*t*Bu-Cl)(**8**)

6 (0.50 g, 3.5 mmol) and DIPEA (0.93 g, 7.2 mmol) were put into a Schlenk flask and dissolved in toluene (15 mL). Chlorodi(terbutyl)phosphine (96 %, 1,301 g, 7.2 mmol) was added dropwise while cooling with an ice bath. Then NaH (181 mg, 7.7 mmol), dissolved in THF (10 mL), was transferred into the Schlenk flask and the mixture was stirred at 80 °C for 24 h.
All volatiles were removed under reduced pressure resulting in the formation of a beige solid which was redissolved in *n*-pentane, filtered through a pad of silica and washed with *n*-pentane. After removing all volatiles under reduced pressure at 80 °C, **8** was afforded as a colorless solid with a yield of 1.048 g (69 %).
^{1}H-NMR (600 MHz, CD_2Cl_2, 20 °C, ppm): δ = 6.91 (t, J = 8.1 Hz, 1H, CH), 6.79 (dd, J = 8.1, 3.5 Hz, 2H, CH), 4.70 (d, J = 10.2 Hz, 2H, NH), 1.14 (d, J = 11.9 Hz, 36H, C(CH_3)$_3$).
^{31}P{^{1}H}-NMR (243 MHz, CD_2Cl_2, 20 °C, ppm): δ = 59.8 (s, P).
^{13}C{^{1}H}-NMR (151 MHz, CD_2Cl_2, 20 °C, ppm): δ = 146.3 (d, J = 18.2 Hz, C-N), 127.41 (s, CH), 108.7 (s, C-Cl), 106.4 (d, J = 22.7 Hz, CH), 34.7 (d, J = 20.3 Hz, *C*(CH_3)$_3$), 28.4 (d, J = 15.4 Hz, C(*C*H_3)$_3$).
HR-MS (ESI$^+$, CH_3CN/MeOH + 1 % H_2O): m/z calcd for $C_{22}H_{41}ClN_2P_2$ $[M+H]^+$ 431.2506, found 431.2512.

3.3. Synthesis of PCP^{CH_2}-*t*Bu-Br

Synthesis of 2-bromo-1,3-(bromomethyl)benzene (**9**)

Into a Schlenk flask were added degassed 2-bromoxylene (20.18 g, 109,0 mmol), N-bromosuccinimide (38.53 g, 216.1 mmol), dibenzoyl peroxide (20 mg, 0.1 mmol) and CCl_4 (200 mL). The reaction mixture was stirred at reflux for 20 h. After 10 h of stirring, another 20 mg of dibenzoyl peroxide were added. The formed succinimide was removed via filtration through a pad of silica and all volatiles were removed under reduced pressure, yielding a pale-yellow solid. The solid was recrystallized form *n*-hexane resulting in the isolation of **9** as colorless needles with a yield of 15.36 g (41 %).
^{1}H-NMR (250 MHz, $CDCl_3$, 20 °C, ppm): δ = 7.48 (d, J = 8.1 Hz, 2H, CH), 7.35 (t, J = 8.1 Hz, 1H, CH), 4.71 (s, 4H, CH_2).

Synthesis of 2-bromophenylen-1,3-dimethylenbis[di(tertbutyl)phosphine] (PCP^{CH_2}-*t*Bu-Br) (**10**)

9 (1.00 g, 2.9 mmol) was put into a Schlenk flask and suspended in methanol (4 mL). Di(tertbutyl)phosphine was added dropwise to the suspension and after complete addition, the mixture was stirred at room temperature for 20 h, whereupon all solid was dissolved. All volatiles were removed under reduced pressure resulting in the formation of a colorless solid
The solid was redissolved in toluene (15 mL) and DIPEA (1.49 g, 11.5 mmol) was added. The mixture was stirred at room temperature for 1.5 h, whereupon the solution turned opaque and a colorless precipitate formed. After the filtration of the suspension through a pad of silica, all volatiles were removed under reduced pressure resulting in the isolation of **10** as a colorless solid with a yield of 1.05 g (76 %).
^{1}H-NMR (400 MHz, CD_2Cl_2, 20 °C, ppm): δ = 7.47 (d, J = 6.5 Hz, 2H, CH), 7.13 (t, J = 7.6 Hz, 1H, CH), 3.07 (d, J = 3.0 Hz, 4H, CH_2), 1.13 (d, J = 10.8 Hz, 36H, $C(CH_3)_3$).
^{31}P{^{1}H}-NMR (162 MHz, CD_2Cl_2, 20 °C, ppm): δ = 34.4 (s, P).
^{13}C{^{1}H}-NMR (101 MHz, CD_2Cl_2, 20 °C, ppm): δ = 142.1 (d, J = 12.2 Hz, *C*-CH_2), 130.0 (dd, J = 17.3, 2.0 Hz, CH), 128.4 (t, 3.4 Hz, C-Br), 126.5 (s, CH), 32.5 (d, J = 23.0 Hz, *C*$(CH_3)_3$), 30.1 (d, 13.4 Hz, C(*C*$H_3)_3$), 29.8 (d, J = 23.9, CH_2).
HR-MS (ESI^+, CH_3CN/MeOH + 1 % H_2O): m/z calcd for $C_{24}H_{43}BrP_2$ $[M+H]^+$ 473.2096, found 472.2087.

3.4. Solvothermalreactions with PCP^{NH}-*i*Pr ligands

Synthesis of [Co(PCP^{NH}-*i*Pr)$(CO)_2$](**11**)

A solution of **3** or **7** (50 mg, 0.12 mmol) and $Co_2(CO)_8$ (22 mg, 0.07 mmol) in MeCN (4 mL) was put into a microwave vial and stirred at 110 °C for 20 h, whereupon the color of the reaction mixture changed from orange-red to green. The mixture was transferred into a Schlenk flask and all volatiles were removed under reduced pressure. The obtained residue was extracted with *n*-pentane and filtered through a syringe filter (PTFE, 0.2 µm). After removing all volatiles under reduced pressure, the product could be isolated as a yellow solid with a yield of 23 mg (43 %). Single crystals were obtained from the slow evaporation of the solvent from a saturated solution of **11** in *n*-pentane at -20 °C.
^{1}H-NMR (600 MHz, CD_2Cl_2, 20 °C, ppm): δ = 6.54 (t, J = 7.6 Hz, 1H, CH), 6.03 (d, J = 7.6 Hz, 2H, CH), 4.18 (s, 2H, NH), 2.33 (m, 4H, C*H*$(CH_3)_2$), 1.23 (m, 24H, CH(C*H*$_3)_2$).
^{31}P{^{1}H}-NMR (243 MHz, CD_2Cl_2, 20 °C, ppm): δ = 158.5 (s, P).
^{13}C{^{1}H}-NMR (151 MHz, CD_2Cl_2, 20 °C, ppm): δ = 207.4 (s, CO), 155.7 (t, J = 12.9 Hz, C-N), 133.1 (t, J = 17.9 Hz, C_{ipso}), 124.1 (s, CH), 100.6 (t, J = 7.0 Hz, CH), 31.5 (t, J = 12.9 Hz, *C*H$(CH_3)_2$), 18.0 (d, J = 92.7 Hz, CH(*C*$H_3)_2$).
IR (ATR, cm^{-1}): 1896 (ν_{CO}), 1956 (ν_{CO}).
HR-MS (ESI^+, CH_3CN/MeOH + 1 % H_2O): m/z calcd for $C_{25}H_{43}OCoP_2$ $[M-CO]^+$ 426.1400, found 426.1401.
XRD (Figure 14).

Synthesis of [Co(PCP^{NH}-*i*Pr)Br$_2$] (**12**)

A solution of **3** (50 mg, 0.12 mmol) and $Co_2(CO)_8$ (22 mg, 0.07 mmol) in MeCN (4 mL) was put into a microwave vial and stirred at 110 °C for 20 h, whereupon the color of the reaction mixture changed from orange-red to green. The mixture was transferred into a Schlenk flask and all volatiles were removed under reduced pressure. The resulting residue was extracted with *n*-pentane in order to remove [Co(PCP^{NH}-*i*Pr)(CO)$_2$] (**11**), to afford **12** as a dark greenish-brown solid with a yield of 31 mg (46 %).
HR-MS (ESI$^+$, CH_3CN/MeOH + 1 % H_2O): m/z calcd for $C_{18}H_{33}N_2CoP_2$ $[M\text{-}2Br+H]^+$ 399.1524, found 399.1528.

Synthesis of [Co(PCP^{NH}-*i*Pr)Cl$_2$] (**13**)

A solution of **7** (50 mg, 0.13 mmol) and $Co_2(CO)_8$ (22 mg, 0.07 mmol) in MeCN (4 mL) was put into a microwave vial and stirred at 110 °C for 20 h, whereupon the color of the reaction mixture changed from orange-red to green. The mixture was transferred into a Schlenk flask and all volatiles were removed under reduced pressure. The resulting residue was extracted with *n*-pentane in order to remove [Co(PCP^{NH}-*i*Pr)(CO)$_2$] (**11**), to afford **13** as a dark greenish solid with a yield of 26 mg (42 %).
HR-MS (ESI$^+$, CH_3CN/MeOH + 1 % H_2O): m/z calcd for $C_{18}H_{33}N_2CoP_2$ $[M\text{-}2Cl+H]^+$ 399.1524, found 399.1534.

Synthesis of [Co^{III}(PCP^{NH}-*i*Pr)(CH_3CN)$_3$](BF_4)$_2$ (**14**)

12 or **13** (20 mg, 0.04 mmol) was dissolved in MeCN-d_3 (1 mL) and a spatula of $AgBF_4$ was added to the solution, whereupon an instantaneous color change from dark green to purple was observed. The suspension was stirred at room temperature for 15 min, before the reaction mixture was filtrated through a syringe filter into an NMR tube.
^{1}H-NMR (400 MHz, MeCN-d_3, 20 °C, ppm): δ = 6.94 (t, J = 7.7 Hz, 1H, CH), 6.43 (d, J = 7.7 Hz, 2H, CH), 4.15 (s, br, 2H, NH), 2.83 (m, 4H, C*H*(CH_3)$_2$), 2.21 (s, br, 9H, CH_3CN), 1.65 (q, J = 7.3 Hz, 12H, CH(C*H$_3$*)$_2$), 1.53 (q, J = (.0 Hz, 12H, CH(C*H$_3$*)$_2$).
^{31}P{^{1}H}-NMR (162 MHz, MeCN-d_3, 20 °C, ppm): δ = 106.5 (s, P).

Synthesis of [Co^{II}(PCP^{NH}-*i*Pr)Br(CO)] (**15**)

A solution of **3** (50 mg, 0.12 mmol) and $Co_2(CO)_8$ (22 mg, 0.07 mmol) in MeCN (4 mL) was put into a microwave vial and stirred at 130 °C for 20 h, whereupon the color of the reaction mixture changed from orange-red to green-brown. The mixture was transferred into a Schlenk flask and all volatiles were removed under reduced pressure. The residue was extracted with *n*-pentane to in order to remove any impurities and **15** was afforded as a brown solid with a yield of 57 mg (94 %).
IR (ATR, cm^{-1}): 1964 (ν_{CO}).

3.5. Solvothermalreactions with PCP^{NH}-*t*Bu ligands

Synthesis of [Co^{I}(PCP^{NH}-*t*Bu)(CO)$_2$] (**16**)

A solution of **4** or **8** (50 mg, 0.12 mmol) and $Co_2(CO)_8$ (21 mg, 0.06 mmol) in MeCN (4 mL) was put into a microwave vial and stirred at 110 °C for 20 h, whereupon the color of the reaction mixture changed from orange-red to green. The mixture was transferred into a Schlenk flask and all volatiles were removed under reduced pressure. The obtained residue was extracted with *n*-pentane and filtered through a syringe filter (PTFE, 0.2 µm). After removing all volatiles under reduced pressure, the product could be obtained as a yellow solid with a yield of 15 mg (27 %).
^{31}P{^{1}H}-NMR (162 MHz, CD_2Cl_2, 20 °C, ppm): δ = 170.0 (s, P).
IR (ATR, cm^{-1}): 1958 (ν_{CO}), 1903 (ν_{CO}).

Synthesis of [Co^{I}(PCP^{NH}-*t*Bu)(CO)] (**17**)

A solution of **4** or **8** (50 mg, 0.12 mmol) and $Co_2(CO)_8$ (21 mg, 0.06 mmol) in MeCN (4 mL) was put into a microwave vial and stirred at 110 °C for 20 h, whereupon the color of the reaction mixture changed from orange-red to green. The mixture was transferred into a Schlenk flask and all volatiles were removed under reduced pressure. The obtained residue was extracted with *n*-pentane in order to remove [Co^{I}(PCP^{NH}-*t*Bu)$(CO)_2$] (**16**). The product could not be isolated in pure form.
IR (ATR, cm^{-1}): 1853 (ν_{CO}).

Synthesis of [Co^{I}(PCP^{NH}-*t*Bu)Br_2] (**18**)

A solution of **4** (50 mg, 0.12 mmol) and $Co_2(CO)_8$ (21 mg, 0.06 mmol) in MeCN (4 mL) was put into a microwave vial and stirred at 110 °C for 20 h, whereupon the color of the reaction mixture changed from orange-red to green. The mixture was transferred into a Schlenk flask and all volatiles were removed under reduced pressure. The obtained residue was extracted with *n*-pentane in order to remove [Co^{I}(PCP^{NH}-*t*Bu)$(CO)_2$] (**16**). The product could not be isolated in pure form. Detection via formation of **20**.

Synthesis of [Co^{I}(PCP^{NH}-*t*Bu)Cl_2] (**19**)

A solution of **8** (50 mg, 0.12 mmol) and $Co_2(CO)_8$ (21 mg, 0.06 mmol) in MeCN (4 mL) was put into a microwave vial and stirred at 110 °C for 20 h, whereupon the color of the reaction mixture changed from orange-red to green. The mixture was transferred into a Schlenk flask and all volatiles were removed under reduced pressure. The obtained residue was extracted with *n*-pentane in order to remove [Co^{I}(PCP^{NH}-*t*Bu)$(CO)_2$] (**16**). The product could not be isolated in pure form. Detection via formation of **20**.

Synthesis of [Co^{III}(PCP^{NH}-*t*Bu)$(CH_3CN)_3$]$(BF_4)_2$ (**20**)

18 or **19** (approx. 20 mg) were dissolved in MeCN-d_3 (1 mL) and a spatula of $AgBF_4$ was added to the solution, whereupon an instantaneous color change from brown to purple was observed. The suspension was stirred at room temperature for 15 min, before the reaction mixture was filtrated through a syringe filter into an NMR tube.
$^{31}P\{^{1}H\}$-NMR (162 MHz, MeCN-d_3, 20 °C, ppm): δ = 93.8 (s, P).

Synthesis of [Co^{II}(PCP^{NH}-*t*Bu)Br] (**21**)

A solution of **4** (50 mg, 0.12 mmol) and $Co_2(CO)_8$ (21 mg, 0.06 mmol) in MeCN (4 mL) was put into a microwave vial and was stirred at 130 °C for 20 h, whereupon the color of the reaction mixture changed from yellow to red. After stopping the heating, the mixture turned orange. The mixture was transferred into a Schlenk flask and all volatiles were removed under reduced pressure. The obtained residue was extracted with *n*-pentane to remove any impurities and **21** was obtained as an orange-red solid with a yield of 53 mg (94 %). Single crystals could be obtained from extracting the reaction mixture with *n*-pentane and slow evaporation of the solvent at -20 °C.
XRD (Figure 17).

Synthesis of [Co^{II}(PCP^{NH}-*t*Bu)Cl] (**22**)

A solution of **8** (50 mg, 0.12 mmol) and $Co_2(CO)_8$ (21 mg, 0.06 mmol) in MeCN (4 mL) was put into a microwave vial and was stirred at 130 °C for 20 h, whereupon the color of the reaction mixture changed from yellow to red. After stopping the heating, the mixture turned orange. The mixture was transferred into a Schlenk flask and all volatiles were removed under reduced pressure. The obtained residue was extracted with *n*-pentane to remove any impurities and **22** was obtained as an orange-red solid with a yield of 52 mg (91 %).
HR-MS (ESI+, CH_3CN/MeOH + 1 % H_2O): m/z calcd for $C_{22}H_{41}CoN_2P_2$ [M-Cl]+ 454.2077, found 454.2079.

Synthesis of [Co^{I}(PCP^{NH}-*t*Bu)(NO)]Br (**23**)

21 (40 mg, 0.07 mmol) was dissolved in CH_2Cl_2 (5 mL) and was exposed to NO gas (1 bar) in a Schlenk flask, whereupon the color changed immediately from brown to dark red and the mixture was stirred at room temperature for 15 min. All volatiles were removed under reduced pressure affording a dark red solid. **23** could not be isolated in pure form and it was not possible to separate it from **24.**
IR (ATR, cm^{-1}): 1803 (ν_{NO}).
^{31}P{^{1}H}-NMR (162 MHz, CD_2Cl_2, 20 °C, ppm): δ = 156.9 (s, P).

Synthesis of [Co^{I}(PCP^{NH}-*t*Bu)Br(NO)] (**24**)

21 (40 mg, 0.07 mmol) was dissolved in CH_2Cl_2 (5 mL) and was exposed to NO gas (1 bar) in a Schlenk flask, whereupon the color changed immediately from brown to dark red and the mixture was stirred at room temperature for 15 min. All volatiles were removed under reduced pressure affording a dark red solid. **24** could not be isolated in pure form and it was not possible to separate it from **23.**
IR (ATR, cm^{-1}): 1651 (ν_{NO}).
^{31}P{^{1}H}-NMR (162 MHz, CD_2Cl_2, 20 °C, ppm): δ = 131.2 (s, P).

3.6. Solvothermalreactions with PCP^{CH_2}-*t*Bu-Br

Synthesis of [Co^{I}(PCP^{CH_2}-*t*Bu)$(CO)_2$ (**25**)

A solution of **10** (50 mg, 0.11 mmol) and $Co_2(CO)_8$ (20 mg, 0.06 mmol) in MeCN (4 mL) was put into a microwave vial and was stirred at 110 °C for 20 h, whereupon the color of the reaction mixture changed from dark orange to green. The mixture was transferred into a Schlenk flask and all volatiles were removed under reduced pressure affording a green solid. The residue was extracted with *n*-pentane and after removing all volatiles under reduced pressure **25** was afforded as a yellow solid with a yield of 23 mg (43 %).
^{31}P{^{1}H}-NMR (162 MHz, CD_2Cl_2, 20 °C, ppm): δ = 117.9 (s, P).
IR (ATR, cm^{-1}): 1962 (ν_{CO}), 1904 (ν_{CO}).
HR-MS (ESI^{+}, CH_3CN/MeOH + 1 % H_2O): m/z calcd for $C_{25}H_{43}OCoP_2$ $[M\text{-}CO]^{+}$ 480.2116, found 480.2116.

Synthesis of [Co^{III}(PCP^{CH_2}-*t*Bu)Br_2] (**26**)

A solution of **10** (50 mg, 0.11 mmol) and $Co_2(CO)_8$ (20 mg, 0.06 mmol) in MeCN (4 mL) was put into a microwave vial and was stirred at 110 °C for 20 h, whereupon the color of the reaction mixture changed from dark orange to green. The mixture was transferred into a Schlenk flask and all volatiles were removed under reduced pressure affording a green solid. The residue was extracted with *n*-pentane in order to remove [Co^{I}(PCP^{CH_2}-*t*Bu)$(CO)_2$ (**25**) and **26** was afforded as a green solid with a yield of 29 mg (45 %).
HR-MS (ESI^{+}, CH_3CN/MeOH + 1 % H_2O): m/z calcd for $C_{24}H_{43}CoP_2$ $[M\text{-}2Br]^{+}$ 452.2166, found 452.2157.

Synthesis of [Co^{III}(PCP^{CH_2}-*t*Bu)$(CH_3CN)_3$]$(SbF_6)_2$ (**27**)

26 (20 mg, 0.03 mmol) was dissolved in MeCN-d_3 (1 mL) and a spatula of $AgSbF_6$ was added to the solution, whereupon an instantaneous color change from green to beige-brown was observed. The suspension was stirred at room temperature for 15 min, before the reaction mixture was filtrated through a syringe filter into an NMR tube.
^{31}P{^{1}H}-NMR (162 MHz, MeCN-d_3, 20 °C, ppm): δ = 68.9 (s, P).

4. Conclusion

It could be demonstrated in this work that the approach of introducing a halide (X = Cl, Br) to the *ipso*-carbon enhances the ability of the cobalt precursor $Co_2(CO)_8$ to accomplish the oxidative addition of PCP-X ligands bearing NH and CH_2 spacers (**3**, **4**, **7**, **8**, **10**) under solvothermal conditions. The halide alters the electronic properties of the ligand by weakening the C–X bond, thus activating the C–X bond and improving the complex formation for first row transition metals like cobalt.
Using this method, a series of cobalt complexes with the PCP^{NH} system could be isolated, which would otherwise not be accessible. Since the hydrogens of the NH spacer groups would interfere in the complex formation process via transmetalation or proton abstraction with a strong base to activate the $P(C\text{-}H)P^{NH}$ ligand, the pathway of oxidative addition is the only viable option to afford the cobalt PCP^{NH} complexes.
During the solvothermal reactions, mostly the disproportionation of the cobalt precursor $Co_2(CO)_8$ was observed, yielding a dicarbonyl species and a dihalide species (**12**, **13**, **18**, **19**, **26**). Hence, a series of cobalt carbonyl complexes (**11**, **16**, **25**) was obtained, although $[Co^{I}(PCP^{Y}\text{-}t\text{Bu})(CO)_2]$ (**16**: Y = NH, **25**: Y = CH_2) were rather unstable in comparison to $[Co^{I}(PCP^{NH}\text{-}i\text{Pr})(CO)_2]$ (**11**). This difference can be reasoned by the steric demand of the bulky *t*-butyl phosphine donors. This is also why the monocarbonyl species (**17**) was only observed with the PCP^{NH}-*t*Bu system. The existence of the paramagnetic dihalide species could be demonstrated via the approach of forming an octahedral cationic Co^{III} complex by abstracting the halides with an halogen scavenger ($AgBF_4$ or $AgSbF_6$) in MeCN, which by extension became diamagnetic and detectable via NMR.
Elevating the temperature of the solvothermal reaction resulted in the formation of the 15-electron complex $[Co^{II}(PCP^{NH}\text{-}t\text{Bu})X)]$ (**21**: X = Br, **22**: X = Cl), which reacted under the exposure to nitric oxide gas (NO), to the cationic $[Co^{I}(PCP^{NH}\text{-}t\text{Bu})(NO)]Br$ (**23**) and to $[Co^{III}(PCP^{NH}\text{-}t\text{Bu})Br(NO)]$ (**24**). The PCP^{NH}-*i*Pr and PCP^{CH_2}-*t*Bu system did not form the square planar complex $[Co^{II}(PCP^{Y}\text{-}R)X)]$ at increased temperatures.

5. Appendix

5.1. NMR spectra

^{1}H-NMR (250 MHz, CD_2Cl_2, 20 °C): 2-Bromo-1,3-dinitrobenzene (**1**)

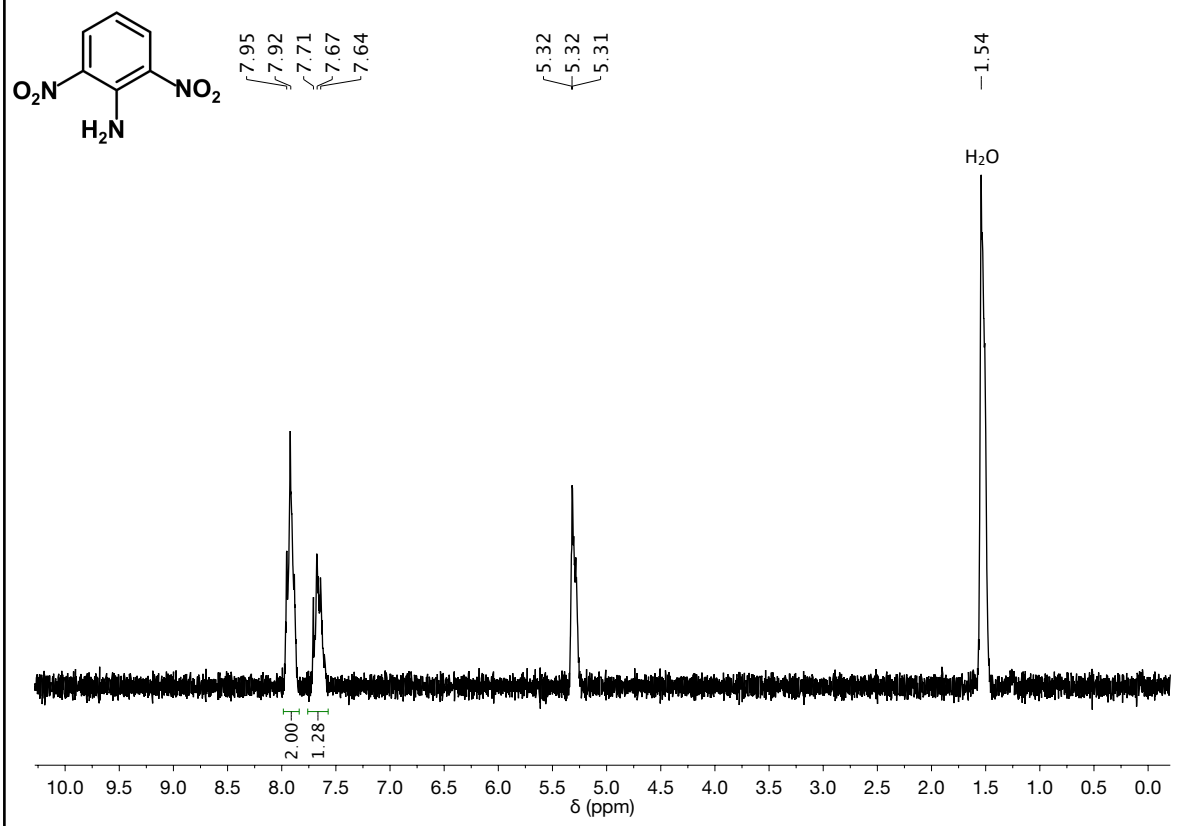

^{1}H-NMR (400 MHz, CD_2Cl_2, 20 °C): 2-Bromo-1,3-benzendiamine (**2**)

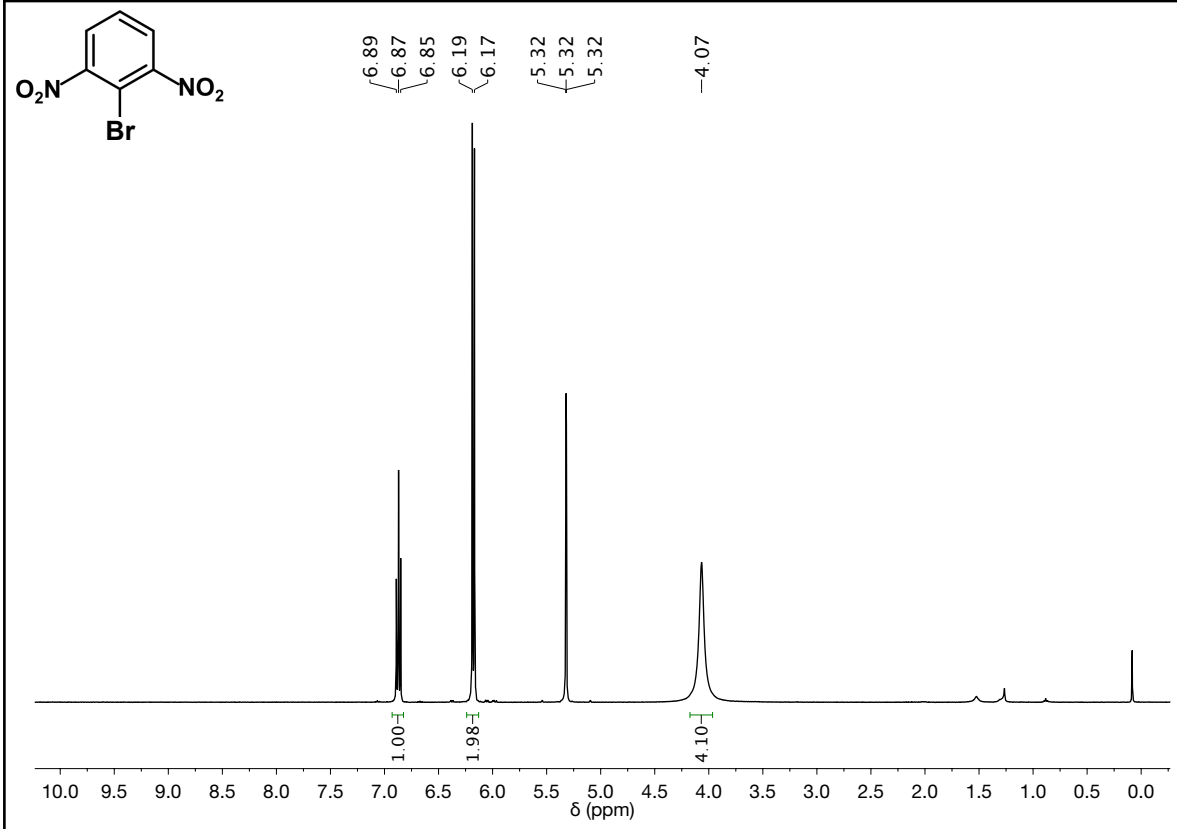

^{1}H-NMR (400 MHz, CD_2Cl_2, 20 °C): PCP^{NH}-*i*Pr-Br (**3**)

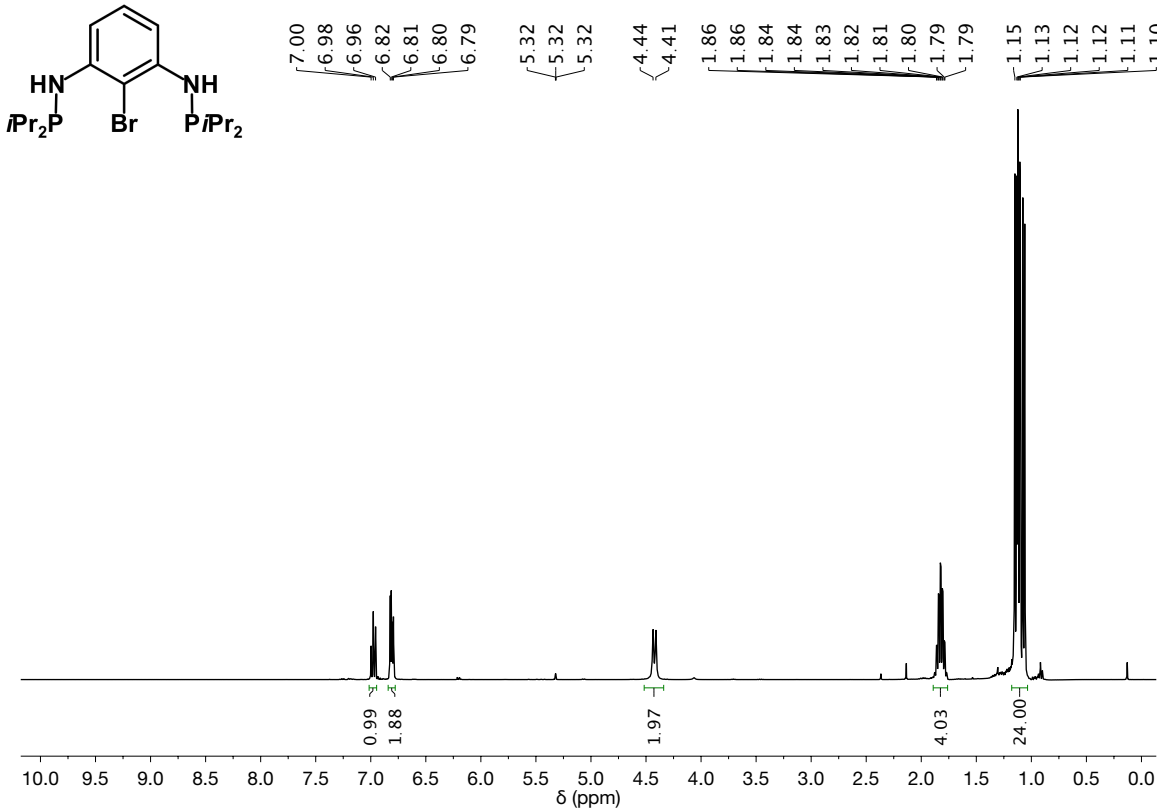

^{13}C{^{1}H}-NMR (101 MHz, CD_2Cl_2, 20 °C): PCP^{NH}-*i*Pr-Br (**3**)

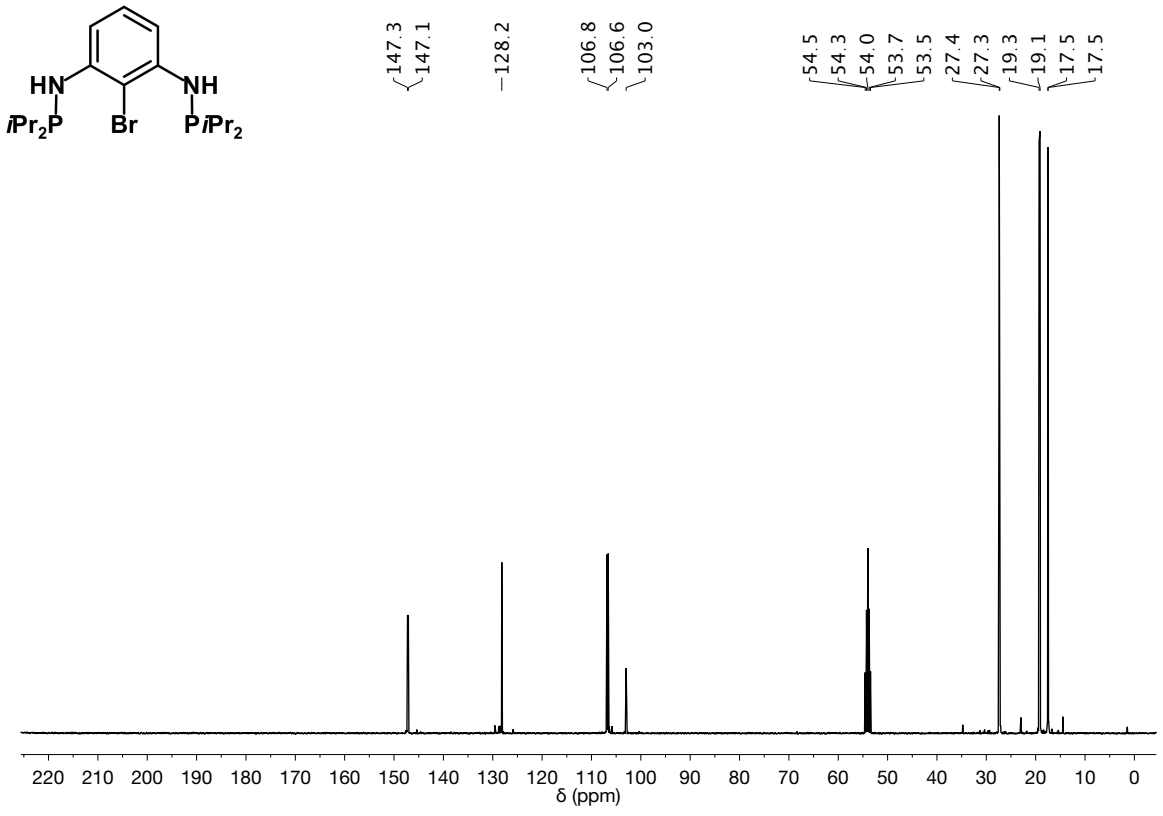

$^{31}P\{^{1}H\}$-NMR (162 MHz, CD_2Cl_2, 20 °C): PCP^{NH}-*i*Pr-Br (**3**)

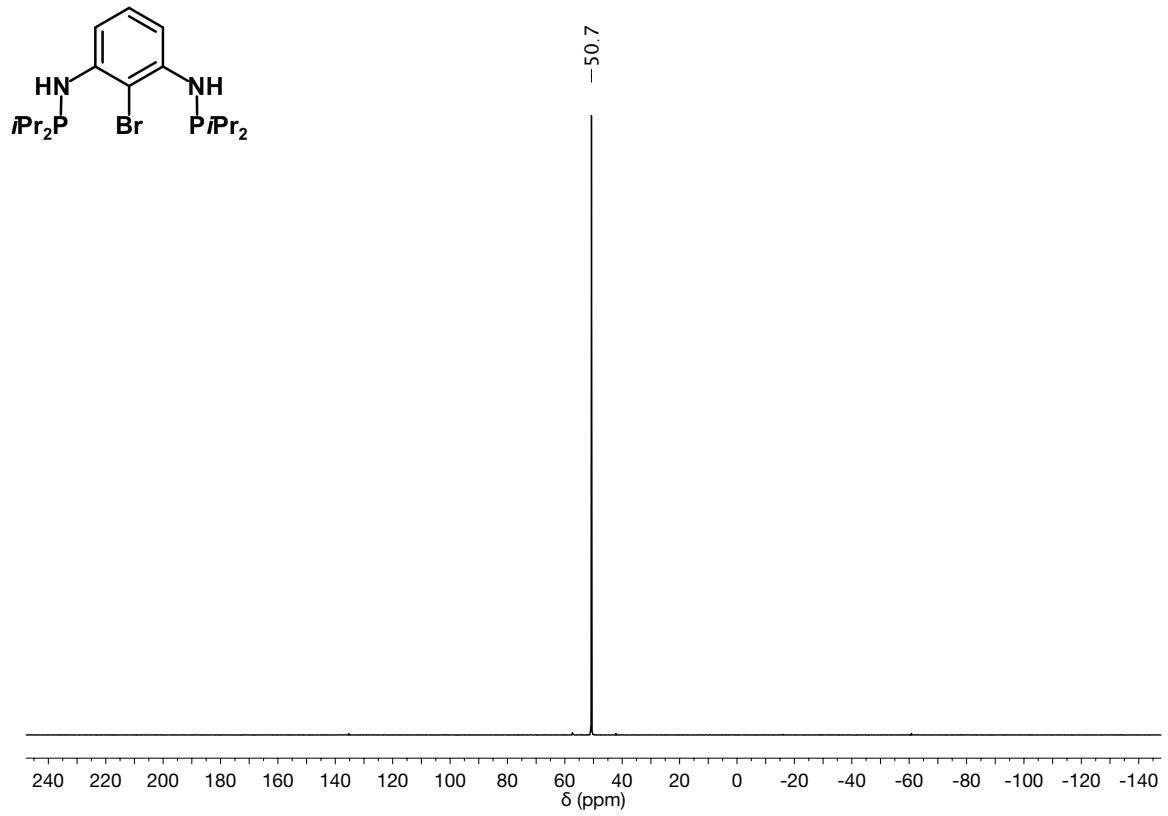

^{1}H-NMR (400 MHz, CD_2Cl_2, 20 °C): PCP^{NH}-*t*Bu-Br (**4**)

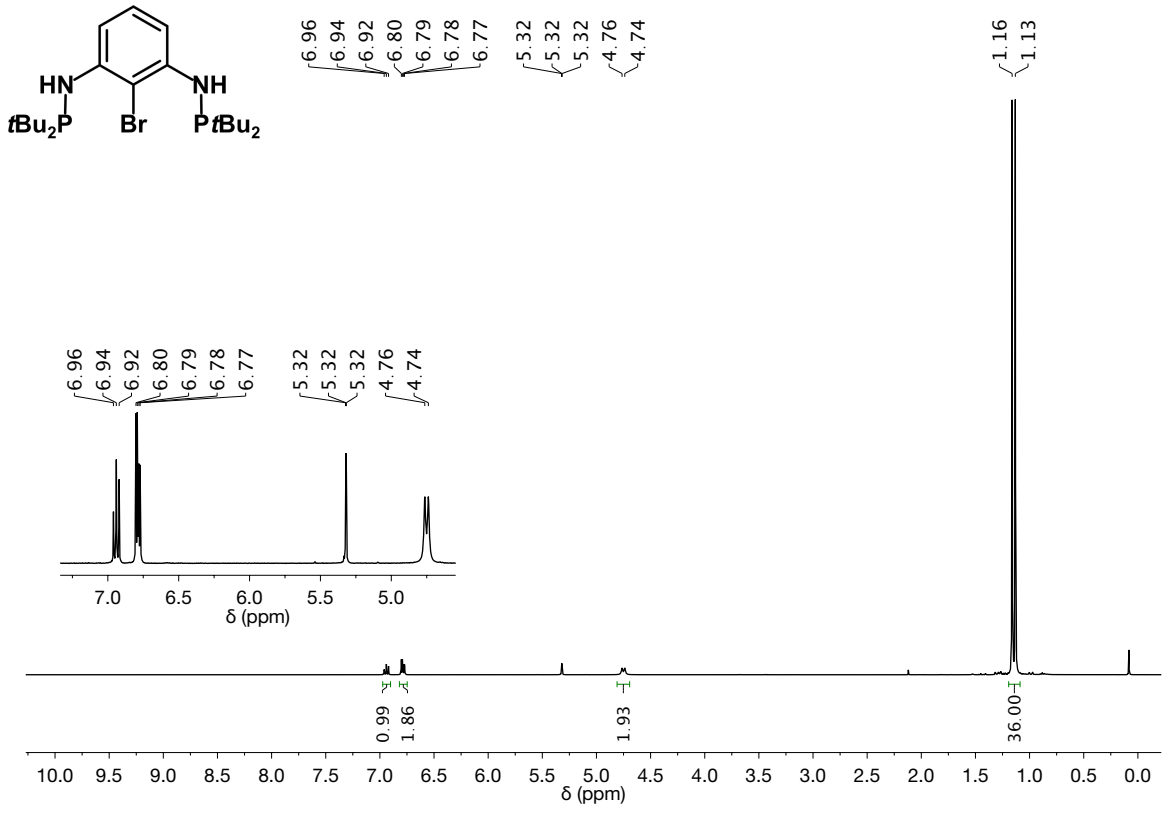

$^{13}C\{^{1}H\}$-NMR (101 MHz, CD_2Cl_2, 20 °C): PCP^{NH}-*t*Bu-Br (**4**)

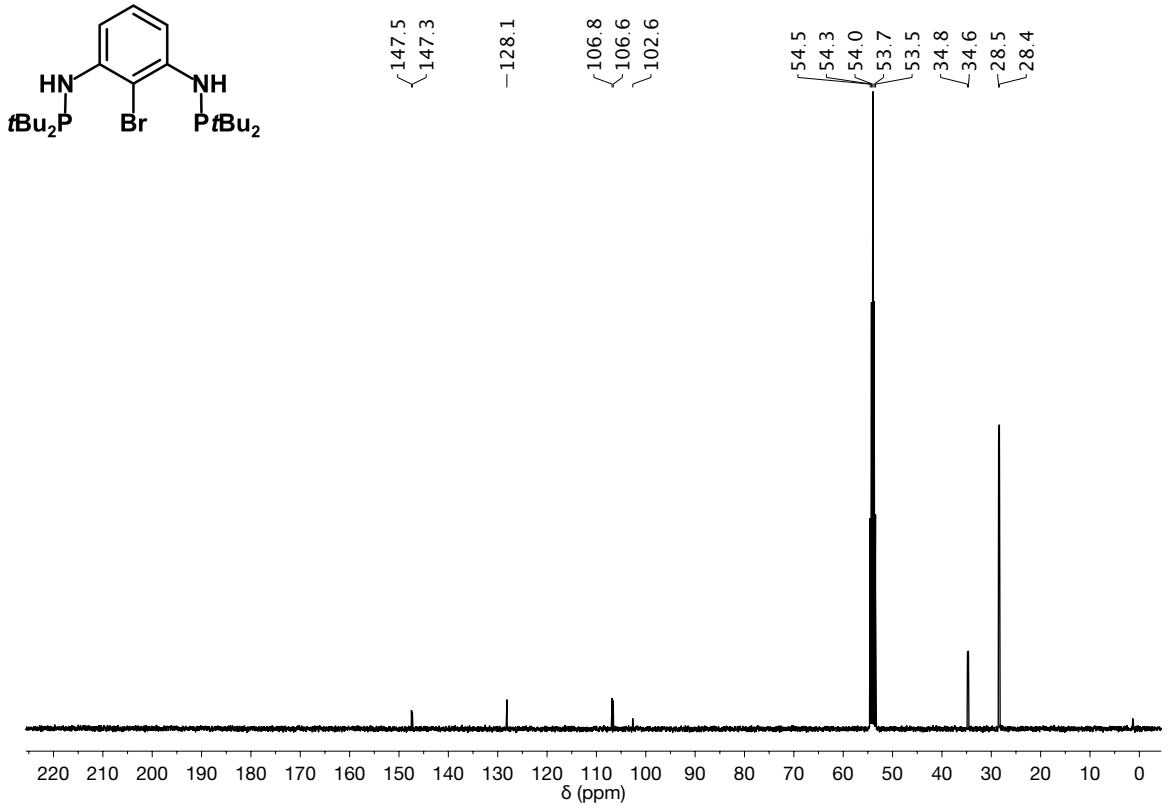

$^{31}P\{^{1}H\}$-NMR (162 MHz, CD_2Cl_2, 20 °C): PCP^{NH}-*t*Bu-Br (**4**)

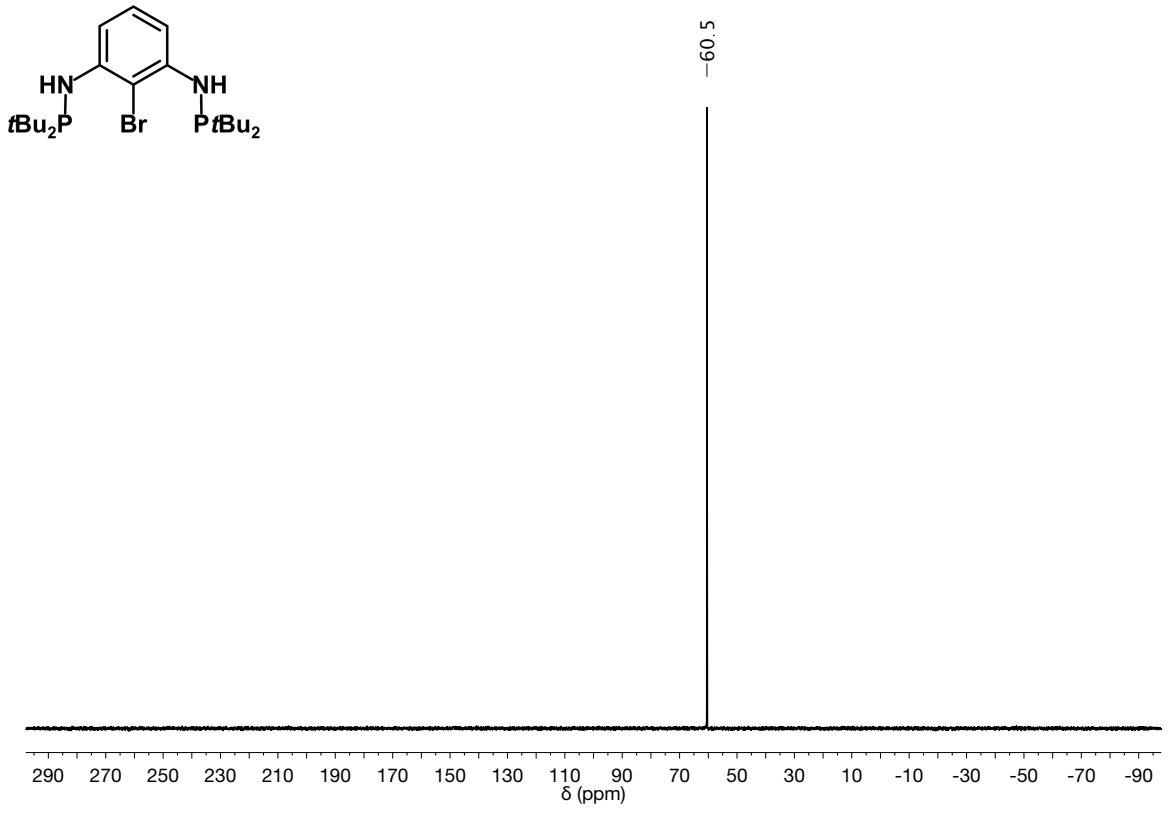

^{1}H-NMR (400 MHz, DMSO-d_6, 20 °C): 2-Chloro-1,3-benzendiamine (**6**)

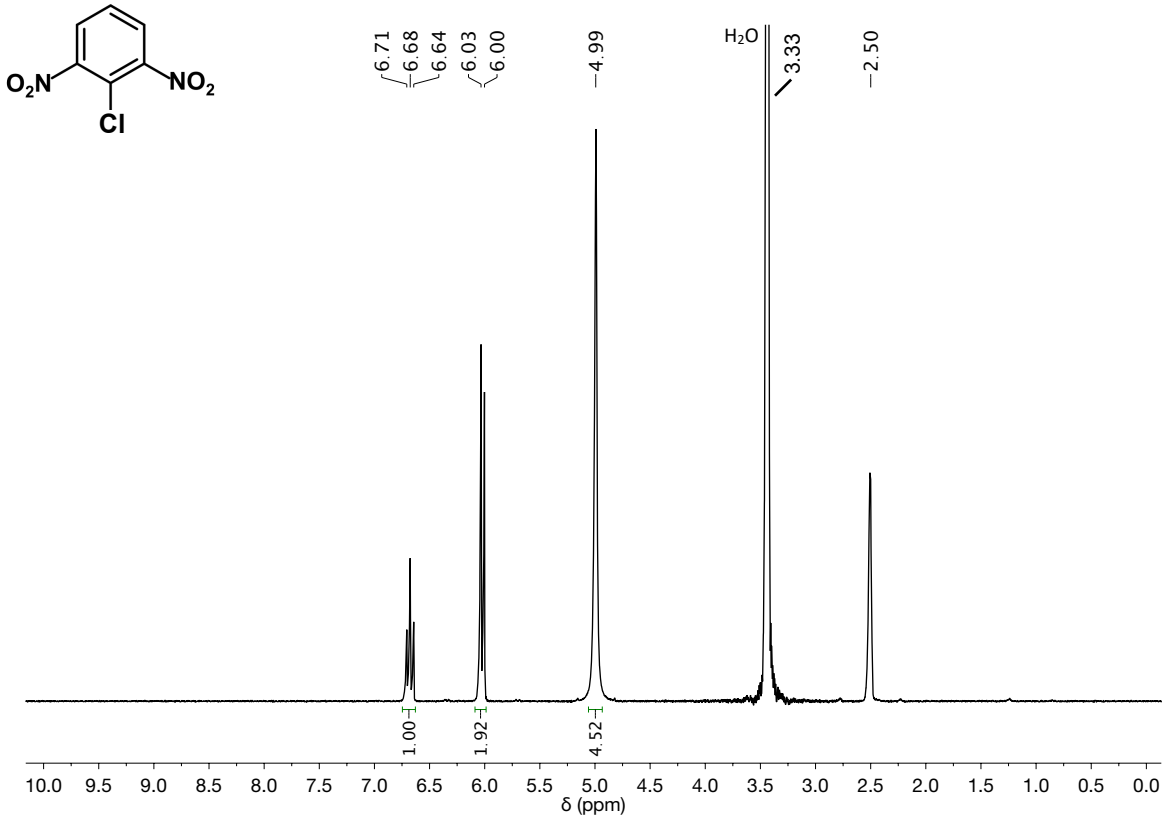

^{1}H-NMR (600 MHz, CD_2Cl_2, 20 °C): PCP^{NH}-*i*Pr-Cl (**7**)

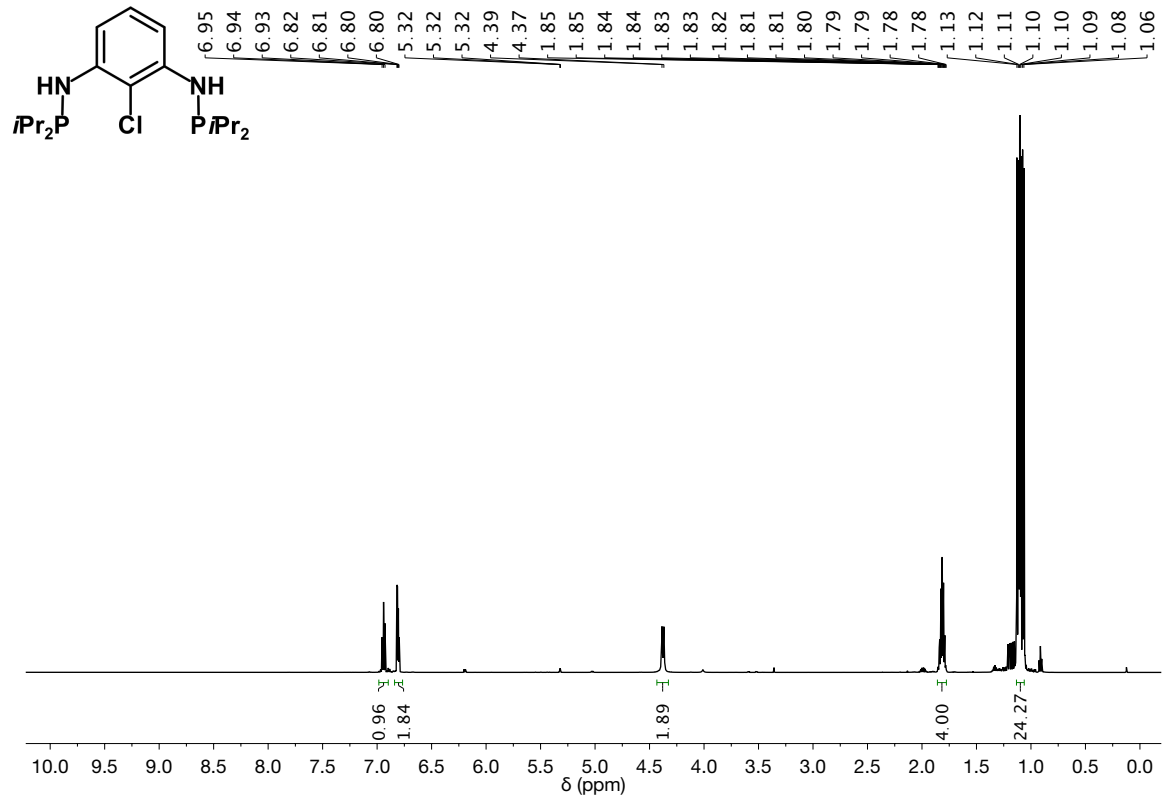

$^{13}C\{^{1}H\}$-NMR (151 MHz, CD_2Cl_2, 20 °C): PCP^{NH}-*i*Pr-Cl (**7**)

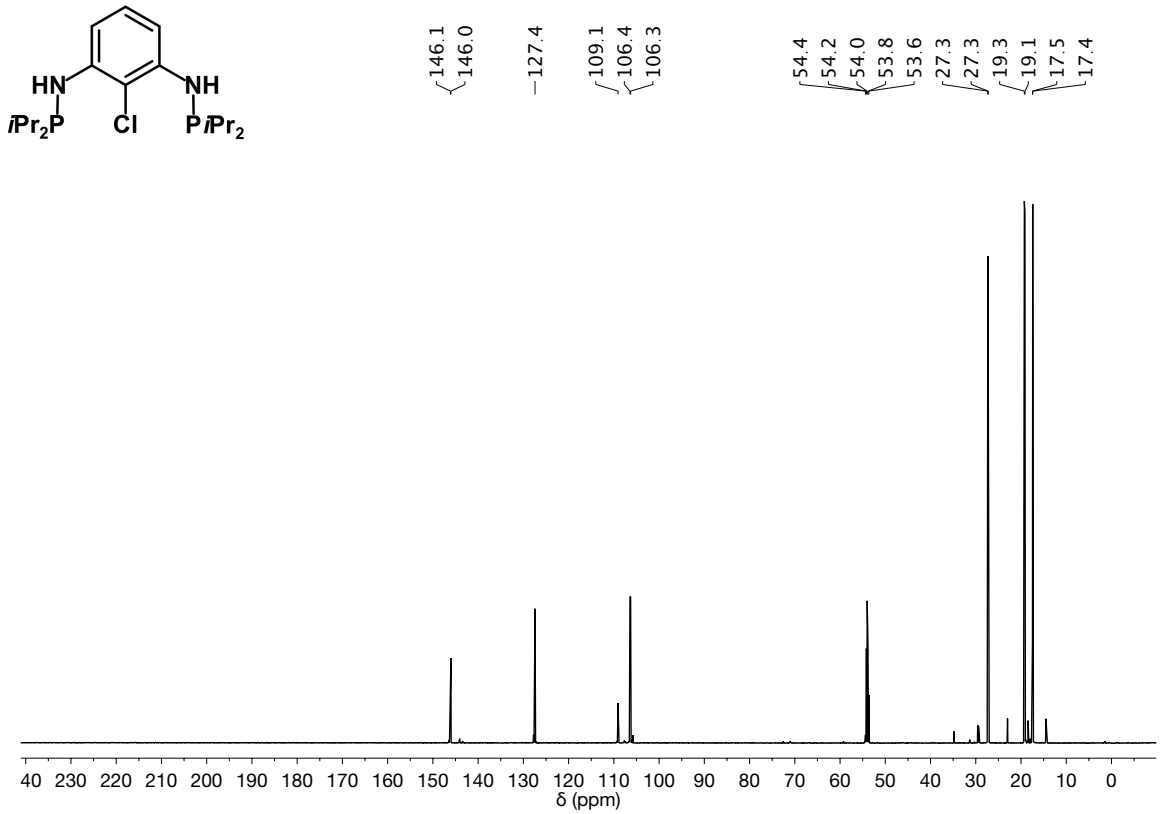

$^{31}P\{^{1}H\}$-NMR (243 MHz, CD_2Cl_2, 20 °C): PCP^{NH}-*i*Pr-Cl (**7**)

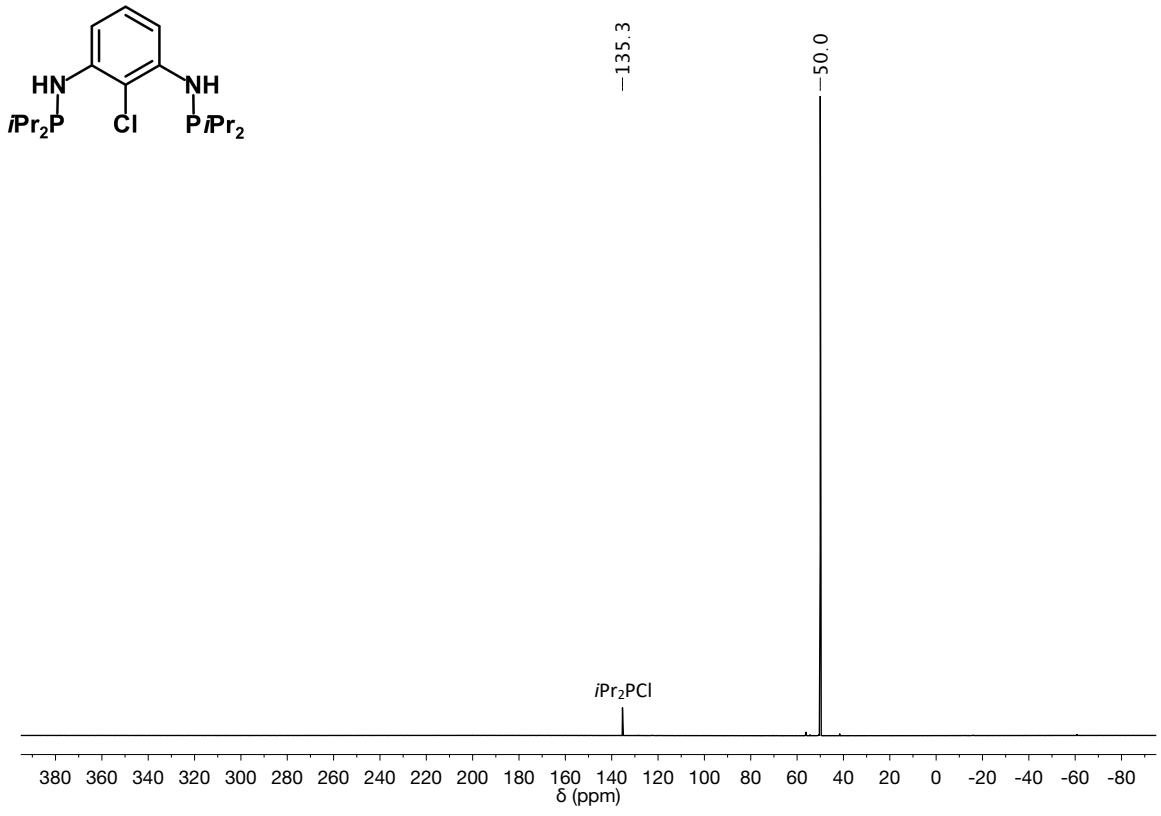

^{1}H-NMR (600 MHz, CD_2Cl_2, 20 °C): PCP^{NH}-*t*Bu-Cl (**8**)

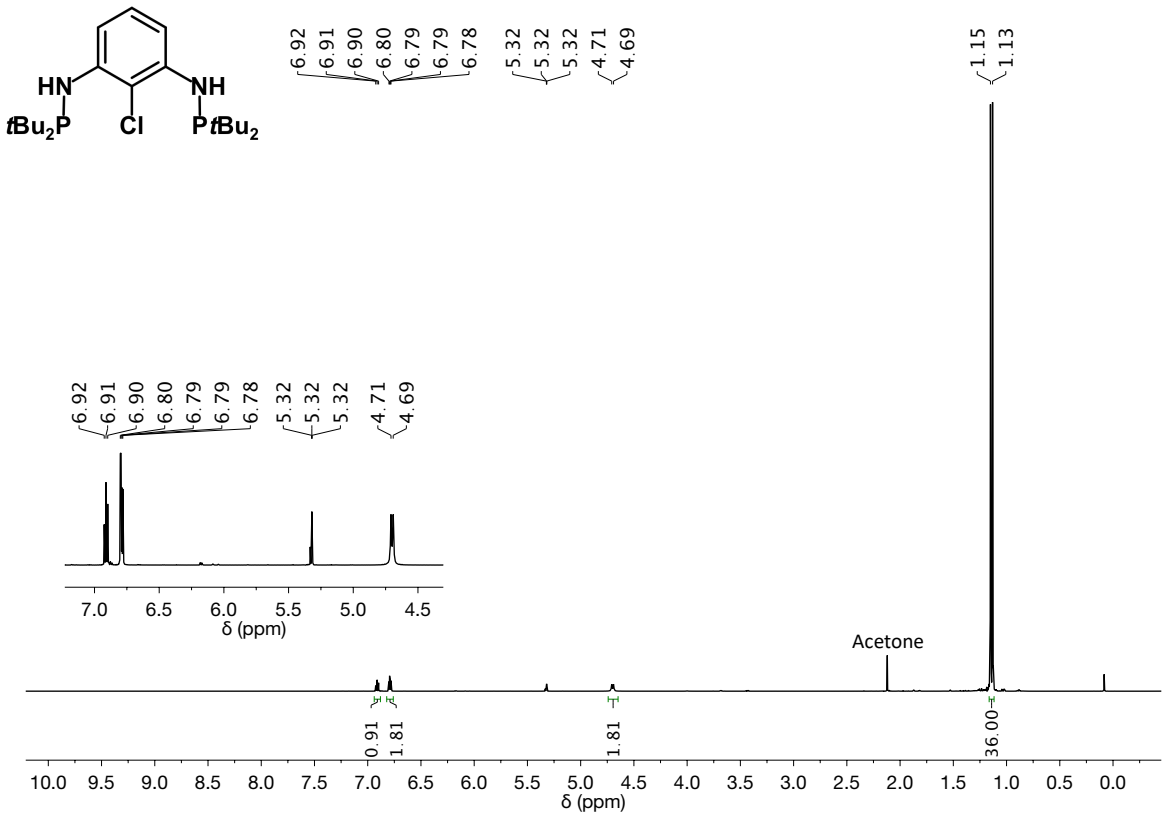

^{13}C{^{1}H}-NMR (151 MHz, CD_2Cl_2, 20 °C): PCP^{NH}-*t*Bu-Cl (**8**)

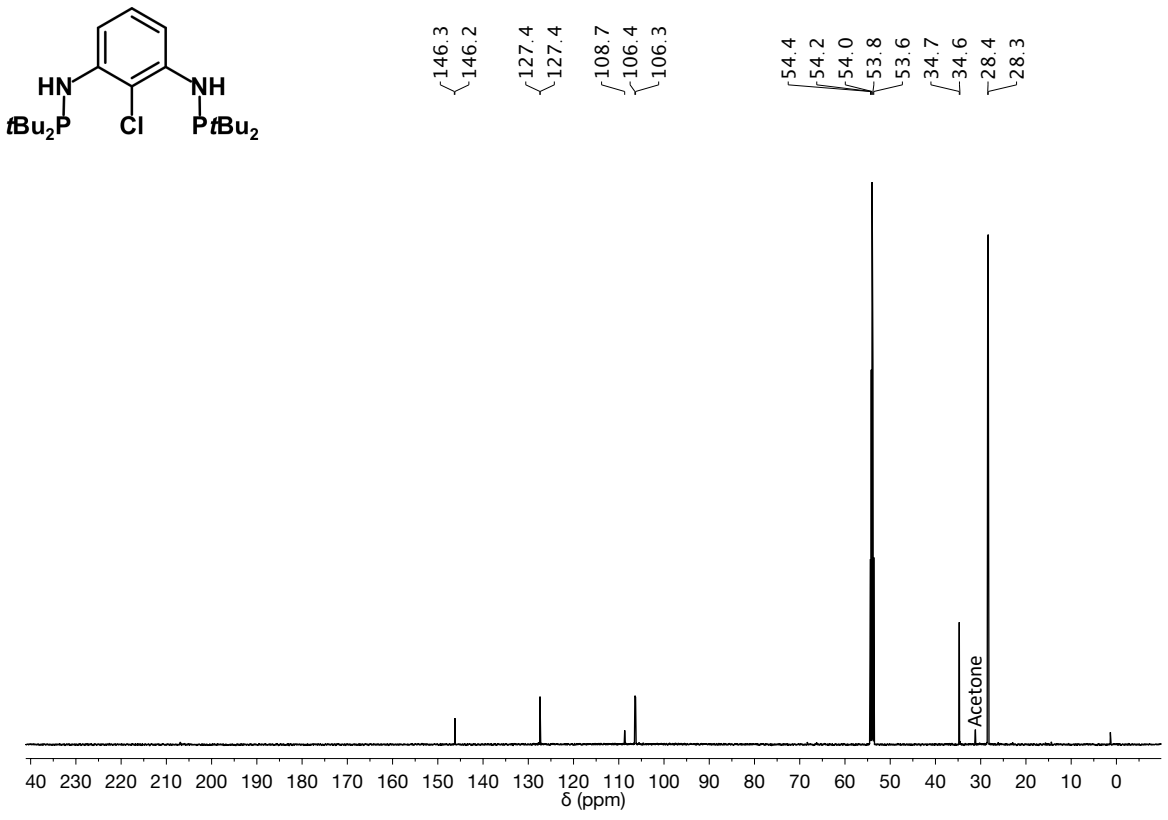

$^{31}P\{^{1}H\}$-NMR (243 MHz, CD_2Cl_2, 20 °C): PCP^{NH}-*t*Bu-Cl (**8**)

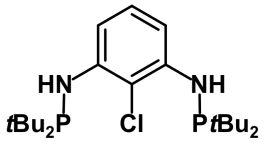

^{1}H-NMR (250 MHz, $CDCl_3$, 20 °C): 2-Bromo-1,3-(bromomethyl)benzene (**9**)

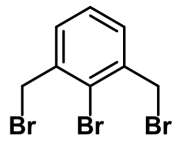

^{1}H-NMR (400 MHz, CD_2Cl_2, 20 °C): PCP^{CH_2}-*t*Bu-Br (**10**)

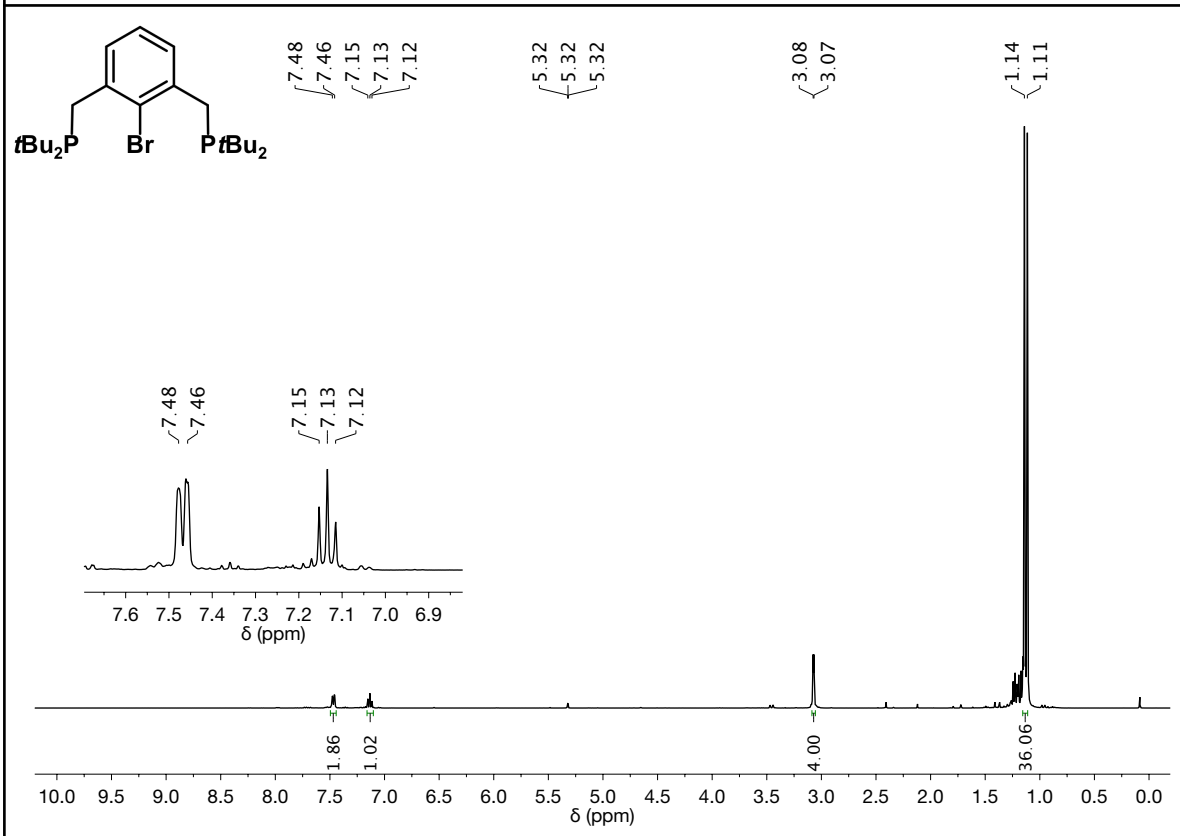

^{13}C{^{1}H}-NMR (101 MHz, CD_2Cl_2, 20 °C): PCP^{CH_2}-*t*Bu-Br (**10**)

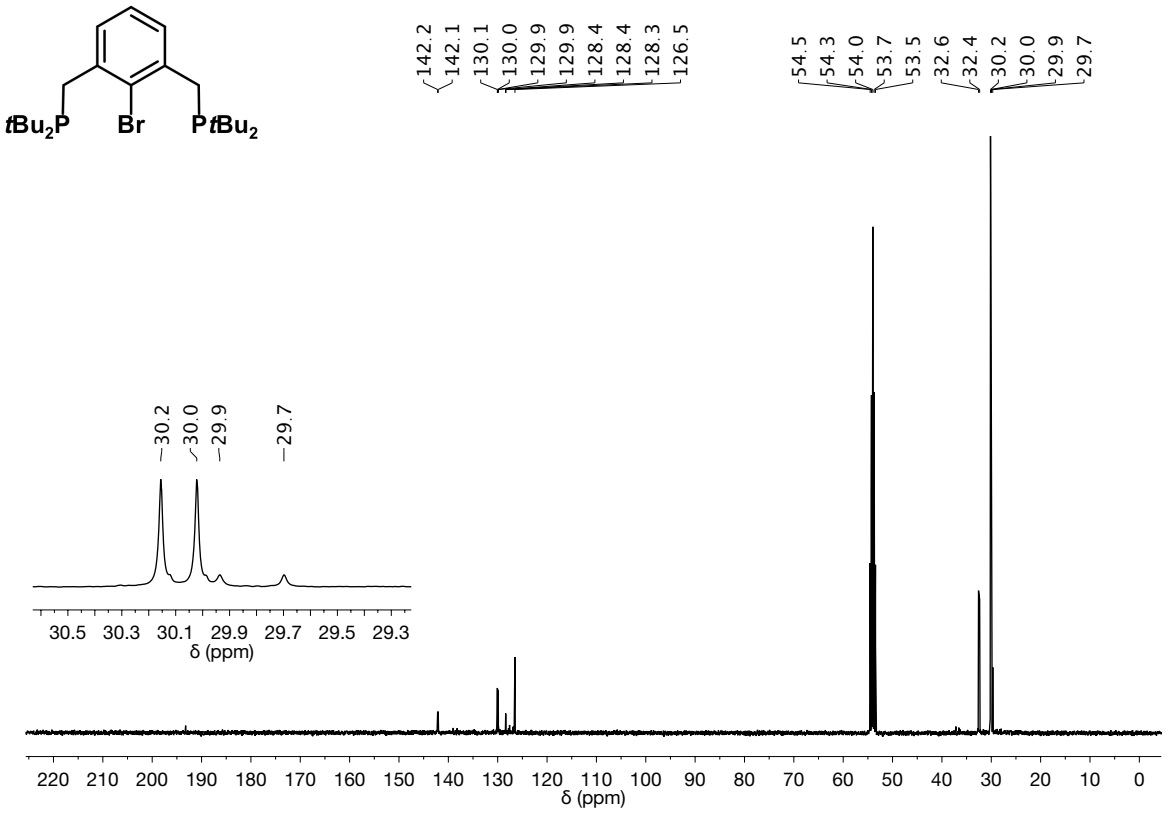

$^{31}P\{^{1}H\}$-NMR (162 MHz, CD_2Cl_2, 20 °C): PCP^{CH_2}-*t*Bu-Br (**10**)

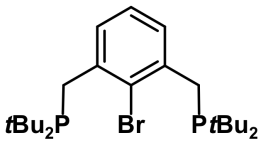

^{1}H-NMR (400 MHz, CD_2Cl_2, 20 °C): [$Co^{I}(PCP^{NH}$-*i*Pr)$(CO)_2$] (**11**)

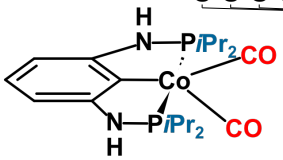

$^{13}C\{^{1}H\}$-NMR (101 MHz, CD_2Cl_2, 20 °C): $[Co^{I}(PCP^{NH}\text{-}iPr)(CO)_2]$ (**11**)

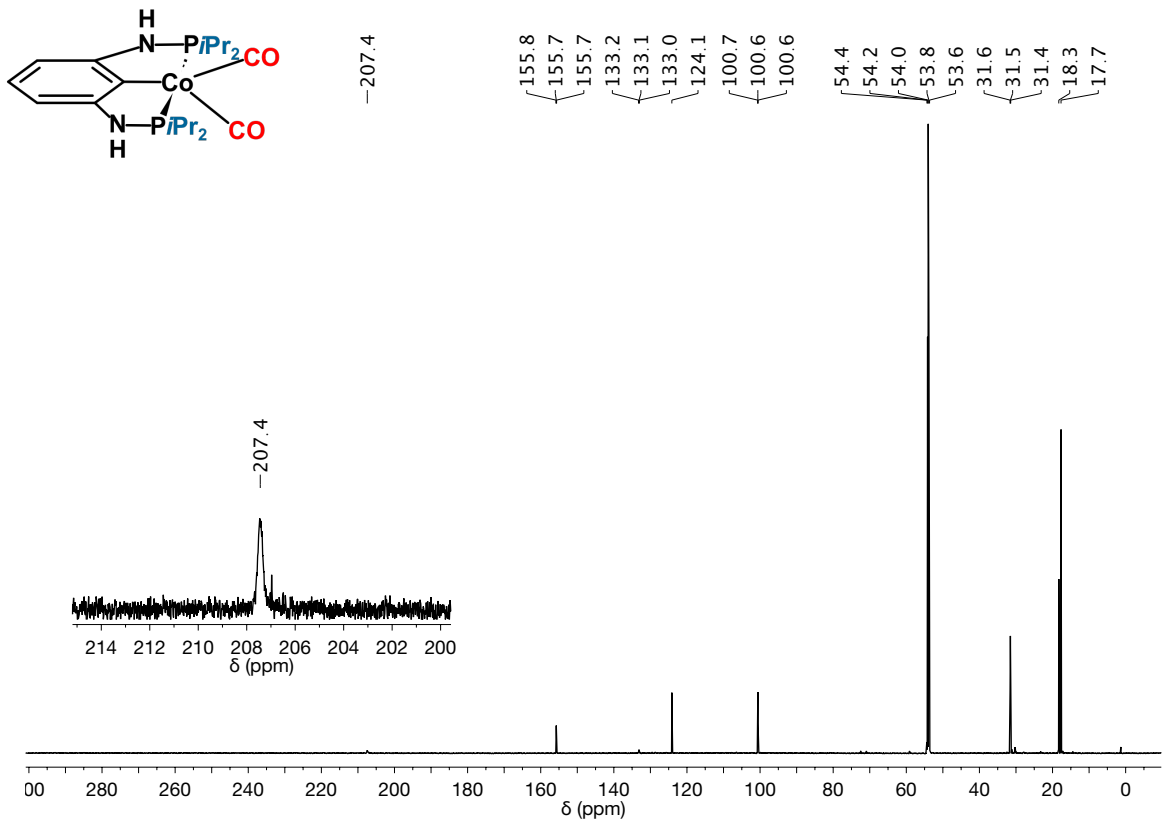

$^{31}P\{^{1}H\}$-NMR (400 MHz, CD_2Cl_2, 20 °C): $[Co^{I}(PCP^{NH}\text{-}iPr)(CO)_2]$ (**11**)

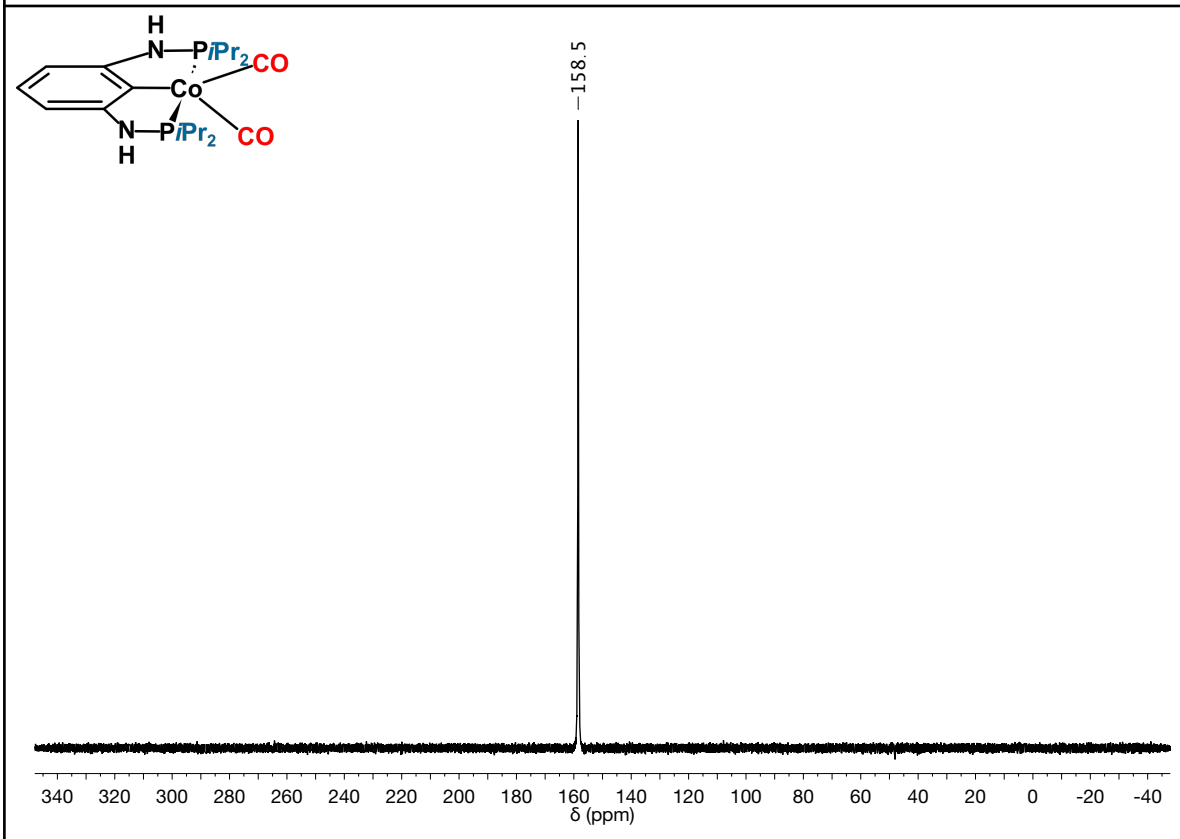

^{1}H-NMR (400 MHz, MeCN-d_3, 20 °C): [Co^{III}(PCP^{NH}-*i*Pr)(CH_3CN)$_3$](BF_4)$_2$ (**14**)

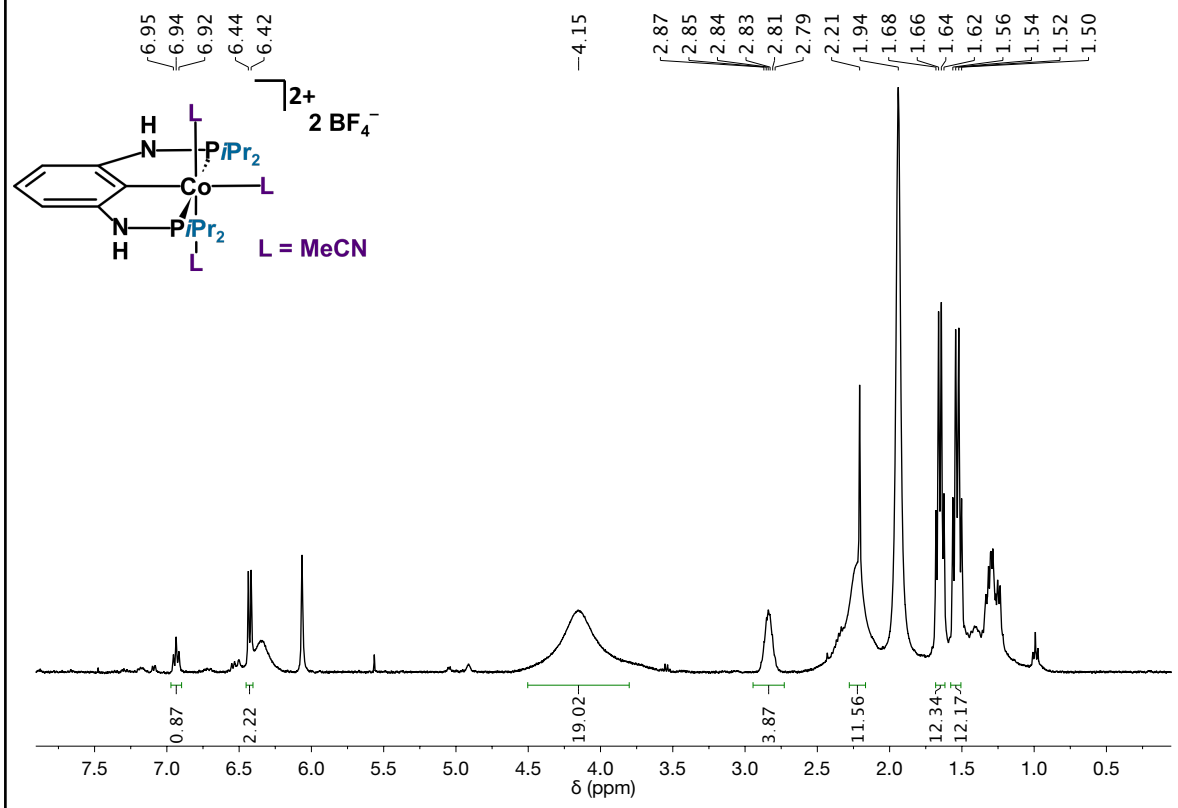

^{31}P{^{1}H}-NMR (162 MHz, MeCN-d_3, 20 °C): [Co^{III}(PCP^{NH}-*i*Pr)(CH_3CN)$_3$](BF_4)$_2$ (**14**)

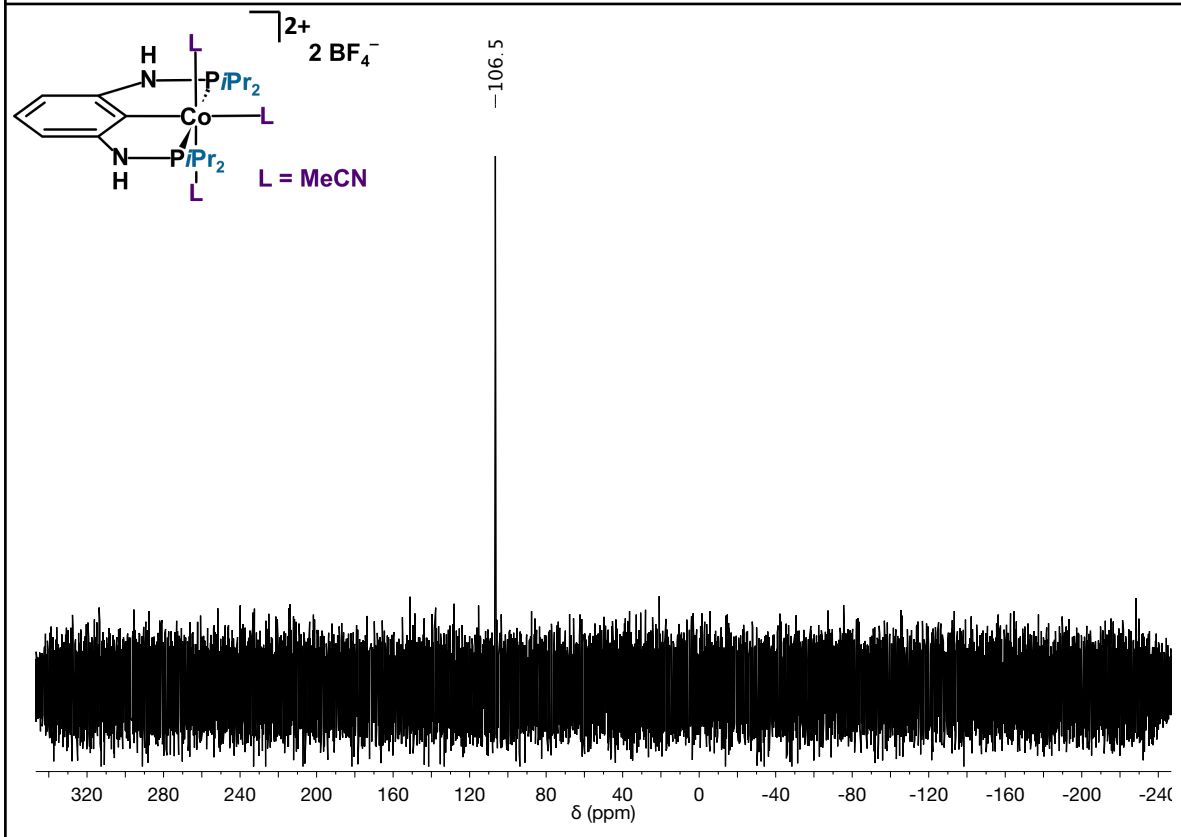

$^{31}P\{^{1}H\}$-NMR (162 MHz, CD_2Cl_2, 20 °C): $[Co^{I}(PCP^{NH}\text{-}t\text{Bu})(CO)_2]$ (**16**)

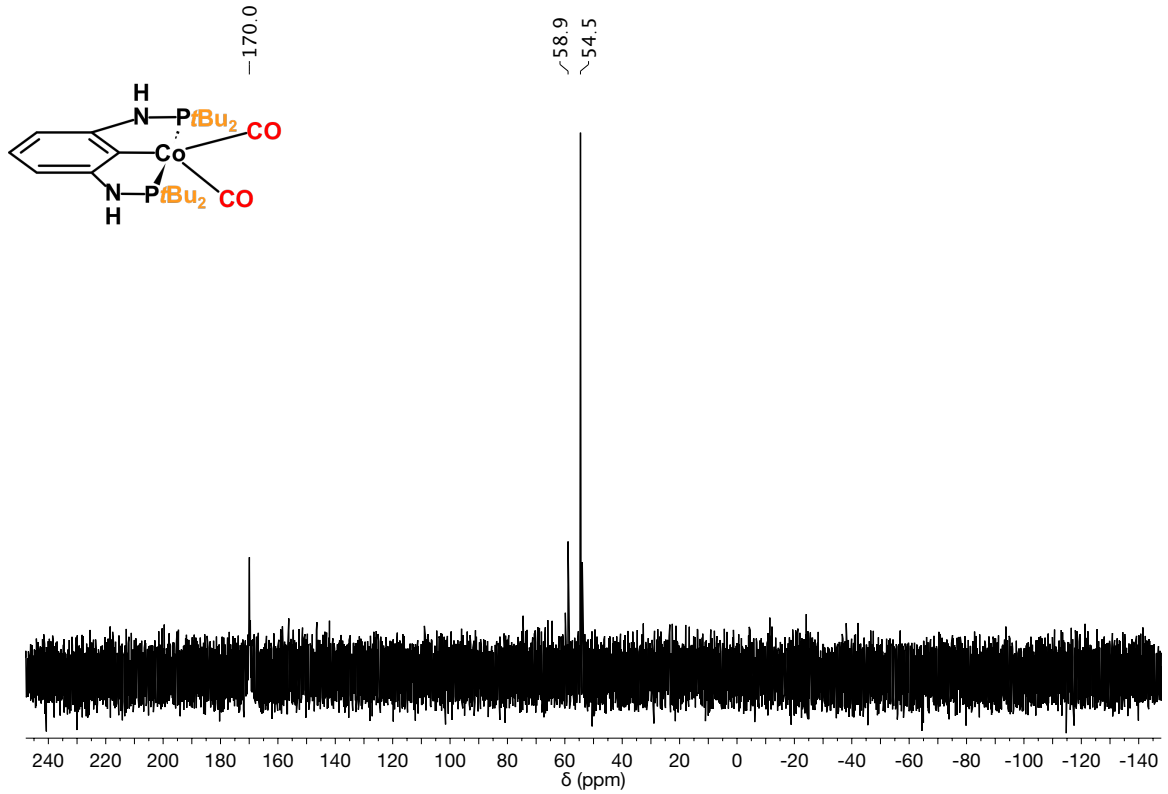

$^{31}P\{^{1}H\}$-NMR (162 MHz, MeCN-d_3, 20 °C): $[Co^{III}(PCP^{NH}\text{-}t\text{Bu})(CH_3CN)_3](BF_4)_2$ (**20**)

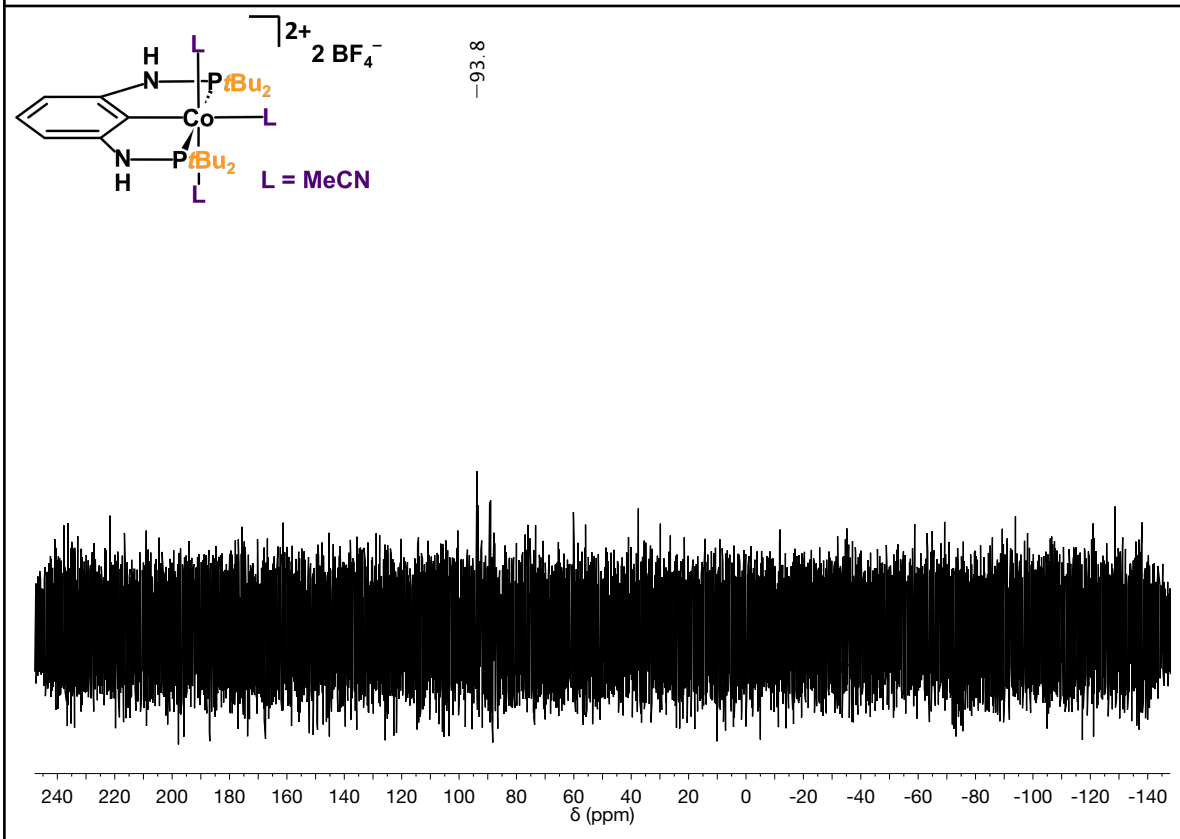

$^{31}P\{^{1}H\}$-NMR (162 MHz, CD_2Cl_2, 20 °C): [Co^{I}(PCP^{NH}-*t*Bu)(NO)]Br (**23**) und [Co^{III}(PCP^{NH}-*t*Bu)Br(NO)] (**24**)

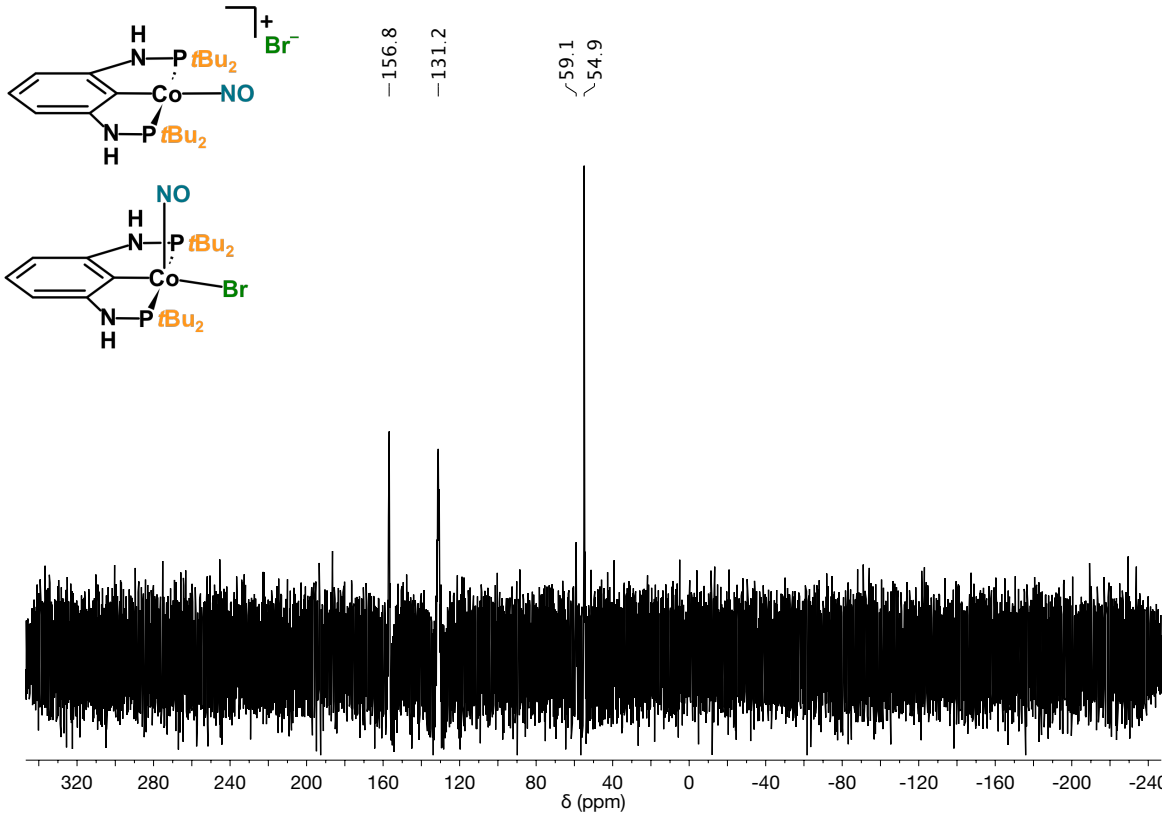

$^{31}P\{^{1}H\}$-NMR (101 MHz, C_6D_6, 20 °C): [Co^{I}(PCP^{CH_2}-*t*Bu)$(CO)_2$](**25**)

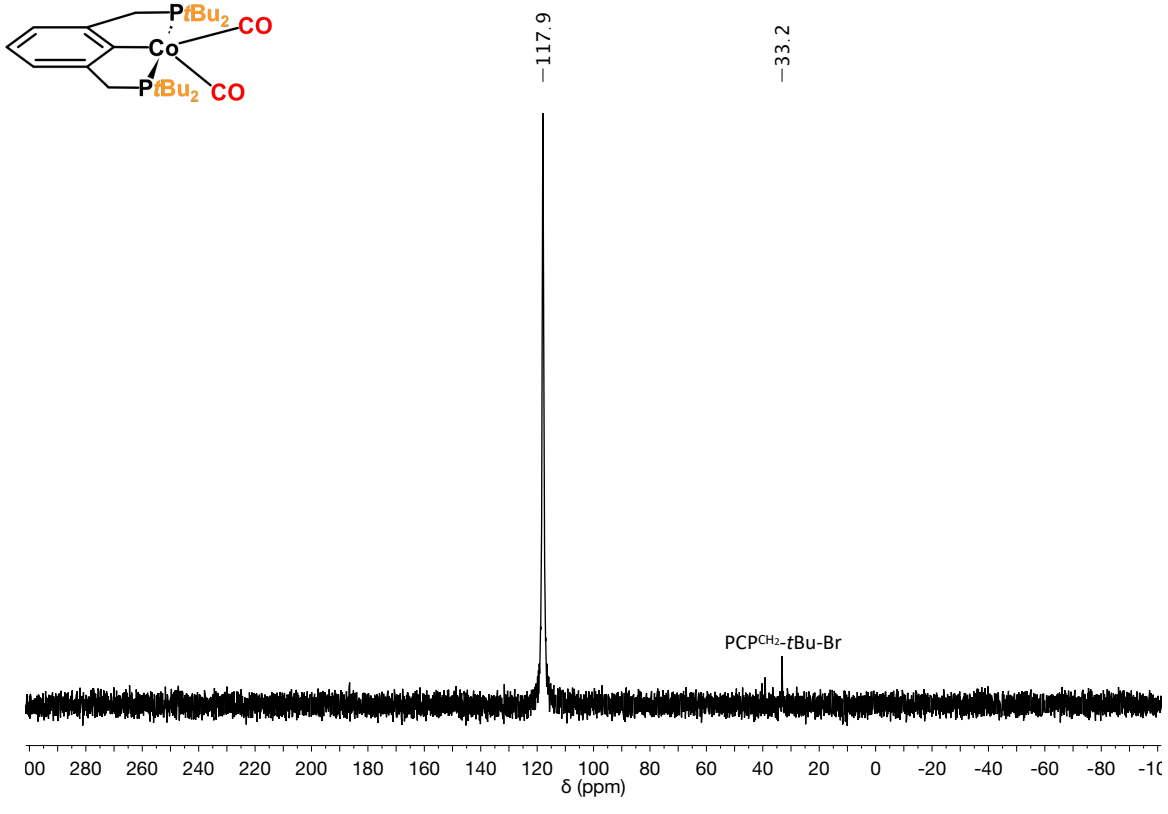

$^{31}P\{^{1}H\}$-NMR (162 MHz, MeCN-d_3, 20 °C): $[Co^{III}(PCP^{CH_2}\text{-}t\text{Bu})(CH_3CN)_3](SbF_6)_2$ (**27**)

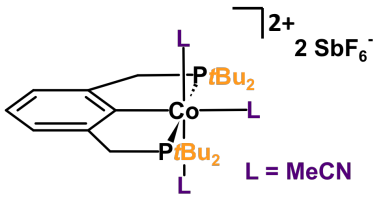

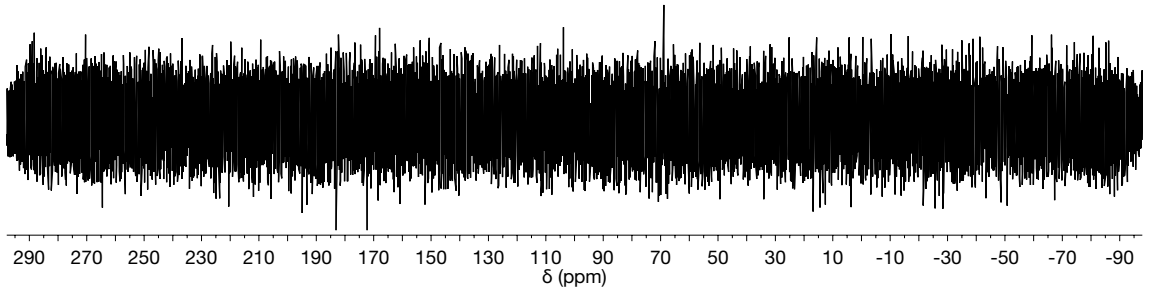

5.2. Crystallographic Data

complex	$[Co^{I}(PCP^{NH}\text{-}i\text{Pr})(CO)_2]$ (**11**)	$[Co^{II}(PCP^{NH}\text{-}t\text{Bu})Br]$ (**21**)
empirical formula	$C_{20}H_{33}CoN_2O_2P_2$	$C_{22}H_{41}BrCoN_2P_2$
MW (g mol^{-1})	454.37	534.36
crystal size (mm)	0.06 x 0.12 x 0.17	0.04 x 0.14 x 0.30
color, shape	yellow, block	orange, plate
crystal system	P 21/n	C 2/c
space group	monoclinic	monoclinic
a (Å)	20.462(2)	28.572(2)
b (Å)	11.1671(12)	15.3293(12)
c (Å)	22.906(3)	14.5716(11)
α (°)	90	90
β (°)	114.298(3)	117.751(2)
γ (°)	90	90
V (Å^3)	4770.6(9)	5648.1(8)
Z	8	12
ρ_{calc} (g cm^{-3})	1.315	1.311
T (K)	100	100
μ (mm^{-1})	0.872	1.620
F (0 0 0)	1992	2350
θ_{min} (°)	1.738	1.553
θ_{max} (°)	28.859	33.642
No. of reflns. measd.	51926	85235
No. of unique reflns.	12476	11063
No. of reflns. I > 2σ	8639	8317
No. of params.	532	302
R_1 (all data)	0.0931	0.0594
wR_2 (all data)	0.1228	0.0872
GooF	1.014	1.036

6. List of Abbreviations

Å	Ångström (0.1 nm)
AcOH	acetic acid
ATR-IR	attenuated total reflection infrared (spectroscopy)
***n*-BuLi**	*n*-butyllithium
CV	cyclic voltammetry
DBPO	dibenzoyl peroxide
DFT	density functional theory
DIPEA	di(isopropyl)ethylamine
EPR	electron paramagnetic resonance
ESI-MS	electrospray ionization mass spectrometry
EtOH	ethanol
Et_2O	diethylether
HOMO	highest occupied molecular orbital
HR-MS	high resolution mass spectrometry
***i*Pr**	isopropyl
LUMO	lowest unoccupied molecular orbital
Me	methyl (i.e. CH_3)
MeCN	acetonitrile
MeOH	methanol
NBS	N-bromosuccinimide
NEt_3	triethylamine
NMR	nuclear magnetic resonance
***t*Bu**	tertbutyl
XRD	X-ray diffraction

7. References

(1) Sheldon, R. A. *Chem. Commun.* **2008**, 3352-3356.

(2) Anastas, P. T.; Warner, J. C. *Green Chemistry: Theory and Practice*, Oxford University Press, Oxford, 1998.

(3) Anastas, P.; Eghbali, N. *Chem. Soc. Rev.* **2010**, *39*, 301-312.

(4) Gebbink, R.; Moret, M. *Non-Noble Metal Catalysis*, 1st ed; Wiley-VCH Verlag GmbH & Co. KGaA; Weinheim, Germany, 2019.

(5) Murugesan, S.; Kirchner, K. *Dalton Trans.* **2016**, *45*, 416.

(6) Moulton, C. J.; Shaw, B. L. *J. Chem. Soc., Dalton Trans.* **1976**, 1020-1024.

(7) van Koten G. *Pure Appl. Chem.* **1989**, *61*, 1681-1694.

(8) Mukherjee, A.; Milstein, D. *ACS Catal.* **2018**, *8*, 11435-11469.

(9) Gorgas, N.; Stöger, B.; Veiros, L. F.; Kirchner, K. *ACS Catal.* **2016**, *6*, 2664-2672.

(10) Garbe, M.; Junge, K.; Walker, S.; Wei, Z.; Jiao, H; Spannenberg, A.; Bachmann, S.; Scalone, M.; Beller M. *Angew. Chem.*, *Int. Ed.* **2018**, *57*, 46-60.

(11) Blanksby, S. J.; Ellison, G. B. *Acc. Chem. Res.* **2003**, *36*, 255-263.

(12) Murugesan, S.; Stöger B.; Weil, M.; Veiros, L. F.; Kirchner K. *Organometallics* **2015**, *34*, 1364-1372.

(13) Himmelbauer, D.; Stöger, B.; Veiros, L. F.; Pignitter, M.; Kirchner, K. *Organometallics* **2019**, *38*, 4669-4678.

(14) Lawrence, M. A. W.; Green, K.-A.; Nelson, P. N.; Lorraine, S. C. *Polyhedron* **2018**, *143*, 11-27.

(15) de Aguiar, S. R. M. M.; Stöger, B.; Pittenauer, E.; Allmaier, G.; Veiros, L. F.; Kirchner, K. *Organometallics* **2016**, *35*, 3032-3039.

(16) Pratihar, S; Pegu, R.; Guha, A. K.; Sarma, P. *Dalton Trans.* **2014**, *43*, 17136-17144.

(17) Junge, K.; Papa, V.; Beller, M. *Chem. Eur. J.* **2019**, *25*, 122-143.

(18) Xu, G.; Sun, H.; Li, X. *Organometallics* **2009**, *28*, 6090-6095.

(19) Lian, Z.; Xu, G.; Li, X. *Acta Crystallogr., Sect. E.: Struct. Rep. Online* **2010***, E66,* m636.

(20) Hebden, T. J.; St. John, A. J.; Gusev, D. G.; Kaminsky, W.; Goldberg, K. I.; Heinekey, D. M. *Angew. Chem. Int. Ed.* **2011**, *50*, 1873-1876.

(21) Mastalir, M.; Tomsu, G.; Pittenauer, E.; Allmaier, G.; Kirchner, K. *Org. Lett.* **2016**, *18*, 3462-3465.

(22) Li, Y.; Krause, J. A.; Guan H. *Organometallics* **2018**, *37*, 2147-2158.

(23) Casey, C. P.; Guan, H. *J. Am. Chem. Soc.* **2009**, *131*, 2499-2507.

(24) Murugesan, S; Stöger, B.; Carvalho, M. D.; Ferreira, L. P.; Pittenauer, E.; Allmaier, G.; Veiros, L. F., Kirchner, K. *Organometallics* **2014**, *33*, 6132-6140.

(25) Guard, L. M.; Hebden, T. J.; Linn, D. E. Jr.; Heinekey, D. M. *Organometallics* **2017**, *36*, 3104-3109.

(26) Murugesan, S.; Stöger, B.; Pittenauer, E.; Allmaier, G.; Veiros, L. F.; Kirchner K. *Angew. Chem. Int. Ed.* **2016**, *55*, 3045-3048.

(27) Pecak, J.; Eder, W.; Stöger, B.; Realista, S.; Martinho, P. N.; Calhorda, M. J.; Linert, W.; Kirchner, K. *Organometallics* **2020**, in press.

(28) Elschenbroich, C., *Organometallchemie*, 6th ed; B. G. Teubner Verlag / GWV Fachverlage GmbH, Wiesbaden, 2008.

(29) Orgel, L. E. *Inorg. Chem.* **1962**, *1*, 25-29.

(30) Wrighton, M. *Chemical Reviews* **1974**, *74,* 401-430.

(31) Tolman, C. A. *Chemical Reviews* **1977**, *77*, 313-348.

(32) Crabtree, R. H., *The Organometallic Chemistry of the Transition Metals*, 4th ed.; John Wiley and Sons, Inc; Hoboken, New Jersey, 2005.

(33) Chen, X.; Engle, K. M.; Wang, D.-H.; Yu, J.-Q. *Angew. Chem. Int. Ed.* **2009**, *48*, 5094-5115.

(34) Huang, S; Zhao, H.; Li, X.; Wang, L.; Sun, H. *RSC Adv.* **2015**, *5*, 15660-15667.

(35) Himmelbauer, D.; Mastalir, M.; Stöger, B.; Veiros, L. F.; Kirchner, K. *Organometallics* **2018**, *37*, 3631-3638.

(36) Himmelbauer, D.; Stöger, B.; Veirson, L. F.; Kircher, K. **2018**, *37*, 3475-3479.

(37) Himmelbauer, D.; Mastalir, M.; Stöger, B.; Veiros, L. F.; Pignitter, M.; Somoza, V.; Kircher, K. *Inorg. Chem.* **2018**, *57*, 7925-7931.

(38) Benito-Garagorri, D.; Bocokić, V.; Mereiter, K.; Kirchner, K. *Organometallics* **2006**, *25*, 3817-3823.

(39) Perin, D. D.; Amerego, W. L. F., *Purification of Laboratory Chemicals*, 3rd ed.; Pergamon: New York, 1988.

(40) Bruker, A. Inc., Madison, Wisconsin, USA,© 2005, COSMO (Version 1.48), SAINT (Version 7.06. A).

(41) Sheldrick, G. M. *Acta Crystallographica Section A* **2008**, *64*, 112-122.